

Session 4. Theory, Reduced Modeling and EP needs

Chairmen: Anne Bourdon and Andrei Smolyakov

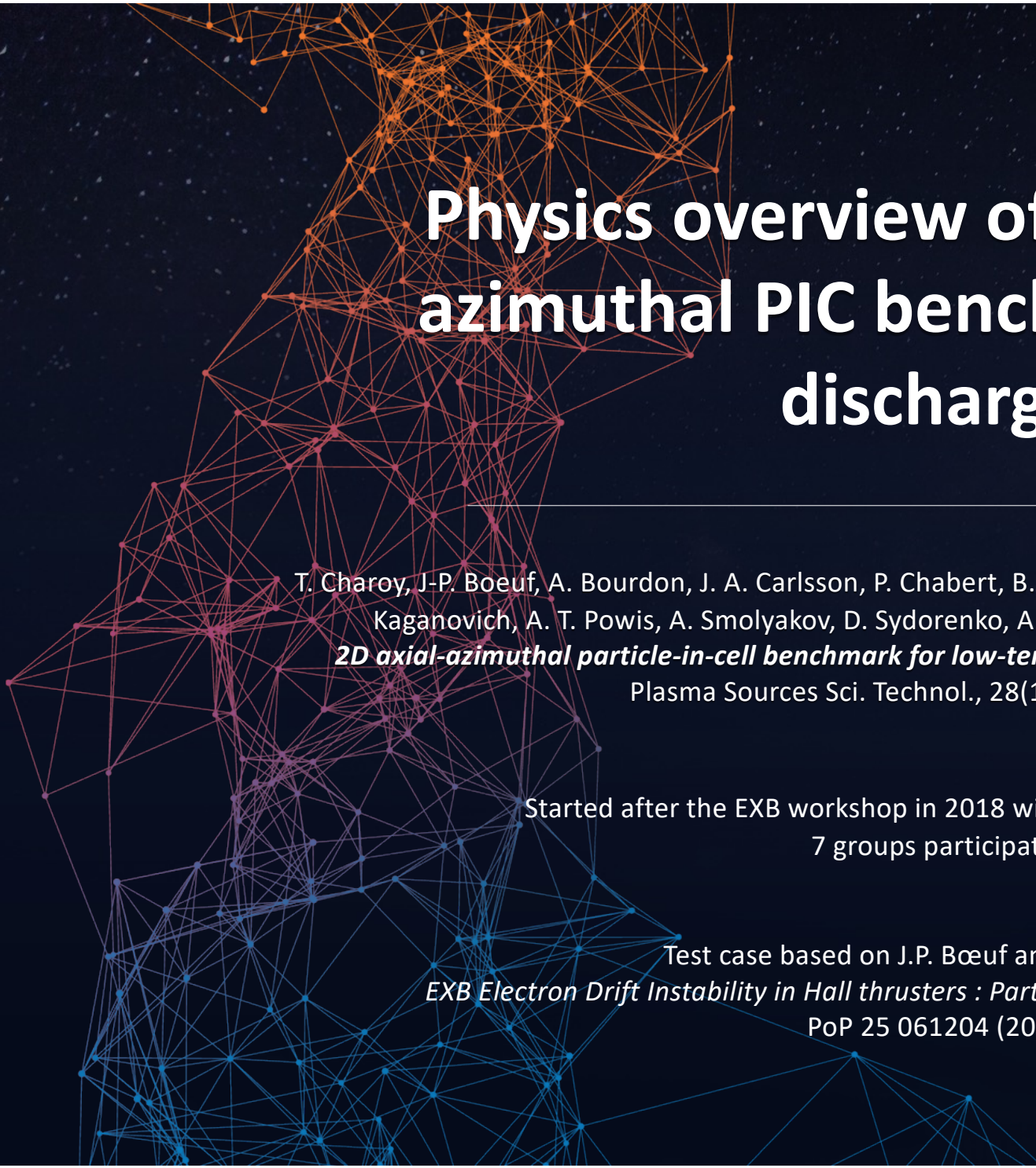
Panelists: Eduardo Ahedo, Trevor Lafleur, Ben Jorns, Tommaso Andreussi



Session 4 - Discussion topics

Introduction

- Physics learned from 2D axial-azimuthal and radial-azimuthal PIC benchmarks Anne Bourdon 10 min
- Comments on (Reduced) Breathing Mode modeling Andrei Smolyakov 10 min
- Simulating Hall thruster discharges with electron fluid models Eduardo Ahedo 10min
- The origin of the breathing mode in Hall thrusters and its stabilization Trevor Lafleur 10 min
- Experimental characterization of Hall thruster breathing mode dynamics and its modelling Ben Jorns 15 min
- Numerical and Experimental Investigation of Longitudinal Oscillations in Hall Thrusters Tommaso Andreussi 15 min
- Discussion 35 min



Physics overview of the 2D axial-azimuthal PIC benchmark for ExB discharges

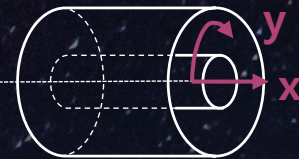
T. Charoy, J-P. Boeuf, A. Bourdon, J. A. Carlsson, P. Chabert, B. Cuenot, D. Eremin, L. Garrigues, K. Hara, I. D. Kaganovich, A. T. Powis, A. Smolyakov, D. Sydorenko, A. Tavant, O. Vermorel, and W. Villafana.

2D axial-azimuthal particle-in-cell benchmark for low-temperature partially magnetized plasmas.

Plasma Sources Sci. Technol., 28(10):105010, 2019.

Started after the EXB workshop in 2018 with a meeting at GEC 2018
7 groups participated

Test case based on J.P. Bœuf and L.Garrigues,
EXB Electron Drift Instability in Hall thrusters : Particle-In-Cell simulations vs. Theory,
PoP 25 061204 (2018)



E_y - azimuthal electric field

n_i - ion density

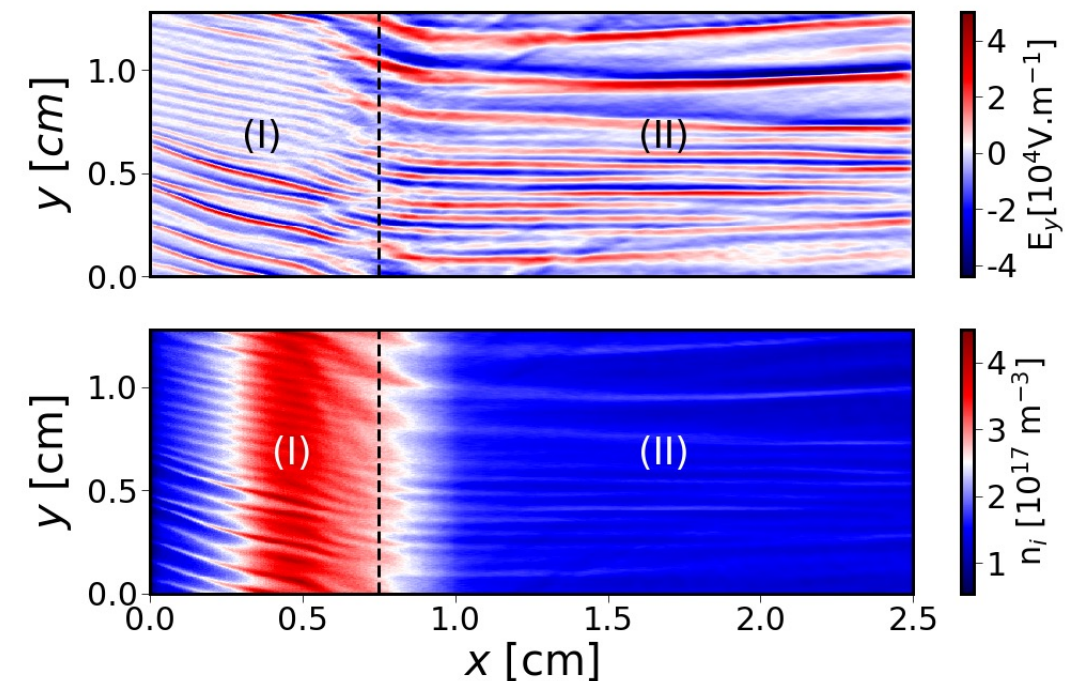
2D PIC axial-azimuthal benchmark

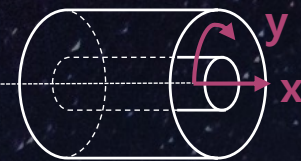
- ✓ Fixed magnetic field
- ✓ No collision
- ✓ Fixed ionization profile => stationnary state reached in $\sim 10 \mu\text{s}$)
- ✓ Azimuthal instabilities (EDI – $\lambda \sim 1 \text{ mm}$, $f \sim 5 \text{ MHz}$).

LIMITATIONS

- Imposed ionization source term
 - No collisions
 - Smaller discharge channel length (0.75 cm)
 - Limited azimuthal length (1.28 cm)
 - Simplified cathode model
-
- ✗ No axial instabilities (BM or ITTI)
 - ✗ Lack of thermalization processes
 - ✗ No long-wavelength azimuthal instabilities

2D maps of azimuthal electric field and ion density at a fixed time (LPP)



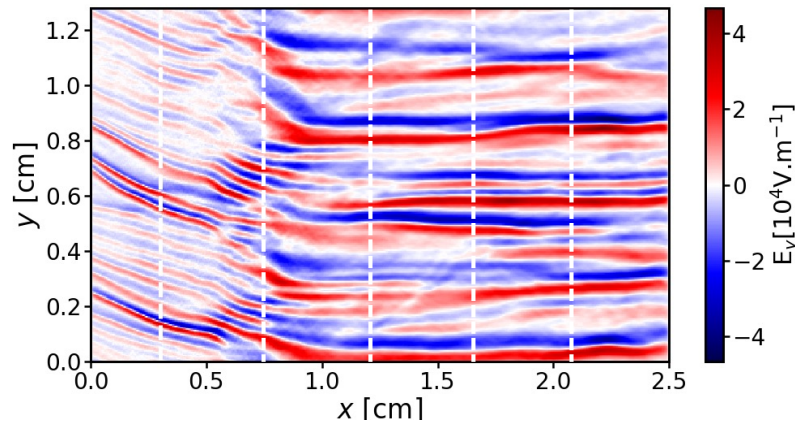


2D PIC axial-azimuthal benchmark

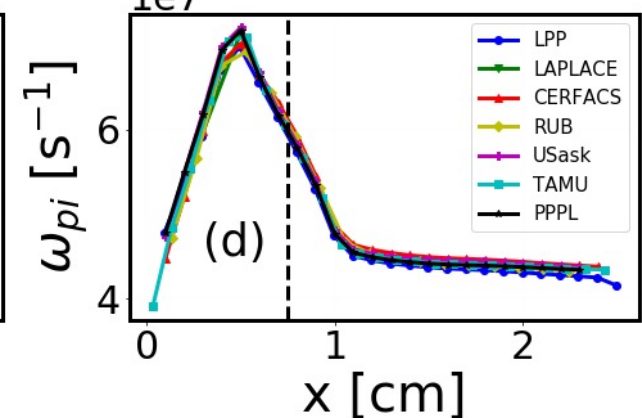
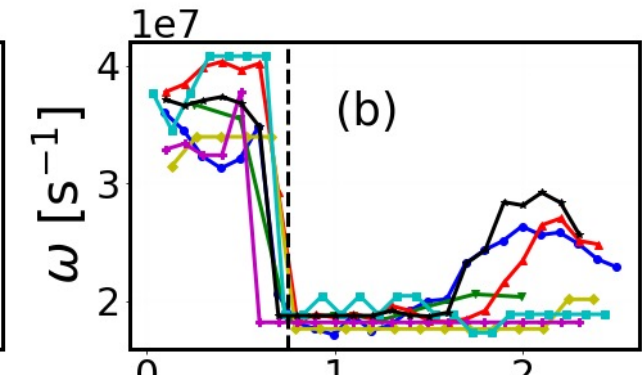
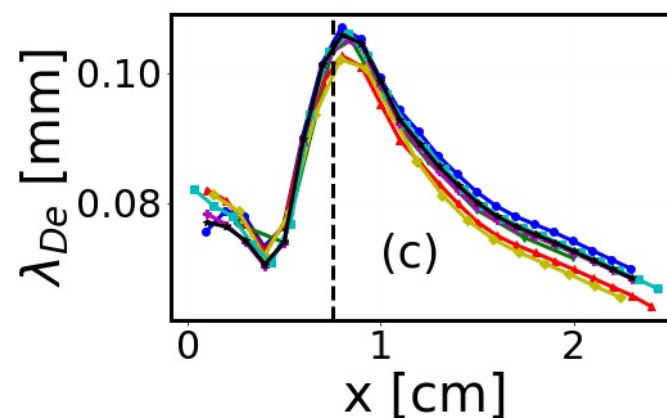
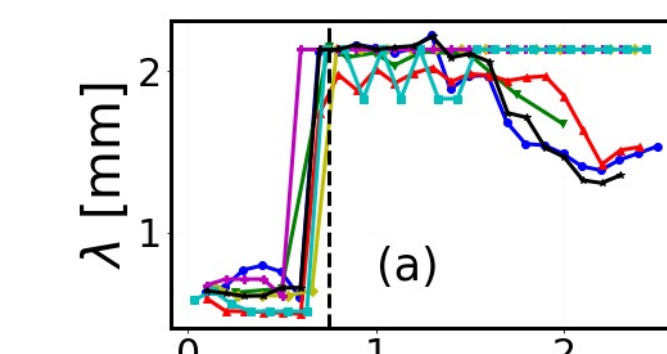
λ - wavelength
 ω - frequency

Study of azimuthal instabilities

Sharp change at the position of maximum radial magnetic field (ion sonic point):
 $\lambda \approx 0.5$ mm to 2 mm and $f \approx 5$ to 3 MHz \Rightarrow not fully understood



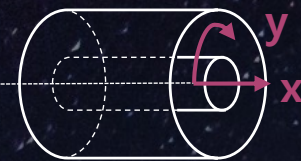
FFT



Very good agreement
 Discrepancies near the cathode

5

Axial evolution of dominant mode characteristics of azimuthal instabilities.
 (a) Wavelength. (b) Frequency. (c) Debye length. (d) Ion plasma frequency.
 Dashed line : Maximum of magnetic field

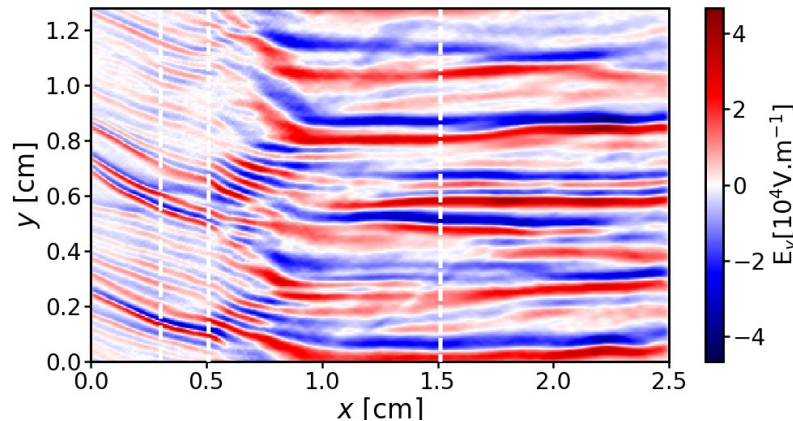


2D PIC axial-azimuthal benchmark

λ - wavelength
 ω - frequency

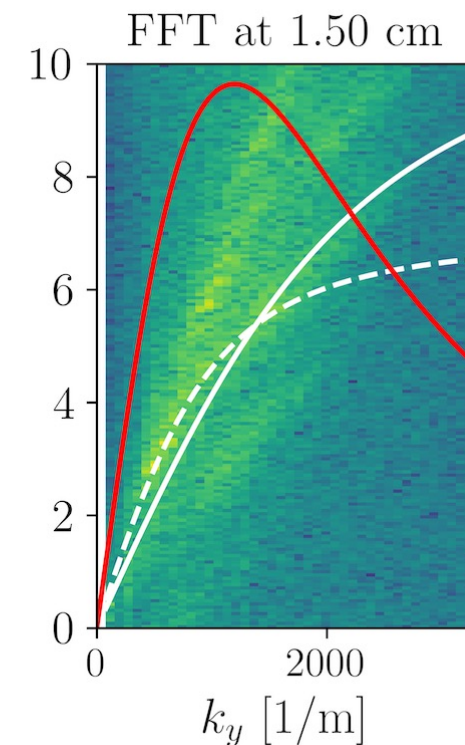
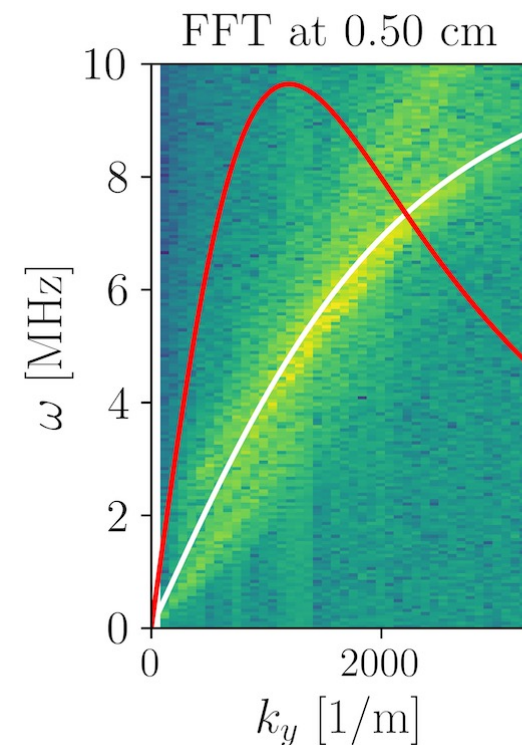
Study of azimuthal instabilities

Sharp change at the position of maximum radial magnetic field (ion sonic point):
 $\lambda \approx 0.5$ mm to 2 mm and $f \approx 5$ to 3 MHz => not fully understood



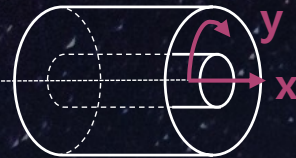
FFT

- Inside the thruster: dominant wavelength close to that predicted by the modified ion-acoustic dispersion relation (validated also by varying current density J [1,2]) => no consensus on saturation mechanisms
- In the plume: more discrete behaviour – fairly good agreement with a shifted DR (with plasma parameters at $x = 0.5$ cm)
- Hypothesis: azimuthal waves are predominately excited in the near anode region (maximum plasma density), and as these waves propagate downstream, the dominant wavelength changes (local dispersion relation continually satisfied).



White line : ion-acoustic dispersion relation
(solid at 0.5cm, dashed at 1.5 cm)
Red line : ion-acoustic growth rate (rescaled)

- [1] J.P. Bœuf and L. Garrigues, *Phys. Plasmas* 25 061204 (2018)
[2] Charoy et al. *Phys. Plasmas* 27, 063510 (2020)



Influence of the azimuthal length L_y

2D maps of ion density

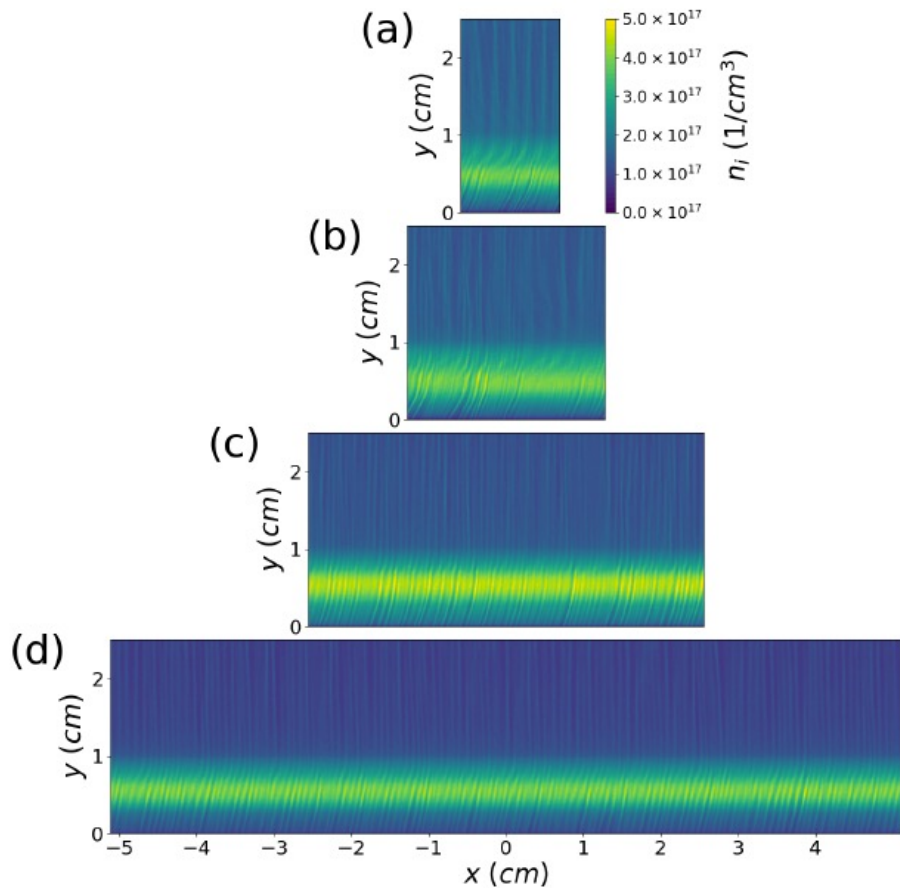


Figure 5.22: Ion density snapshot at $20 \mu\text{s}$ of an axial-azimuthal slice of a Hall thruster channel for various azimuthal extensions, (a) 1.28 cm (nominal case), (b) 2.56 cm, (c) 5.12 cm, and (d) 10.24 cm.

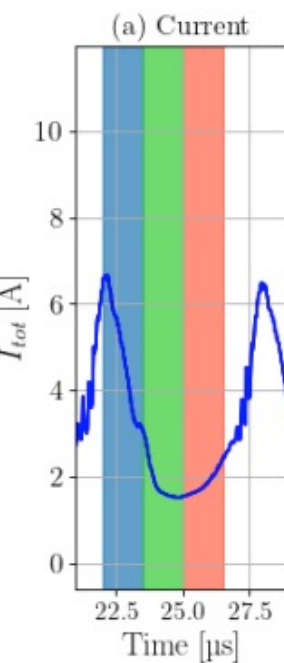
$L_y = 1.28 \text{ cm}$ limits the development of long-wavelength structures

$2L_y, 4L_y, 8L_y$ in [1] and $8L_y = 10.24 \text{ cm}$ in [2]

No long-wavelength structures in [1] and [2]

The azimuthal instability has a dominant wavelength close to that predicted by the modified ion-acoustic dispersion relation inside the thruster [2]

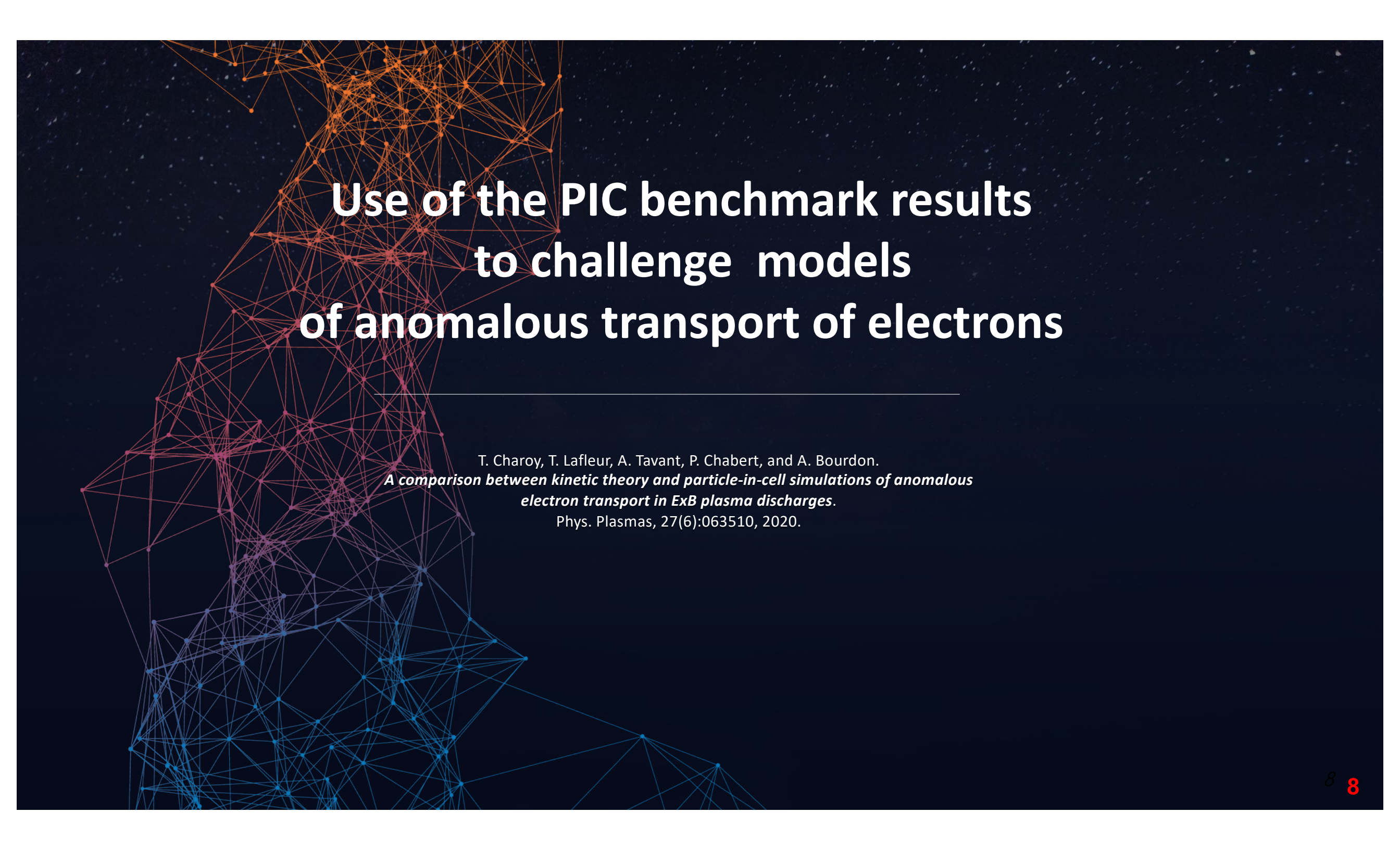
For 10.24 cm , current oscillations are observed [3]



[1] T Powis et al. in Scaling of spoke rotation frequency within a penning discharge and code development updates IEPC 2019 and T. Powis PhD thesis

[2] T Charoy et al. The interaction between ion transit-time and electron drift instabilities and their effect on anomalous electron transport in Hall thrusters 2021 *Plasma Sources Sci. Technol.* **30** 065017

[3] F. Petronio et al. Poster at this EXB workshop

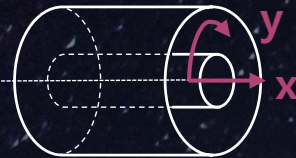


Use of the PIC benchmark results to challenge models of anomalous transport of electrons

T. Charoy, T. Lafleur, A. Tavant, P. Chabert, and A. Bourdon.

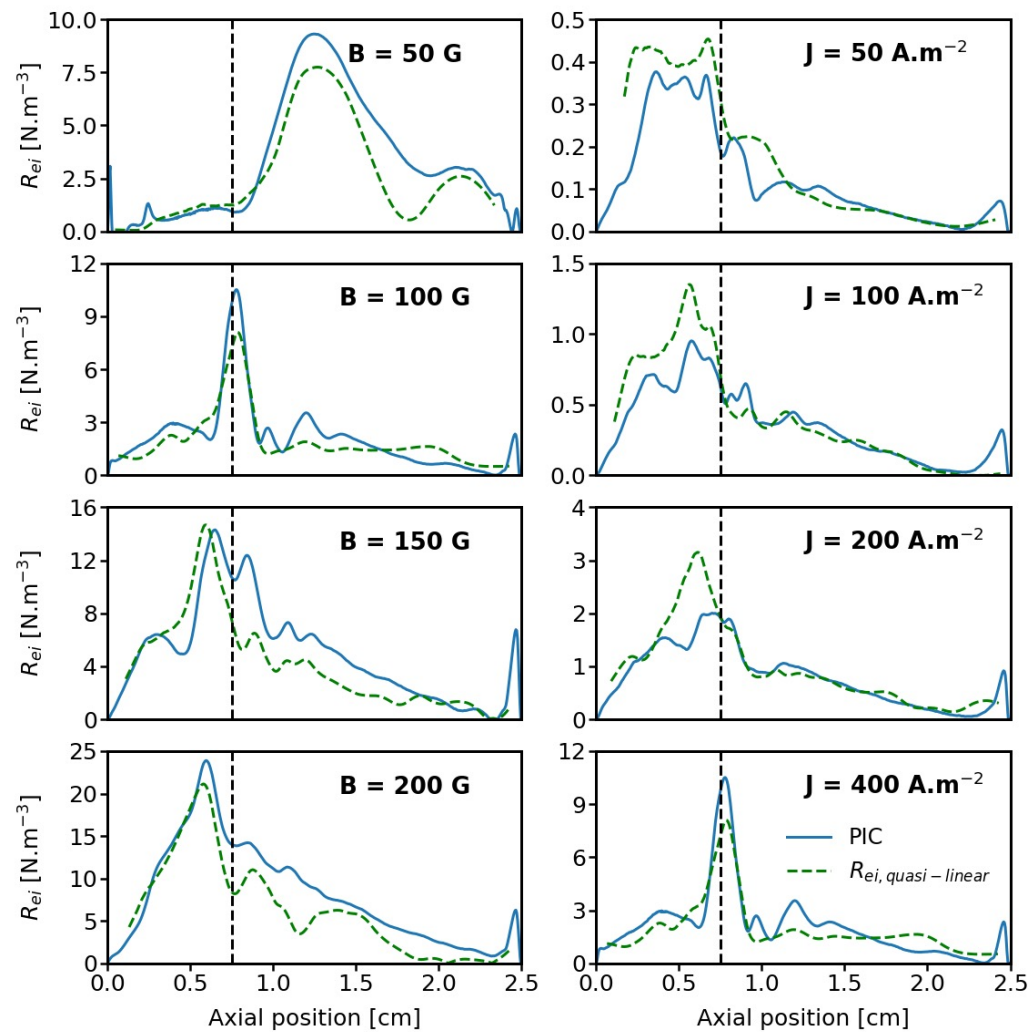
*A comparison between kinetic theory and particle-in-cell simulations of anomalous
electron transport in ExB plasma discharges.*

Phys. Plasmas, 27(6):063510, 2020.



Benchmark PIC results used to stress-test models

Extensive parametric study: Variation of magnetic field maximum value and discharge current density



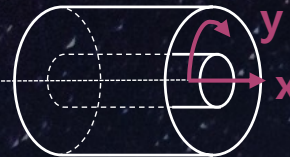
Axial evolution of the instability-enhanced force for different values of magnetic field maximum value B (left) and current density J (right)

$$R_{\text{quasi-linear}} = 2\sqrt{2}\pi\omega_{pe}^2\lambda_d\varepsilon_{\text{wave}} \frac{dF_{e,0}}{d\nu_{e,y}}|_{\nu_{e,y}=0}$$

- Various shapes and amplitudes for the instability-enhanced force

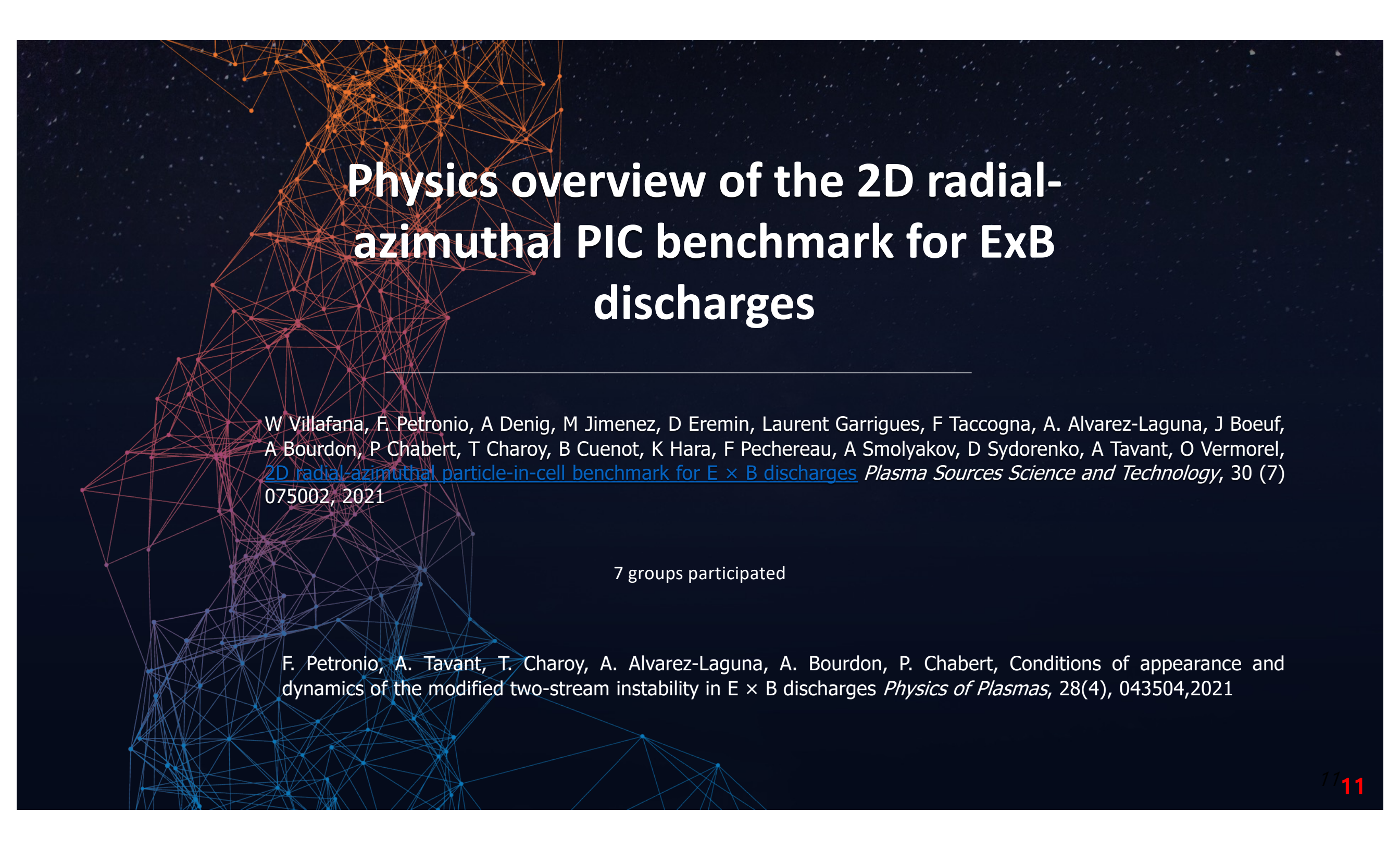


Quasi-linear theoretical model approximates very well the instability-enhanced force
 ⇒ Validity in the context of electron drift instabilities in HETs still requires further investigation
 ⇒ The EDF is in general strongly non-Maxwellian and diverse in shape throughout the discharge: Challenge in modeling anomalous electron transport for fluid simulations



Other works based on the 2D PIC axial-azimuthal benchmark test case

- **Study of multiply charged ions:** The presence of multiply charged ions causes another short-wavelength phenomenon: ion–ion two-stream instability (IITSI). The interactions between IITSI and ECDI-perturbations leads to complex plasma behaviour
 - K. Hara and S. Tsikata, Cross-field electron diffusion due to the coupling of drift-driven microinstabilities, *Phys. Rev. E*, 102, 023202 (2020)
 - P. Kumar, S. Tsikata and K. Hara, Effects of multiply charged ions on microturbulence-driven electron transport in partially magnetized plasmas, *Journal of Applied Physics*, 130, 173307 (2021)
- **Virtual Collective Thomson Scattering: mode propagation, electron density fluctuations:** T. Ben Slimane et al., Analysis of small scale fluctuations in Hall effect thrusters using virtual Thomson scattering on PIC simulations, *Physics of Plasmas* 29, 023501 (2022) + Poster at this workshop
- **3D /2D comparisons:** W. Villafana PhD + Poster at this workshop

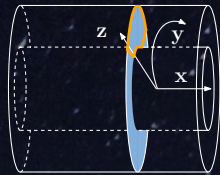


Physics overview of the 2D radial-azimuthal PIC benchmark for ExB discharges

W Villafana, F Petronio, A Denig, M Jimenez, D Eremin, Laurent Garrigues, F Taccogna, A Alvarez-Laguna, J Boeuf, A Bourdon, P Chabert, T Charoy, B Cuenot, K Hara, F Pechereau, A Smolyakov, D Sydorenko, A Tavant, O Vermorel, [2D radial-azimuthal particle-in-cell benchmark for \$E \times B\$ discharges](#) *Plasma Sources Science and Technology*, 30 (7) 075002, 2021

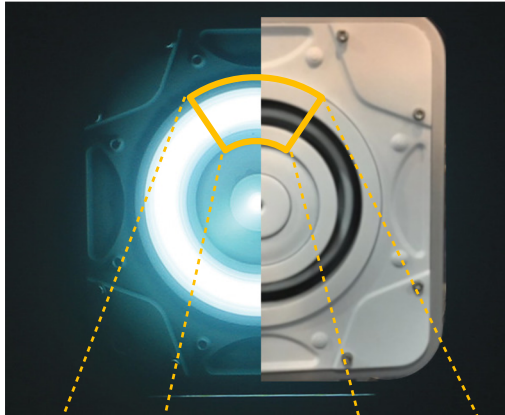
7 groups participated

F. Petronio, A. Tavant, T. Charoy, A. Alvarez-Laguna, A. Bourdon, P. Chabert, Conditions of appearance and dynamics of the modified two-stream instability in $E \times B$ discharges *Physics of Plasmas*, 28(4), 043504, 2021



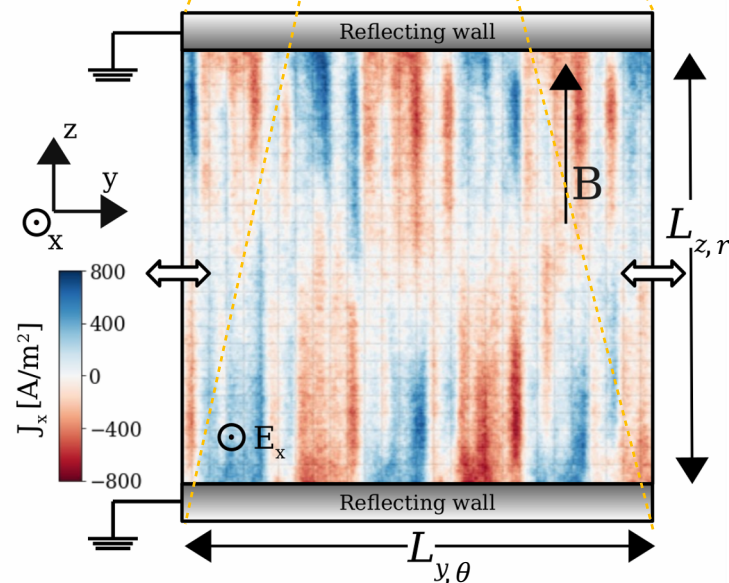
2 D P I C radial-azimuthal benchmark

Radial-azimuthal ($r \theta$) plane



Several instabilities develop in these discharges, in particular **ECDI** and **MTSI (Modified Two-Stream Instability)**

ECDI: Well studied in literature, $\lambda \sim 1$ mm and $\omega \sim 5$ MHz

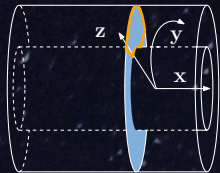


MTSI: Observed by Janhunen *et al.*¹, $\lambda \sim 5$ mm and $\omega \sim 1$ MHz but not in other works, such Tavant *et al.*²

Choice of a collisionless test-case with both instabilities

¹S. Janhunen *et al.*, "Evolution of the electron cyclotron drift instability in two-dimensions" Physics of Plasmas, 2018.

²A. Tavant *et al.*, "The Effects of Secondary Electron Emission on Plasma Sheath Characteristics and Electron Transport in an $E \times B$ Discharge via Kinetic Simulations". PSST, 2018



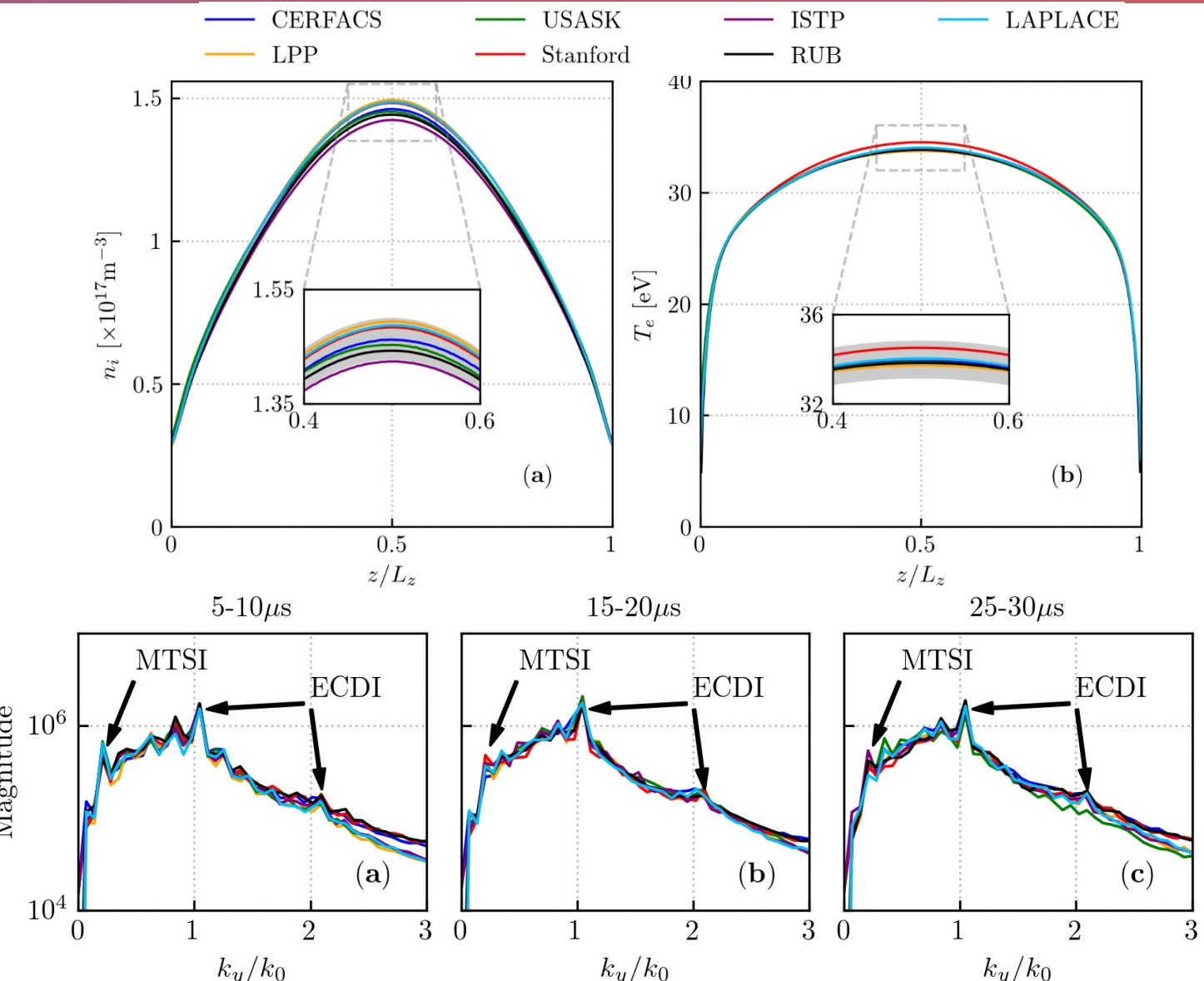
2 D radial - azimuthal configuration

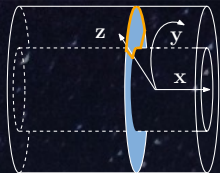
Main plasma parameters (1D mean radial profiles)

Spectral analysis

All groups observe the 2 instabilities on the test-case

Verification / results





2 D radial-azimuthal configuration

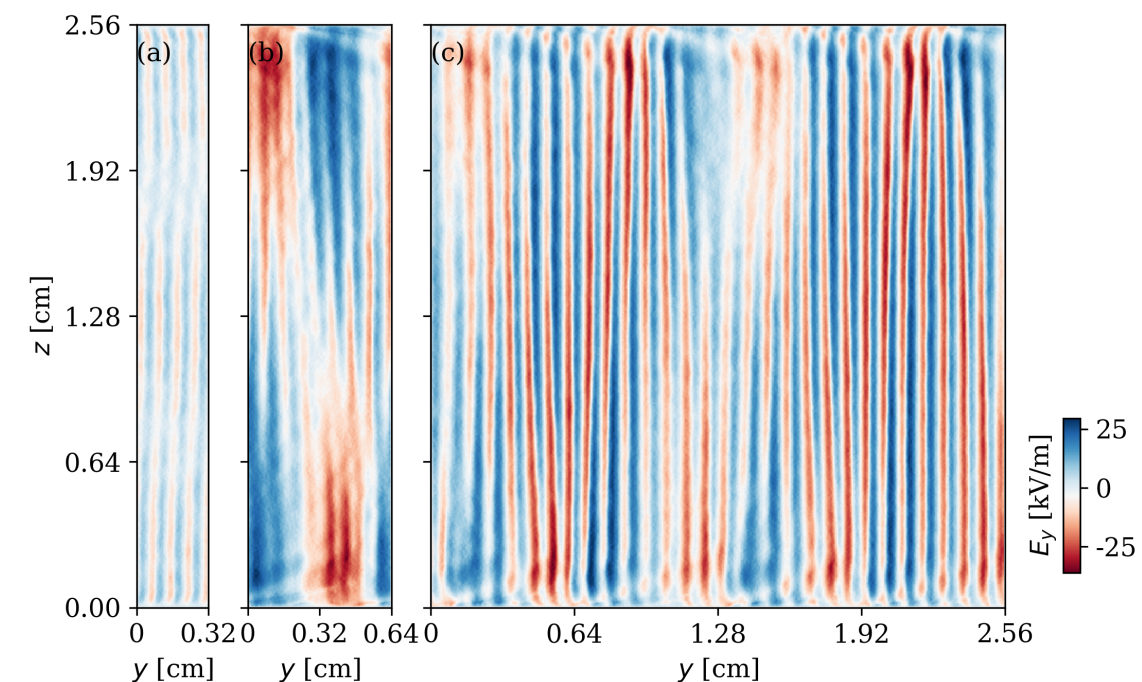
Derivation in [1] of a stability condition for the apparition of the MTSI modes.

This model has been challenged with several PIC simulations in different discharge conditions (density, electric field, domain dimensions, ...)

Example : Change of simulation domain dimensions¹:

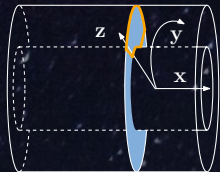
- Reducing L_y below a certain threshold, **switches off** the MTSI instability. See (a) and (b).
- **Prediction of the number of MTSI wavelengths** knowing the domain dimensions
- Oscillating mode is always the one closest to the instability limit.

Effect of the MTSI on some important thruster's parameters:
electron temperature and electron mobility



Azimuthal = $\theta = y$
Radial = $r = z$

¹F. Petronio *et al.*, *Conditions of appearance and dynamics of the Modified Two-Stream Instability in $E \times B$ discharges*, PoP, 2021



2D PIC radial-azimuthal benchmark - Conclusion

Benchmark with both MTSI and ECDI instabilities : good agreement between 7 independent PIC codes

Better understanding of the conditions of appearance of MTSI in PIC simulations of $E \times B$ discharges

The dispersion relation has been challenged with several PIC simulations in different discharge conditions (density, electric field, domain dimensions, ...)

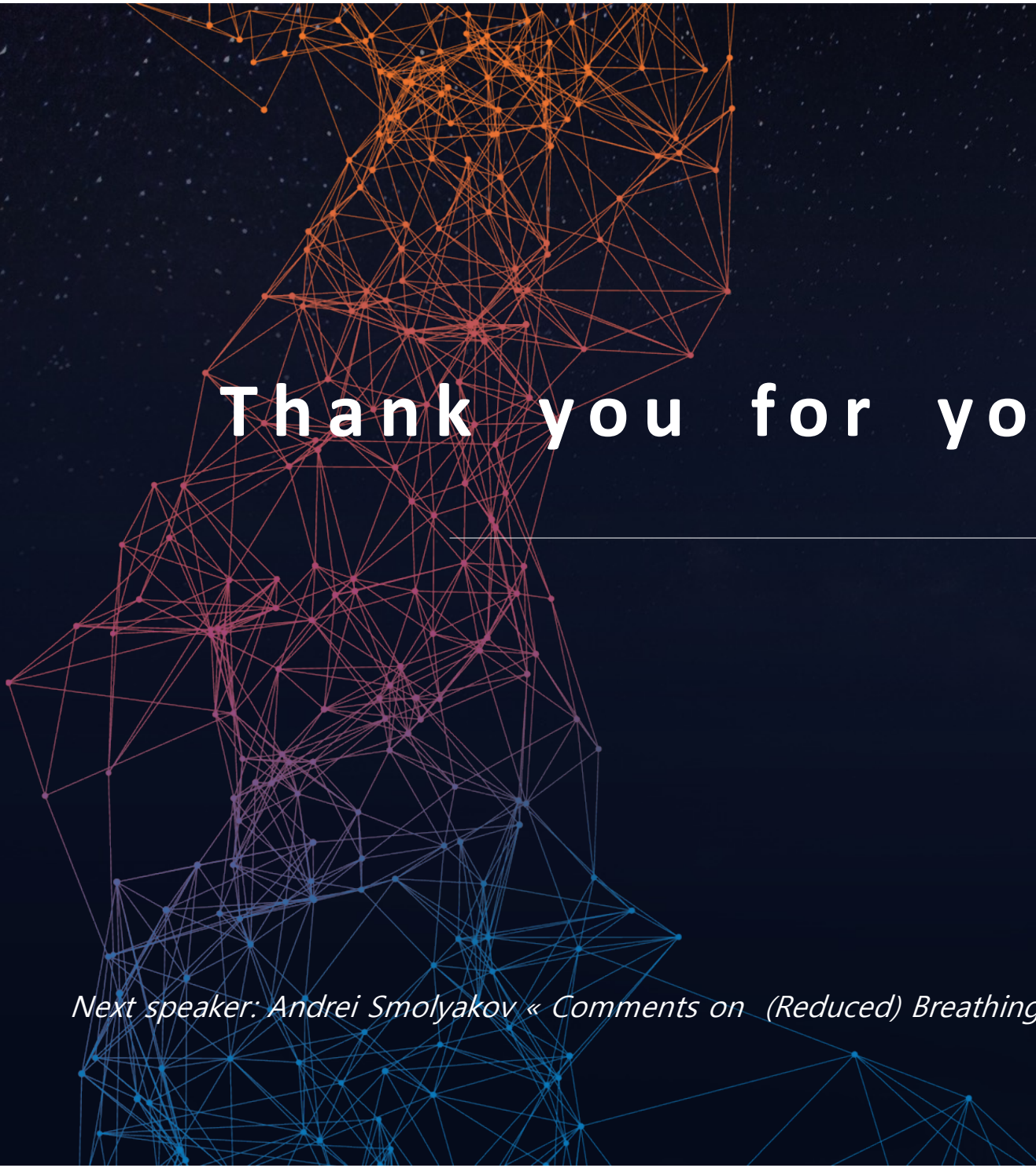
Effect of the MTSI on some important thruster's parameters (electron temperature, electron mobility)

Limits:

- Fixed ionization source term
- No collisions
- Simplified BC at the walls.

Open question:

- How does SEE impact the conditions of appearance of the MTSI, influence on the ECDI/MTSI coupling?



Thank you for your attention

Next speaker: Andrei Smolyakov « Comments on (Reduced) Breathing Mode modeling »

Comments on (Reduced) Breathing Mode modeling

Andrei Smolyakov
ExB Workshop, 2022

Mechanisms of ionization oscillations; Fluid and hybrid breathing mode (LANDMARK) benchmark, A.Chapurin et al , JAP 2021, 129, 233307, <http://arxiv.org/abs/2201.11280>

The origin of the breathing mode in Hall thrusters and its stabilization, T Lafleur; JAP 130, 053305 (2021)

Experimental characterization of plasma properties on time scale of breathing mode in acceleration zone, B Jorns; E. Dale and B. Jorns, JAP **130** 133302 (2021),...

Numerical and Experimental Investigation of Longitudinal Oscillations in Hall Thrusters, T Andreussi; Aerospace 2021, 8(6), 148,...

- Full 3D modeling is (currently) out of reach due to immense scale separation, some exploratory work exist
- 2D kinetic (azimuthal-axial) still very difficult (rescaling is needed), 2D fluid are rare
 - Existing work clearly shows coupling and synergy of axial mode (e.g. BM) and azimuthal modes (responsible for transport)
- “Full” 1D (axial) models: fluid and hybrid (fluid electrons + kinetic ions and neutrals)
- Further reductions: various 0D models, e.g. neutral-ion interactions (predator-prey), neutral-ion+electron energy (ionization), ...

Key questions:

- Conditions for the instability
- Predict the characteristics of oscillations, e.g. current amplitude

Reduced-reduced, e.g. 0D models

Coupling to ionization suggests:

$$\frac{\partial n_i}{\partial t} + \frac{\partial}{\partial x}(n v_i) = \beta n N \quad \frac{\partial N}{\partial t} + \frac{\partial}{\partial x}(N v_a) = -\beta n N$$

0D predator-prey
(Fife 1998)

$$\frac{\partial n_i}{\partial t} + \frac{1}{L} n v_i = \beta n N; \quad \frac{\partial N}{\partial t} - \frac{1}{L} n v_a = -\beta n N$$

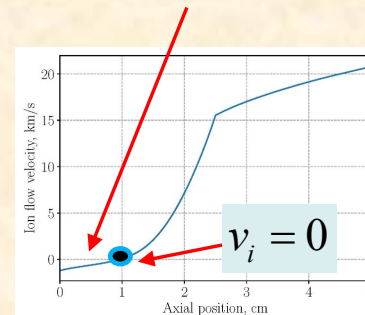
Predator-prey: does not have the instability, nor the condition for the instability...
Various improvements and fixes: neutral influx variations, temperature fluctuations, two-zone, (Barral, Hara, Jorns, ...) + further Lafleur + Jorns in this session

1D Continuum predator-prey with the ion backflow region near the anode is unstable

Chapurin et al 2021,

$$\frac{\partial N}{\partial t} + \frac{\partial}{\partial x}(N v_a) = -\beta n N$$

$$\frac{\partial n_i}{\partial t} + \frac{\partial}{\partial x}(n v_i) = \beta n N$$



The ion back-flow region occurs as a result of the electron diffusion near the anode

The breathing mode frequency scales with the width of the back-flow region is $f * L / v_a = 4$. Good agreement with full model (LANDMARK)

Some mathematical questions of plasma ionization, Gavrikov, Tayurskiy, https://keldysh.ru/papers/2021/prep2021_94.pdf

(Keldysh Institute of Applied Mathematics, Russian Academy of Science)

Cauchy problem: single zero of the ion velocity is required as the sufficient and required condition for BM

“Full” 1D (axial) fluid (and hybrid) models for BM

$$\frac{\partial n}{\partial t} + \frac{\partial}{\partial x} (n v_i) = \beta n N - \nu_w n$$

$$\frac{\partial N}{\partial t} + \frac{\partial}{\partial x} (N v_a) = -\beta n N + \nu_w n$$

$$m_i n \left(\frac{\partial v_i}{\partial t} + v_i \frac{\partial v_i}{\partial x} \right) = e n E - \beta N m_i (v_i - v_a) \quad J_d = n v_i - n \mu_e E - \frac{\mu_e}{e} \frac{\partial (T_e n)}{\partial x} = \text{const}$$

$$\frac{3}{2} \frac{\partial (n T_e)}{\partial t} + \frac{5}{2} \frac{\partial}{\partial x} (n T_e v_{ex}) + \frac{\partial}{\partial x} q_x = -e n v_{ex} E - n N_a K - n W \quad q_x = -n \mu_e T_e \frac{\partial T_e}{\partial x}$$

$$\mu_e = \frac{e}{m_e v_m} \frac{1}{1 + \omega_{ce}^2 / v_m^2}$$

$$v_m = v_{en} + v_{wall} + v_B$$

$$v_B = (\beta / 16) \frac{e}{m_e B}$$

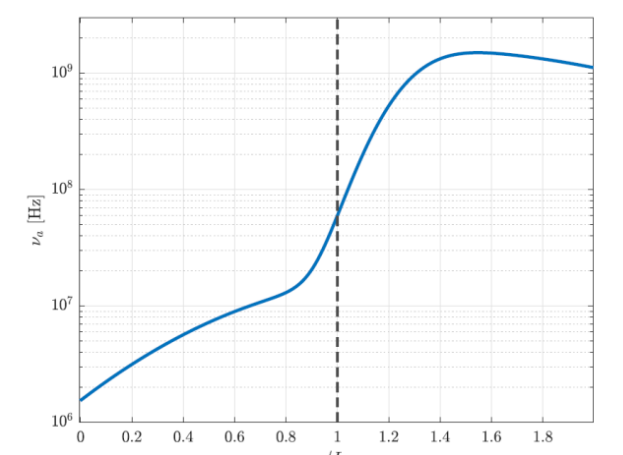
Morozov & Savel'ev, 1995, 2000; Boeuf & Garrigues 1998, Barral et al 2001, Barral & Ahedo 2009, Hagelaar et al, 2004, Hara & Mikellides 2018, ...+ this session (Lafleur, Andreussi)

- All models include several phenomenological (“calibration”) parameters
- With some “calibration” (and enthusiasm) every model is able to reproduce experimental data (with varying degrees of success)

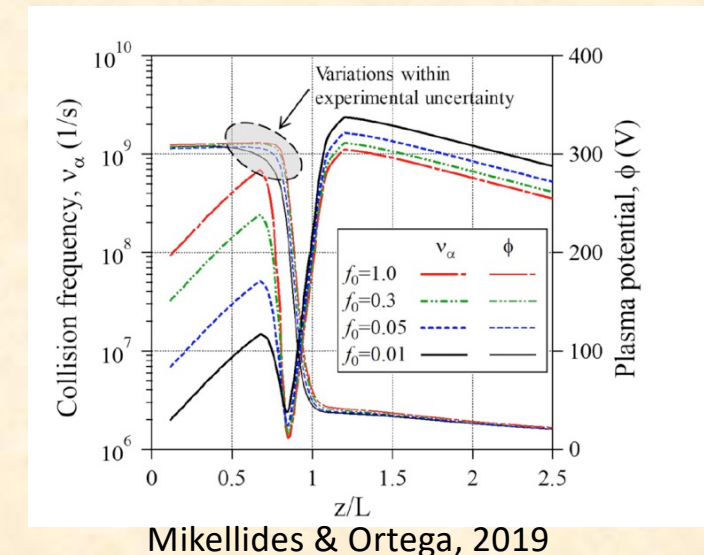
$\mu_e, v_B, q_e, W, \dots$

anomalous transport (current and heat),
electron energy losses (kinetic and anomalous)

		Anomalous mobility	Electron energy losses (sheath)	Heat flux	Comment
Lafleur et al.	$\alpha_B = 0.1 \times (1/16)$	Classical, SEE (fluid)	No	Nonlinearity $p_{abs} \sim \mu_e n E^2$ in power absorption triggers BM	
Andreussi et al.	Large variation across the whole region	Classical, SEE (fluid)	anomalous, same as mobility	Calibrated by the comparison with exp. data	
Chapurin et al. Fluid vs hybrid LANDMARK study	$\alpha_{B,in} = 0.1 \times (1/16)$ $\alpha_{B,out} = 1 \times (1/16)$	“anomalous” $W = \nu_e \varepsilon \exp\left(-\frac{U}{\varepsilon}\right)$	anomalous, same as mobility	High sensitivity* to anomalous energy losses, and anomalous mobility profile (*noted by many others)	



Giannetti et al 2021



Mikellides & Ortega, 2019

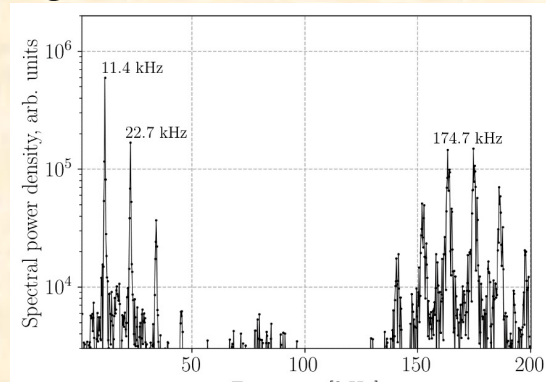
Role of ion/neutral kinetic effects: fully fluid model vs kinetic ions and neutrals with identical fluid electron physics, Chapurin et al, 2022

Fluid vs hybrid benchmark, LANDMARK, <https://www.landmark-plasma.com>

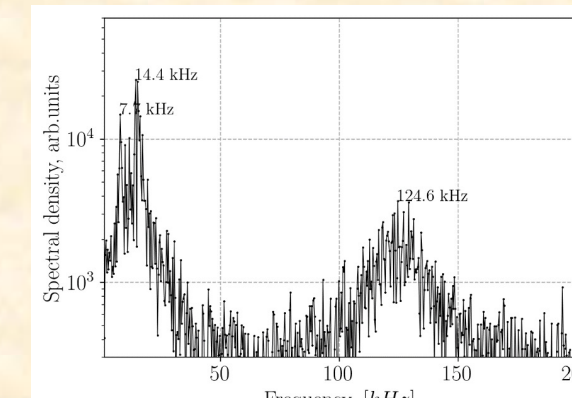
- Generally similar features in fluid and hybrid simulations
- Good agreement on stationary/average profiles and frequencies, 30-50% discrepancy for amplitude of fluctuations, agreement is improved with finite ion pressure
- Two different regimes of BM are identified in both models
- Large sensitivity to “phenomenological” parameters (both models), e.g. energy losses

	Anomalous energy losses	
Case 1	$\nu_{\varepsilon,in} = 0.95 \times 10^7 \text{ s}^{-1}$	Single Breathing Mode, similar to the reduced model due to back-flow instability
Case 2	$\nu_{\varepsilon,in} = 0.4 \times 10^7 \text{ s}^{-1}$	BM coexist with resistive modes (transit frequency), both in fluid and hybrid simulations
Case 3	Injection of neutrals with a finite temperature spread	Hybrid: Strong suppression of BM oscillations ampl. (sensitive to the shift of the acceleration region)

Fluctuations spectra in fluid and hybrid models for the regime of BM ($\sim 10 \text{ kHz}$) coexisting with resistive modes ($\sim 120-160 \text{ kHz}$)



Fluid



Hybrid

- Key questions:
 - Conditions for the instability
 - Predict the characteristics of oscillations, e.g. current amplitude
- Physics insights provided by reduced models are valuable as they may point to the critical parameters controlling the mode excitation and mechanisms
 - e.g. Ion velocity with a backflow is unstable (“solo” BM regime)
 - However (LANDMARK study): BM exist in different regimes, role of resistive modes, high sensitivity to anomalous energy losses (and mobility)

(for the discussion) ...
- Do existing models have predictive power?
- How to deal with uncertainties and sensitivities on anomalous transport/losses models?
 - e.g. simple questions are
 - How different are “fits” for anomalous mobility obtained from calibration on thruster performance and on BM characteristics?
 - Is characterization in terms of the anomalous collision is sufficient?
 - e.g. $D_a / \mu_a = T_e / e$?

Next:

Eduardo Ahedo: On magnetized electron fluid models for thruster discharges

Simulating Hall thruster discharges with electron fluid models

Eduardo Ahedo



**ExB Plasmas
Workshop
2022**

Madrid, online event

Introduction

- Plasma discharge in HET, EPT (HPT, ECRT), GIT ... is weakly collisional
 - Some kinetic effects relevant, but difficult to include in fluid models,
 - PIC models adequate, although noisy
- Full PIC-3D codes have huge computational cost since $\Delta t_n \sim 10^2 \Delta t_i \sim 10^4 \Delta t_e$
 - Often 3D is simplified into axisymmetry 2D(z,r)
 - Some physics must be sacrificed. Depending on goals:
 - neutral dynamics are simplified for fundamental phenomena (e.g. instabilities, plasma-wall):
 - electron dynamics are simplified for performance studies of whole, long-range discharge (~1 ms)
- Common simplified electron model: fluid, 2D(z,r), magnetized, slow-dynamics, drift-diffusion
 - Coupled to ion+neutral models, leads to
 - Fully-fluid codes: Hall2De, 1D axial, ...
 - Hybrid codes [PIC-ions + fluid-electrons]: HPHall (Fife, 1997) and sequels (e.g. HYPHEN)
 - HYPHEN yields steady-state 1ms behavior in ≥ 10 hours of workstation

Introduction

- 2D(z-r) fluid models:
 1. What effects are misrepresented?
 2. How serious are these limitations?
 3. How e-kinetic models can validate e-fluid models?
- 3D dynamics
 - 3D high-freq dynamics: e.g. electron θ -instabilities responsible of anomalous $\bar{1}_\theta \times \bar{B}$ transport
 - No model for θ -averaged turbulent force \rightarrow use of fitted expressions
 - 3D effects created by some elements (lateral cathode, ...) \rightarrow some are quickly θ -homogenized [1]
- Non-Maxwellian velocity distribution function (VDF) effects
 - Weakly-collisional electrons are well-confined inside the discharge \rightarrow is VDF quasi-Maxwellian ?
 - Non-Maxwellian VDF affects mainly
 - plasma-wall interaction fluxes
 - plume expansion (e.g. electron collisionless cooling)
 - A non-Maxwellian VDF affects mainly two fluid terms (besides boundary conditions)
 - The **pressure tensor**: is $\bar{\bar{P}}_e = p_e \bar{\bar{I}}$?
 - The **heat flux vector**: is $\bar{q}_e = -\bar{\bar{K}}_e \cdot \nabla T_e$?
- Electron inertia and finite Larmor radius (FLR) effects

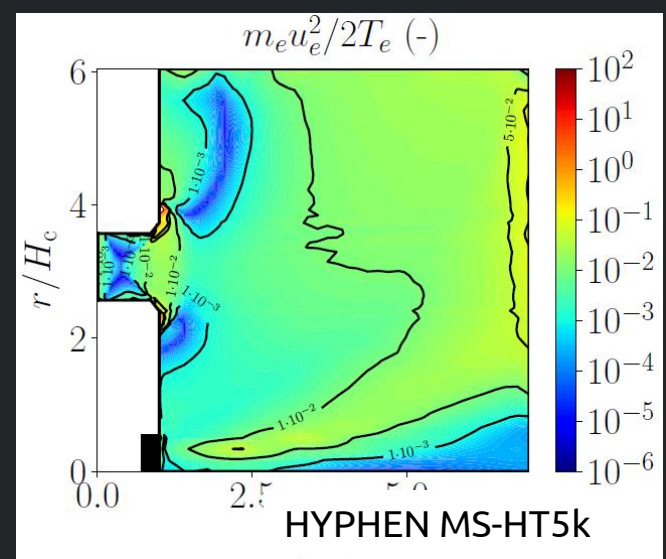
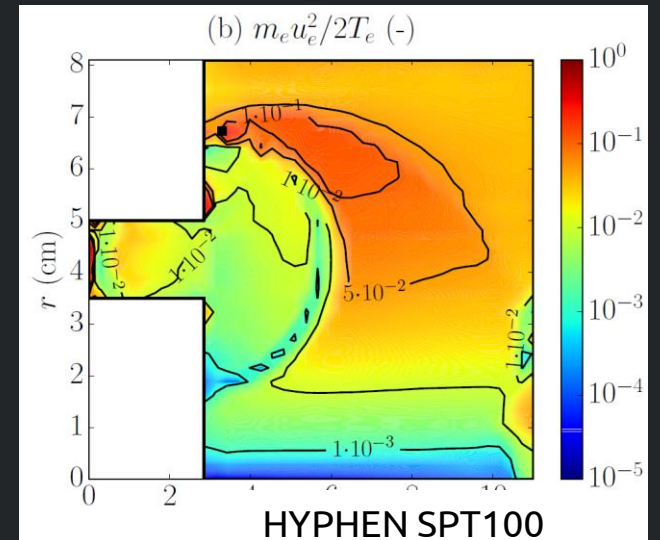
[1] Cichocki et al. *Acta Astronautica* 187, 498 (2021)

On the electron momentum equation

- Momentum vector equation:

$$m_e \nabla \cdot n_e \vec{u}_e \vec{u}_e = -\nabla \cdot \bar{\bar{P}}_e - e n_e (\vec{E} + \vec{u}_e \times \vec{B}) + \vec{F}_{col} + \vec{F}_{turb}$$

- Drift-diffusion approximation (DDA): $u_e^2 \ll c_e^2 = \frac{T_e}{m_e}$
 - $m_e \nabla \cdot n_e \vec{u}_e \vec{u}_e$ can be neglected
 - Momentum equation becomes generalized Ohm's law for \vec{J}_e
 - Simpler treatment
- DDA is satisfied in HETs except for certain operation points and localized regions.
- In HET, axisymmetric discharges $\chi = \frac{\omega_{ce}}{v_e} \gg 1$ (say $\chi \sim 10^2$)
 - $u_{\theta e} \approx \chi u_{ze} \rightarrow$ azimuthal inertia \gg axial, radial inertia



On the azimuthal inertia

(Let us take $\bar{B} = B\bar{1}_r$ and $\partial/\partial t = 0$ for illustration)

- Scalar equations for electron momentum are not of the same order

$$F_{z,inert} = +en_e u_{\theta e} B - (\nabla \cdot \bar{P}_e)_z - en_e E_z + F_{z,col} + F_{z,turb}$$

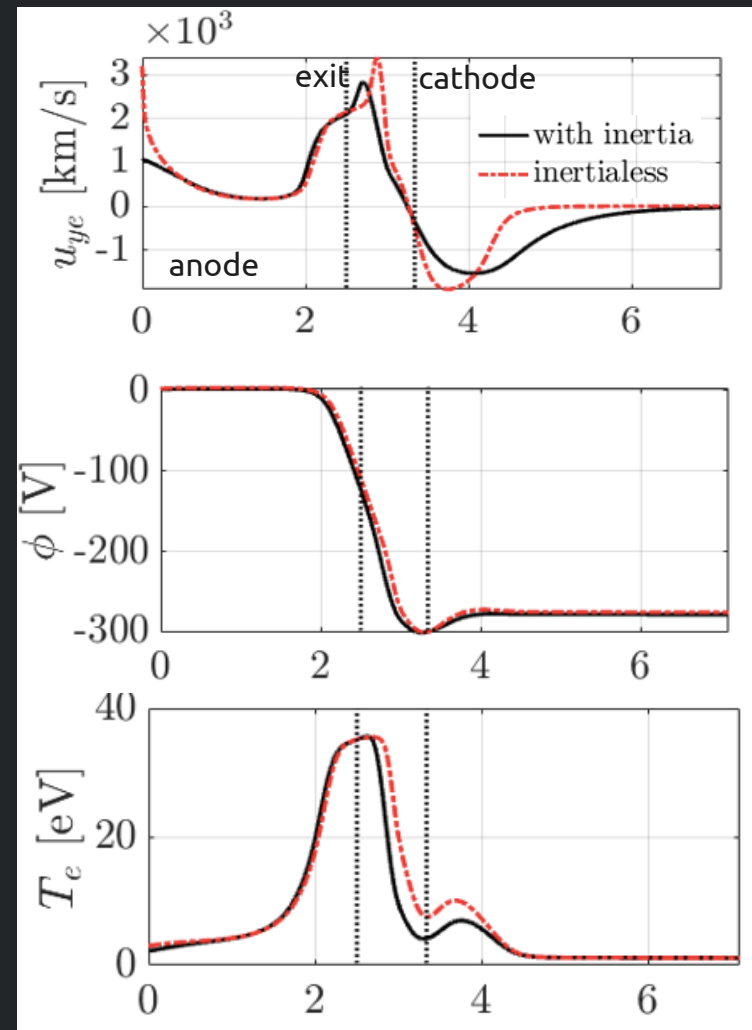
$$F_{\theta,inert} = -en_e u_{ze} B - (\nabla \cdot \bar{P}_e)_{\theta} + F_{\theta,col} + F_{\theta,turb}$$

- $(\theta\text{-equation}) \sim 10^{-2}$ ($z\text{-equation}$)
 - In θ -equation, ‘small’ contributions matter
 - They come from collisions, turbulence, inertia, gyroviscosity

- Bello et al. [2] included θ -inertia in a 1D(z) model:

$$m_e u_{ze} \frac{du_{\theta e}}{dz} = -eu_{ze} B - m_e u_{\theta e} (\nu_{col} + \nu_{turb})$$

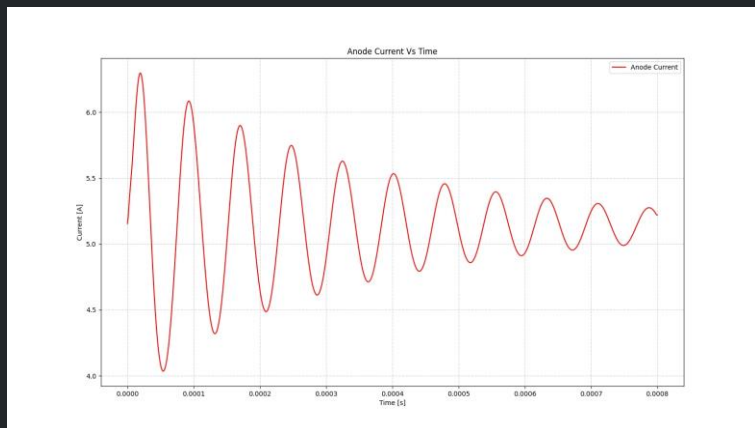
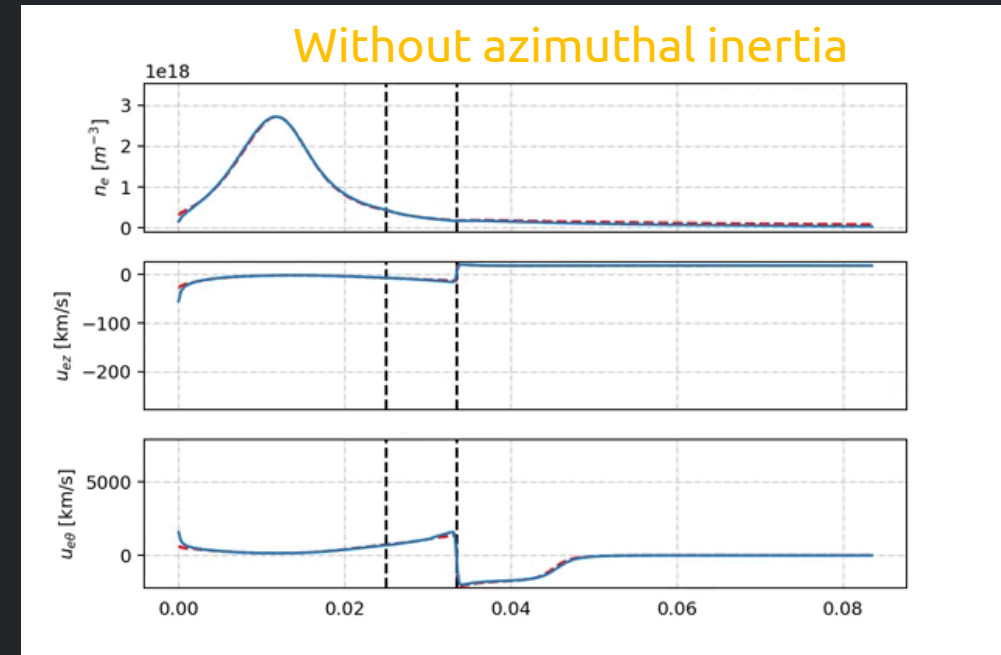
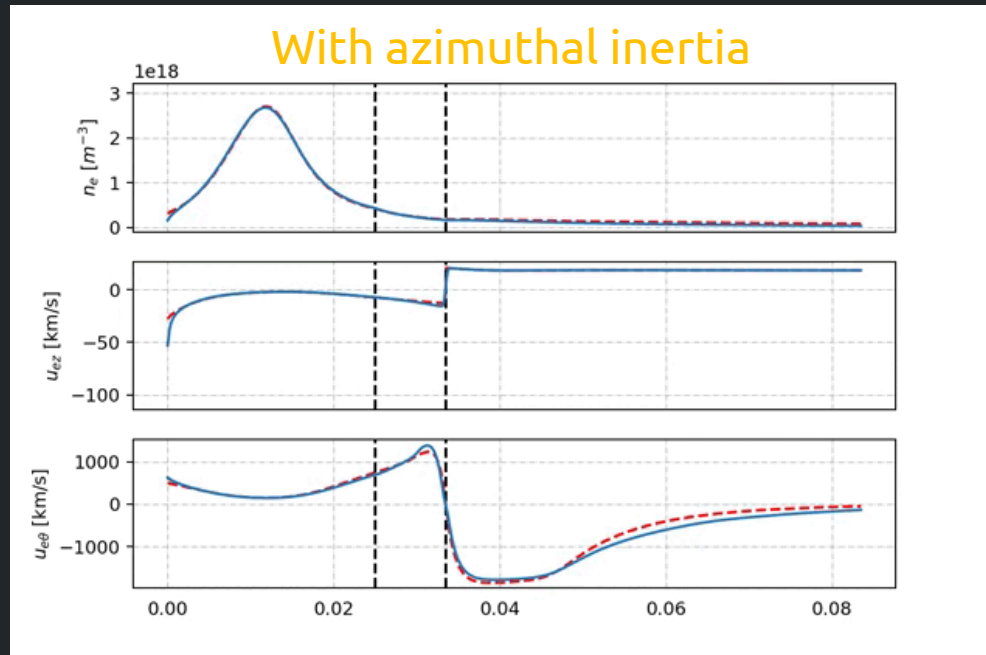
- θ - inertia is important: (1) near the anode if n_e is very low, (2) around the neutralizer, (3) around the maximum E-field, (4) in the far plume
- θ - inertia upper- bounds $u_{\theta e} \leq O(c_e)$
- In 2D(z,r) models, including θ -inertia is expensive [3]
 - In HYPHEN we opted for including a velocity limiter, e.g. $u_{\theta e} \leq 2c_e$



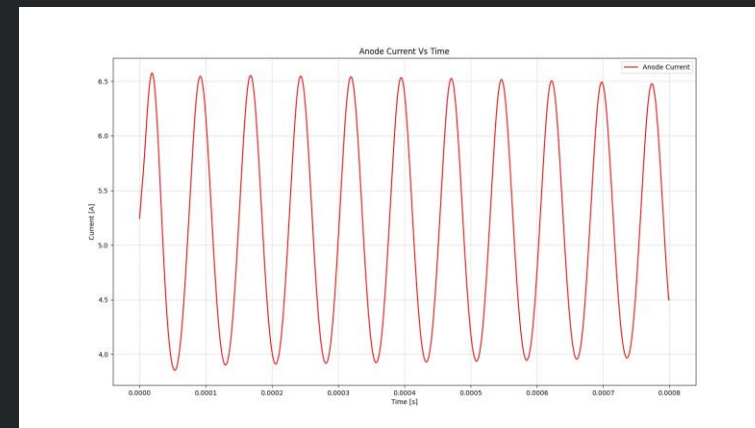
[2] Bello et al., SP2020 00133 (2021) and ongoing work

[3] Perales-Díaz et al. PSS 30, 105023 (2021)

Azimuthal inertia and breathing mode



[4] Poli et al., ongoing work



On the pressure tensor

- Fluid models generally use $\bar{\bar{P}}_e = p_e \bar{I}$ instead of $\bar{\bar{P}}_e \simeq [p_{\parallel e} \bar{1}_{\parallel} \bar{1}_{\parallel} + p_{\perp e} (\bar{I} - \bar{1}_{\parallel} \bar{1}_{\parallel})] + \bar{\bar{P}}_{GV,e}$
- $p_{\parallel e} \neq p_{\perp e}$ introduces **macroscopic magnetic mirror** effects, $(p_{\parallel e} - p_{\perp e}) \nabla \ln B$, in momentum equation
 - $p_{\parallel e} \neq p_{\perp e}$ requires to use 2 energy equations (for $T_{\parallel e}$ and $T_{\perp e}$) + 2 (uncertain) closure laws for \bar{q}_e 's
 - 1D kinetic models provide some results on these issues
- **Gyroviscous** (off-diagonal) part. We expect $|\bar{\bar{P}}_{GV,e}| \ll p_{\parallel e}, p_{\perp e}$
 - But still $(\nabla \cdot \bar{\bar{P}}_e)_{\theta} = (\nabla \cdot \bar{\bar{P}}_{GV,e})_{\theta}$ and $(\nabla \cdot \bar{\bar{P}}_{GV,e})_{\theta} \leq O(F_{\theta,inert})$
 - Gyroviscous force can matter in θ -equation: $F_{\theta,inert} = -en_e u_{ze} B - (\nabla \cdot \bar{\bar{P}}_{GV,e})_{\theta} + F_{\theta,col} + F_{\theta,turb}$
- Two recent results on this:
 - Bello [2], with 1D(z) fluid model, found that $\frac{(\nabla \cdot \bar{\bar{P}}_{GV,e})_{\theta}}{(m_e \nabla \cdot n_e \vec{u}_e \vec{u}_e)_{\theta}}$ small
 - This is fortunate since $(\nabla \cdot \bar{\bar{P}}_{GV,e})_{\theta}$ introduces 2nd order derivatives
 - Marín [5], with a 1D(r) kinetic model, found non-negligible radial effects of $(\nabla \cdot \bar{\bar{P}}_{GV,e})_{\theta}$

[5] Marín et al. *PSST30*, 115011 (2021)

On the energy equation

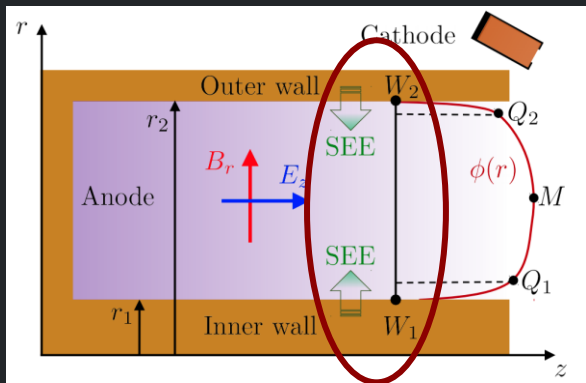
- Total energy equation:
$$\nabla \cdot \left[\left(\frac{m_e u_e^2}{2} + \frac{3}{2} T_e \right) n_e \vec{u}_e + \bar{\vec{P}}_e \cdot \vec{u}_e + \vec{q}_e \right] = \vec{J}_e \cdot \vec{E} + Q_{col} + Q_{turb}$$
- Using $\bar{\vec{P}}_e = p_e \bar{I}$:
$$\nabla \cdot \left[\left(\frac{m_e u_e^2}{2} + \frac{5}{2} T_e \right) n_e \vec{u}_e + \vec{q}_e \right] = \vec{J}_e \cdot \vec{E} + Q_{col} + Q_{turb}$$
- Internal energy equation:
$$\nabla \cdot \left[\frac{5}{2} T_e n_e \vec{u}_e + \vec{q}_e \right] = \vec{u}_e \cdot \nabla p_e + Q_{col} - (\vec{F}_{col} \cdot \vec{u}_e + \vec{F}_{turb} \cdot \vec{u}_e) + Q_{turb}$$
 - $Q_{col} (< 0) \approx$ inelastic losses; $(-\vec{F}_{col} - \vec{F}_{turb}) \cdot \vec{u}_e \approx m_e u_{\theta e}^2 n_e (\nu_{col} + \nu_{turb})$ = Joule heating
- Open question (besides using a more genera, anisotropic $\bar{\vec{P}}_e$):
 - Is $Q_{turb} \sim \langle J'_{\theta e} E'_{\theta} \rangle$ negligible? Fluid models assume this.
- Heat flux closure law. The DDA yields $\bar{q}_e = -\bar{\vec{K}}_e \cdot \nabla T_e$, $\bar{\vec{K}}_e = (5T_e/2e^2)\bar{\sigma}_e$ = thermal conductivity tensor.
 - Evidences in divertors [6], laser-plasma [7], EP magnetic nozzles [8,9] that this diffusive law does not hold along magnetic lines (for weakly-collisional, magnetized electrons)

[6] Stangeby et al. Nucl. Fusion 50, 125003 (2010); [7] Malone PRL 34, 721 (1975); [8] Ahedo et al. PSST 29, 045017 (2020); [9] Zhou et al. PSST 30, 045009 (2021)

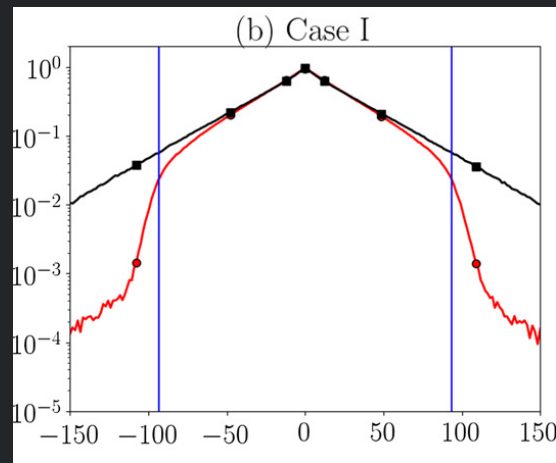
Kinetic validation of fluid model

- The way to validate the macroscopic momentum and energy equations is to construct them from kinetic solutions
- We have done this with
 - a 1D (radial) model of a HET discharge, Marín at al. [5]
 - 1D (paraxial) models of a magnetic nozzle, Ahedo, Zhou et al. [8,9]

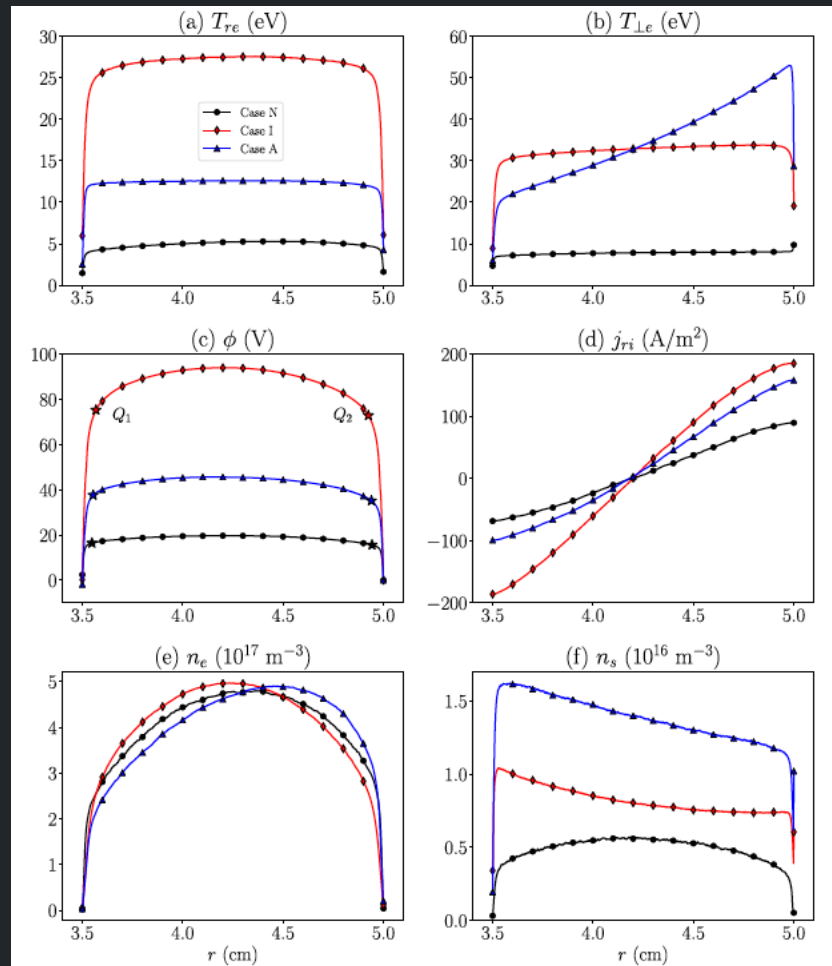
1Dr kinetic model [5]



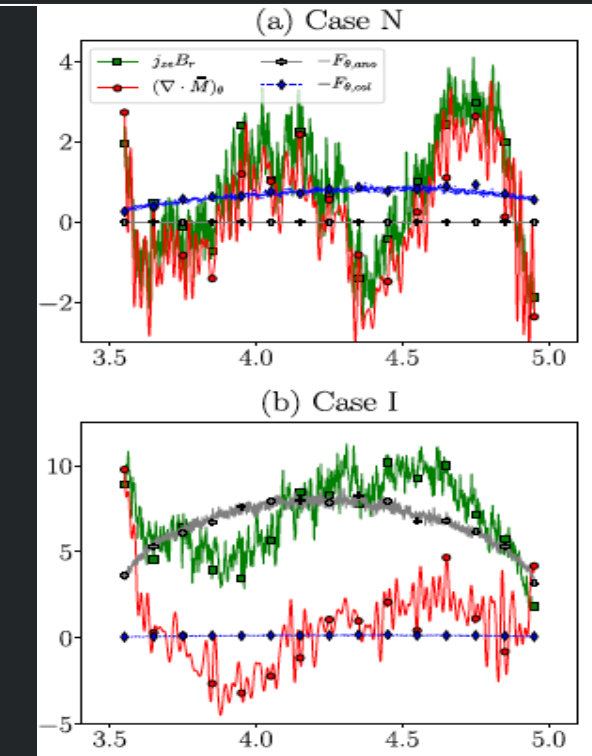
1) The region we solve



2) The VDF shows wall depletion in r-direction (affects plasma-wall parameters)



3) Profiles of macroscopic magnitudes: T_e anisotropy; cylindrical asymmetries; dependence on anomalous diffusion model

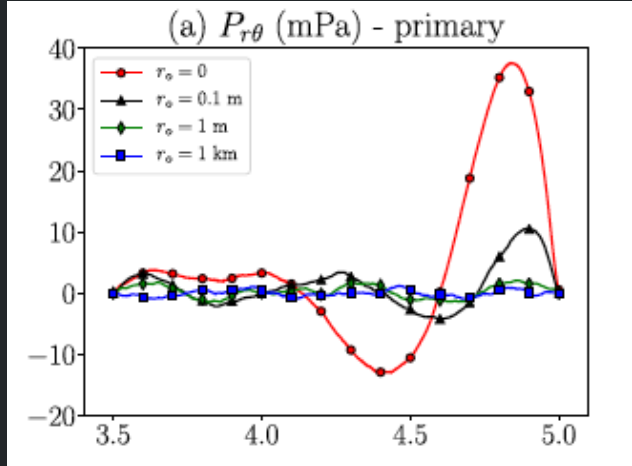


$$j_{ze} = -en_e u_{ze} = \frac{1}{B_r} [(\nabla \cdot \bar{M})_\theta - F_{\theta,col} - F_{\theta,ano}] .$$

4) Gyroviscosity $P_{r\theta}$ matters and affects $j_{ze}(r)$, which presents near-wall conductivity features

1Dr kinetic model [5]

- Electron energy balance
- Flux of electron energy
- Fluid representation

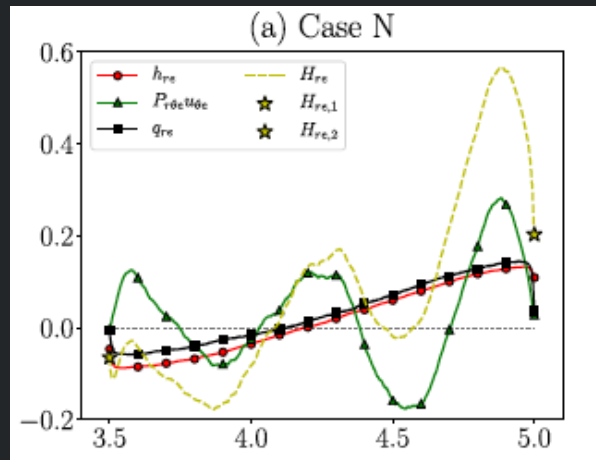


5) Gyroviscosity effects are much weaker in planar channel

$$\nabla \cdot \mathbf{H}_e \equiv \frac{1}{r} \frac{d(rH_{re})}{dr} = \mathcal{P}'_{\text{col}} + \mathcal{P}'_{E_z} + \mathcal{P}'_{E_r},$$

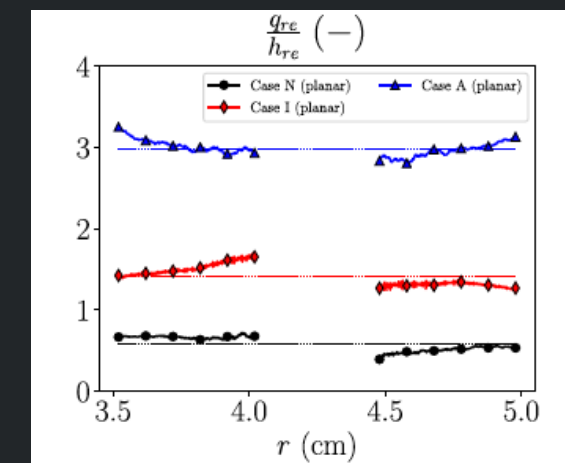
$$\mathbf{H}_e = \int (m_e \mathbf{v}^2 / 2) \mathbf{v} f_e(\mathbf{v}) d\mathbf{v}$$

$$\mathbf{H}_e = \left(\frac{1}{2} m_e u_e^2 n_e + \frac{1}{2} \text{trace} \bar{\bar{P}} \right) \mathbf{u}_e + \bar{\bar{P}} \cdot \mathbf{u}_e + \mathbf{q}_e,$$



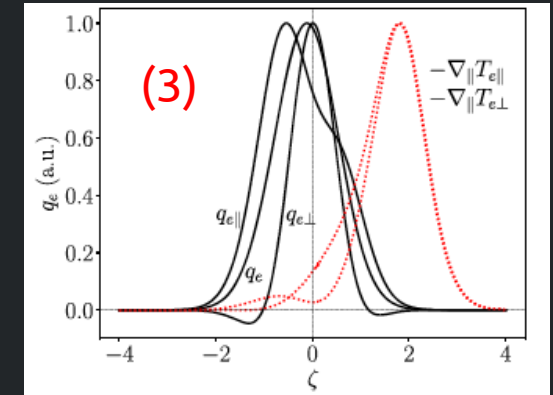
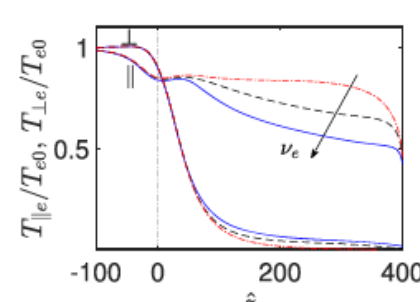
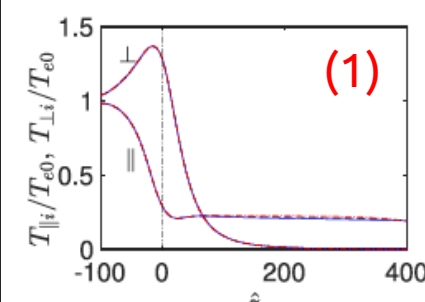
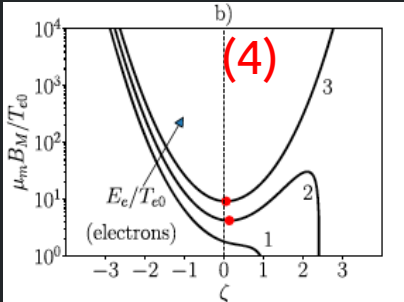
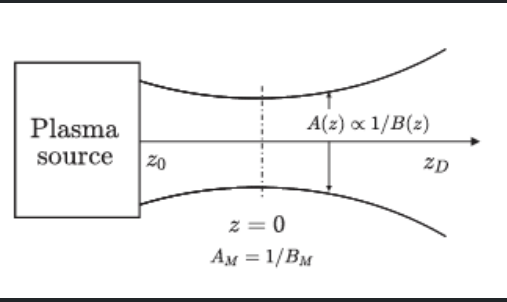
6) Dominant fluid terms for energy transport

$$H_{re} \simeq h_{re} + q_{re} + P_{r\theta} u_{\theta e},$$



7) Heat flux \propto enthalpy flux (instead of $\propto dT_e/dr$)

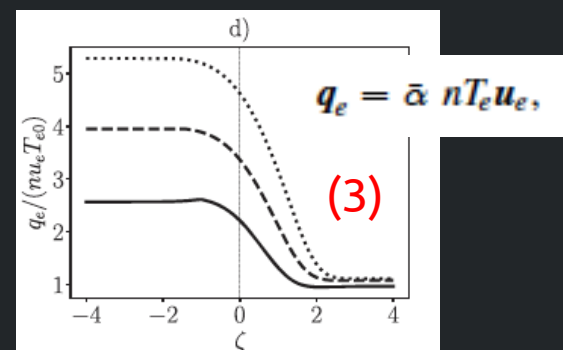
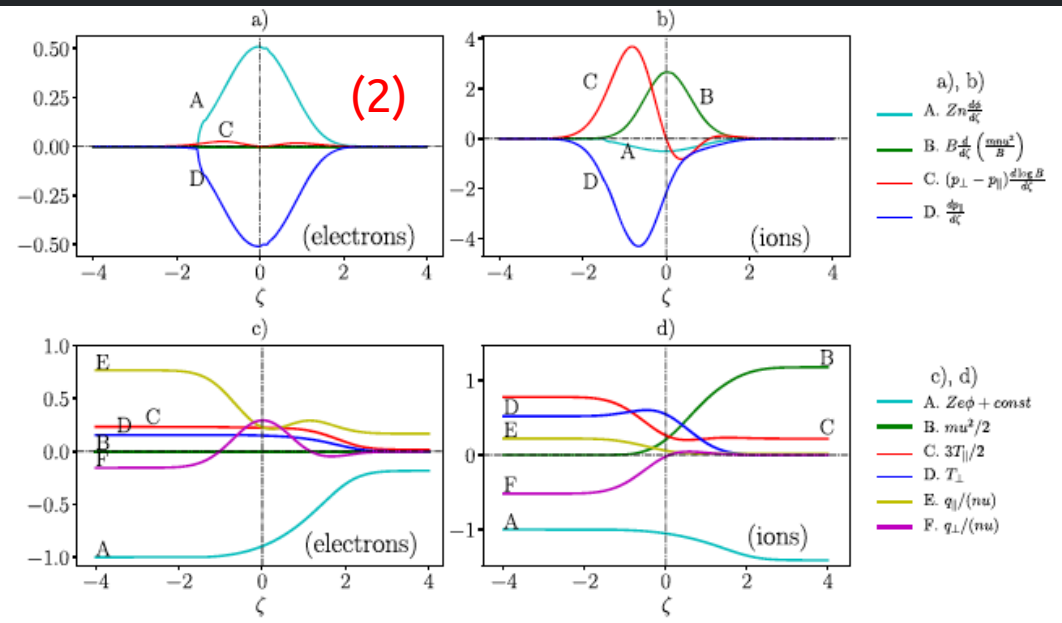
Paraxial magnetic nozzle kinetic model [8,9]



$$m_\alpha n_\alpha u_\alpha \frac{\partial u_\alpha}{\partial z} + Z_\alpha e n_\alpha \frac{\partial \phi}{\partial z} + \frac{\partial p_{||\alpha}}{\partial z} + (p_{\perp\alpha} - p_{||\alpha}) \frac{d \ln B}{dz} = 0,$$

$$\left(Z_\alpha e \phi + \frac{m_\alpha}{2} u_\alpha^2 + h_\alpha + \frac{q_\alpha}{n_\alpha u_\alpha} \right) n_\alpha u_\alpha A = \text{const.}$$

Fully magnetized ions & electrons



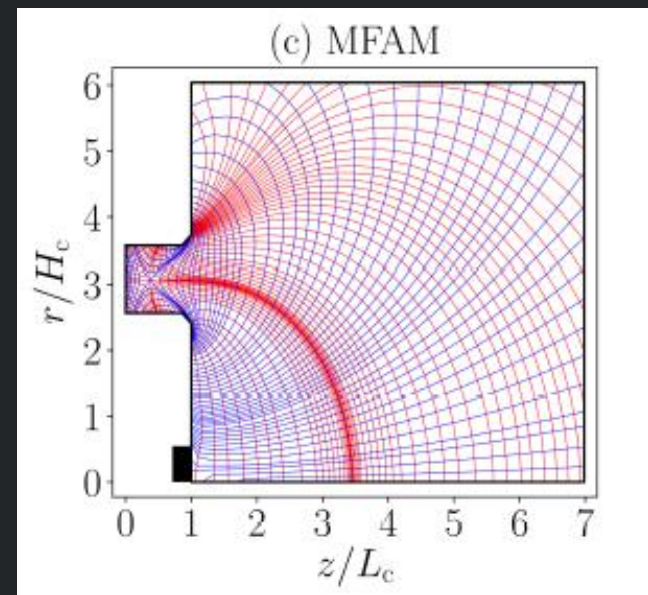
(4)

$$T_e \propto n^{\bar{\gamma}-1} \quad \text{with} \quad \bar{\gamma} = \frac{5 + 2\bar{\alpha}}{3 + 2\bar{\alpha}},$$

- 1) T_i develops **large anisotropy** on conv. side; T_e mainly in div. side
- 2) The **macroscopic B-mirror effect** is more important for ions than electrons
- 3) Electrons: **no Fourier's law** heat flux \propto enthalpy flux (roug.)
- 4) Instead of a monoatomic gas, electrons behave more as **mixture of 3 subpopulations** with an average $\gamma \sim 1.2 - 1.3$

Conclusions

- A physical macroscopic model of turbulent transport continues to be the most serious limitation for e-fluid models of HET and EPTs
- Other uncertainties are on: the heat flux closure and boundary conditions(BCs)
- Finally, azimuthal inertia and pressure tensor effects are not to be ignored.
- Beyond physics there are important numerical challenges with 2D e- fluid models
- The large anisotropy of $\bar{\sigma}_e$ and \bar{K}_e
 - Spurious numerical diffusion can ruin solutions in regular Cartesian meshes
 - Hall2De and HYPHEN opted for using a MFAM (magnetic field aligned mesh) [10]
 - MFAM avoids numerical diff. but involves complex numerical algorithms [11,12]
 - Is it worth working on very irregular MFAM or should we develop diffusion-free algorithms on regular meshes? [13]
- Addressing the infinite plume expansion with a finite domain
 - Issue arises because of nonlocal kinetic effects
 - Downstream BCs on finite plume are not obvious
 - Simulated thruster performances affected by plume size [14]



HPT case	F [mN]	η_F	η_{ene}	η_{div}	η_{disp}
Nominal case	7.64	0.097	0.178	0.74	0.74
Double plume	8.69	0.126	0.178	0.85	0.83

[10] Perez et al., Appl. Sci. 6, 354 (2016)

[11] Zhou et al. PSST28, 115004 (2019)

[12] Perales et al. JAP (accepted)

[13] Modesti et al. ongoing work

[14] Zhou et al. ,PSST (submitted)

Acknowledgments

This presentation is based on work supported by:

- The PROMETEO project, funded by the Comunidad de Madrid, under Grant reference Y2018/NMT-4750 PROMETEO-CM.
- The HIPATIA project, funded by the European Union's Horizon 2020 Research and Innovation Program, under Grant Agreement number 870542.
- The CHEOPS LOW POWER project, funded by the European Union's Horizon 2020 Research and Innovation Program, under Grant Agreement number 101004331.



THRUSTME



The origin of the breathing mode in Hall thrusters and its stabilization



Trevor Lafleur

ThrustMe, 91370 Verrières-le-Buisson, France

Pascal Chabert and Anne Bourdon

LPP, Ecole Polytechnique, France

- **Breathing mode:** A low-frequency (~ 10 kHz) axial oscillation observed in Hall thrusters
- **“Classical” explanation:** Simple predator-prey interaction

$$\frac{dn_g}{dt} + \frac{n_g v_g}{L} = -n_e n_g K_{iz}$$

$$\frac{dn_i}{dt} + \frac{n_i v_i}{L} = n_e n_g K_{iz}$$

Perturbation analysis gives a real frequency in the kHz range

- More accurate analysis including injection mass flow rate

$$\frac{dn_g}{dt} + \frac{(n_g - n_{g,inj}) v_g}{L} = -n_e n_g K_{iz}$$

$$\frac{dn_i}{dt} + \frac{n_i v_i}{L} = n_e n_g K_{iz}$$

Unconditionally stable ($\gamma < 0$)

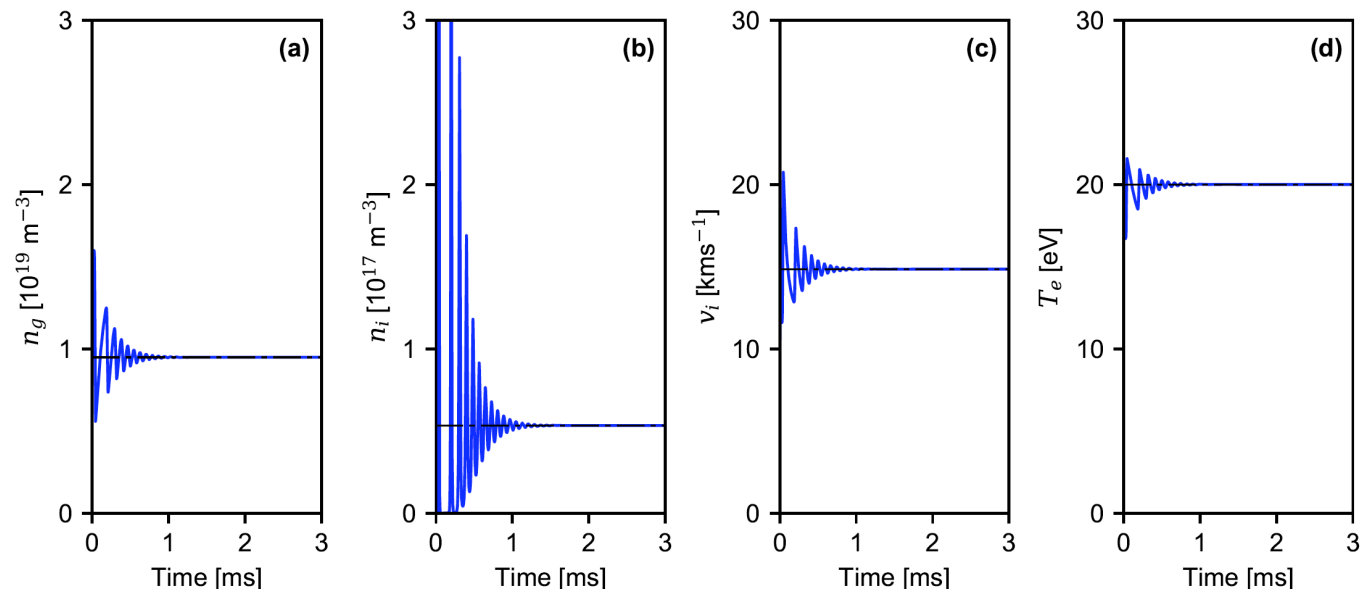
$$\frac{dn_g}{dt} + \frac{(n_g - n_{g,inj}) v_g}{L} = -n_e n_g K_{iz}$$

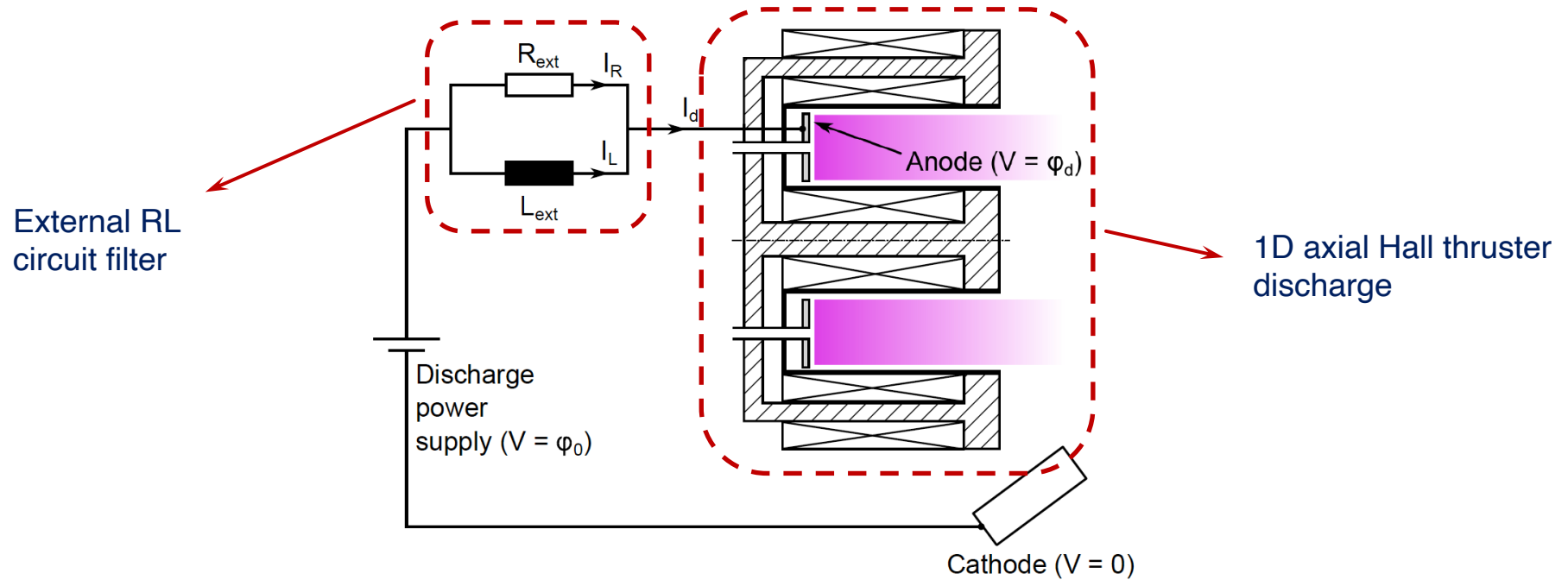
$$\frac{dn_i}{dt} + \frac{n_i v_i}{L} = n_e n_g K_{iz}$$

$$\frac{d}{dt} (m_i n_i v_i) + \frac{m_i n_i v_i^2}{L} = e n_i E - m_i n_i v_i \nu_{iw}$$

$$\frac{d}{dt} \left(\frac{3}{2} n_e T_e \right) + \frac{5}{2} \frac{n_e v_e T_e}{L} = -n_e v_e E - n_e \nu_{ew} \varepsilon_{ew} - n_e n_g K_{iz} \varepsilon_{iz} \chi$$

Stable, so what causes the breathing mode?





$$\frac{\partial n_g}{\partial t} + v_g \frac{\partial n_g}{\partial x} = -n_e n_g K_{iz} + n_i \nu_{iw}$$

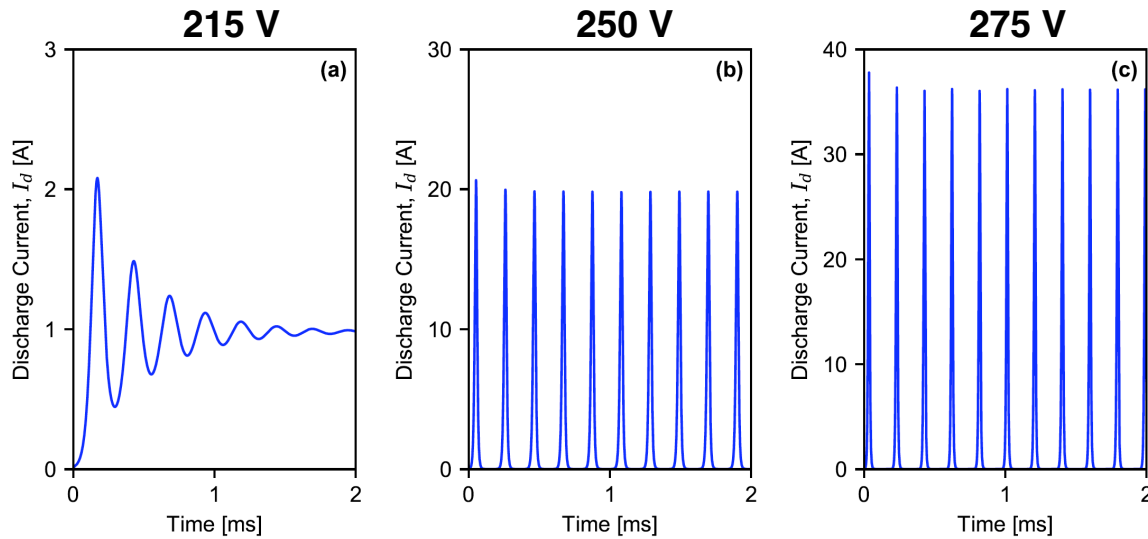
$$\frac{\partial n_i}{\partial t} + \frac{\partial}{\partial x} (n_i v_i) = n_e n_g K_{iz} - n_i \nu_{iw}$$

$$\frac{\partial}{\partial t} (m_i n_i v_i) + \frac{\partial}{\partial x} (m_i n_i v_i^2) = e n_i E_x + m_i n_i n_g K_{iz} v_g - m_i n_i \nu_{iw} v_i$$

$$\frac{\partial}{\partial t} \left(\frac{3}{2} n_e T_e \right) + \frac{\partial}{\partial x} \left(\frac{5}{2} n_e v_{ex} T_e \right) = -n_e v_{ex} E_x - n_e \nu_{ew} \varepsilon_w - n_e n_g K_{iz} \varepsilon_{iz} \chi$$

1D extensions of
the previous 0D
equations

- **Reference case (circuit off):** Breathing mode oscillations observed

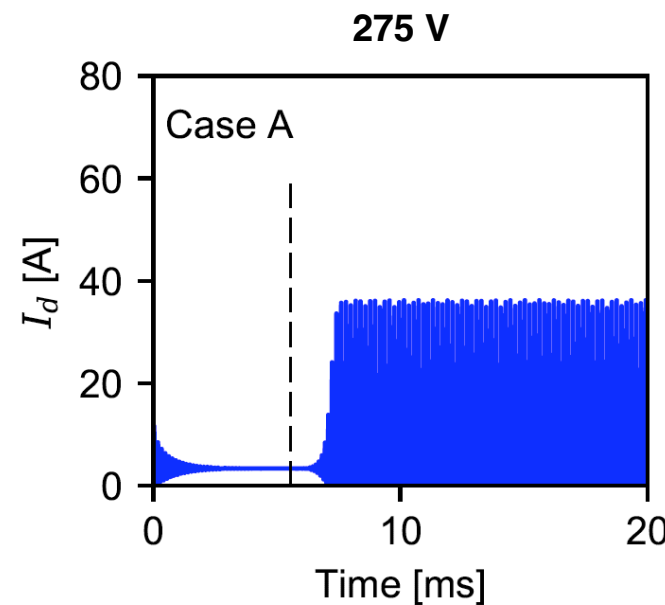
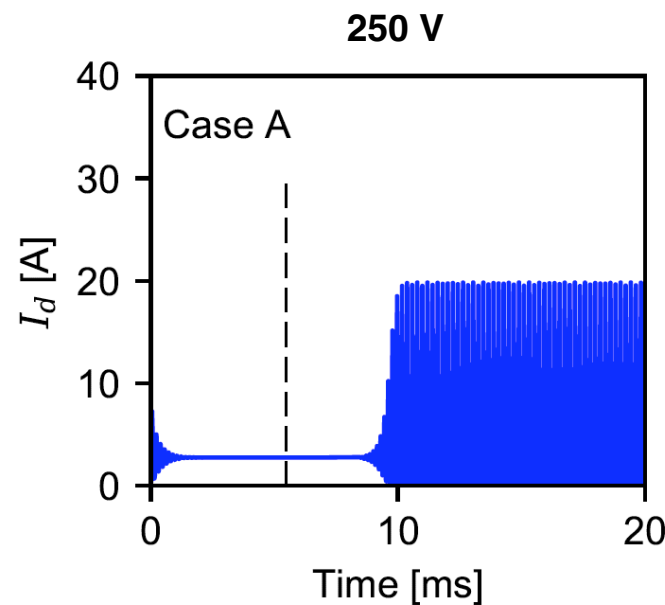
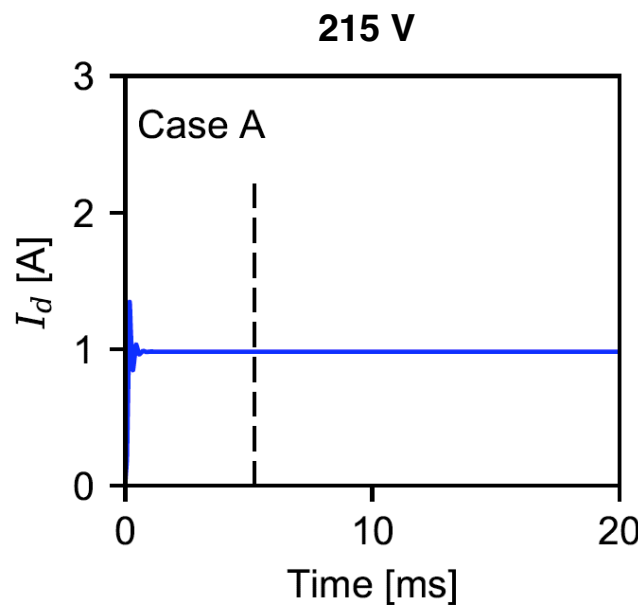


- **Test cases:** Circuit on to obtain a stationary state, then circuit turned off to study system evolution for different cases

Case A	No change to plasma equations
Case B	v_i profile fixed in time
Case C	v_i and T_e profiles fixed in time
Case D	p_{abs} profile fixed in time

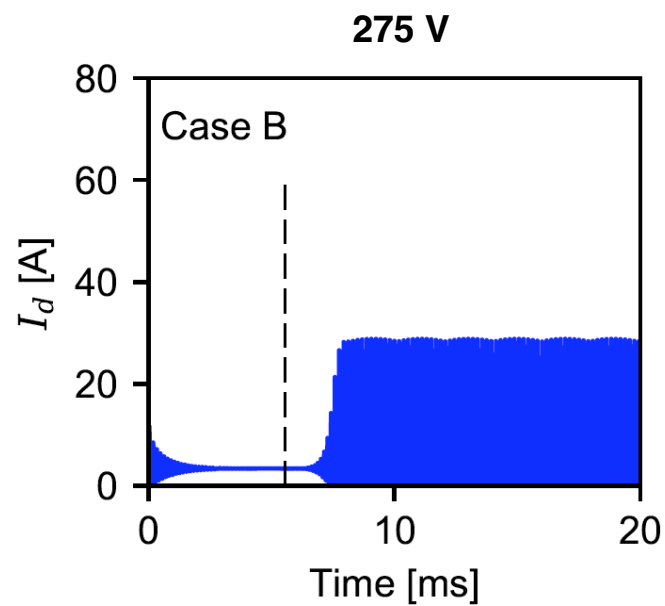
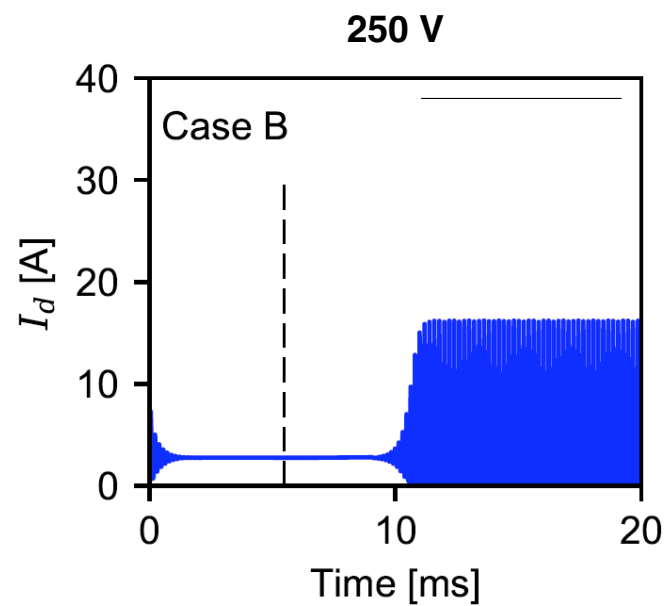
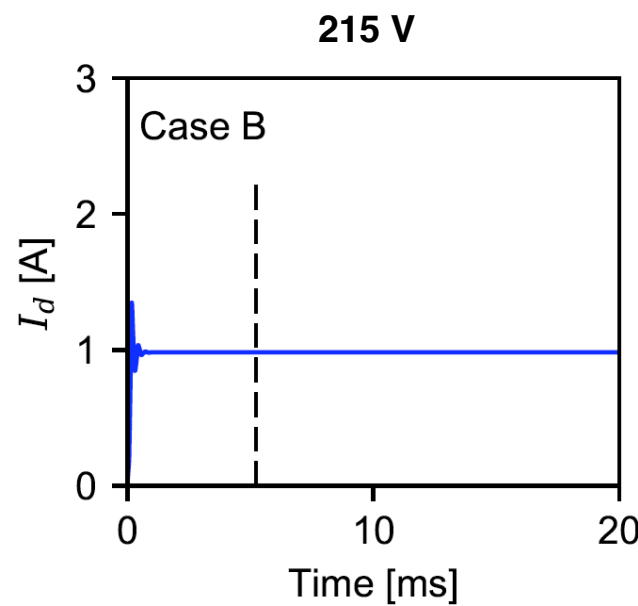
Breathing mode trigger (case A)

- **Case A:** No change to the plasma equations
- Breathing mode reforms after the circuit is turned off for higher voltages



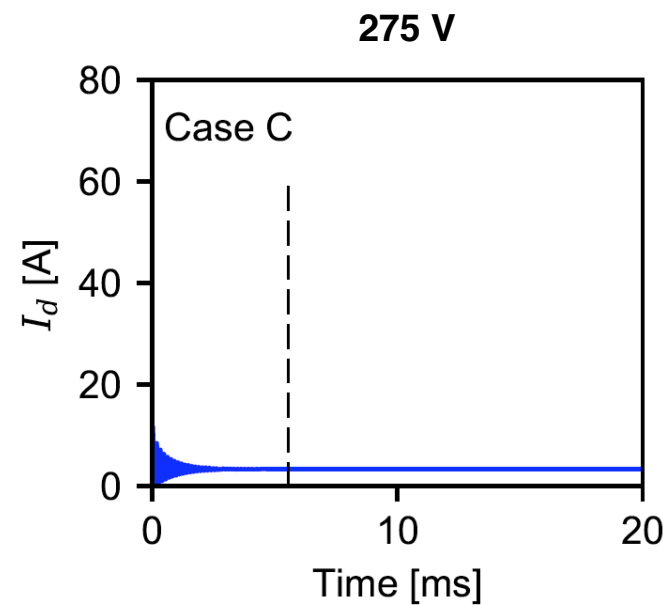
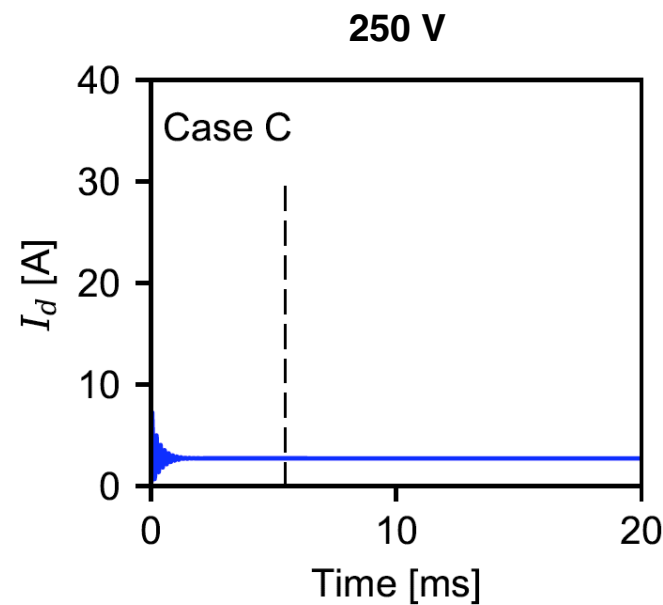
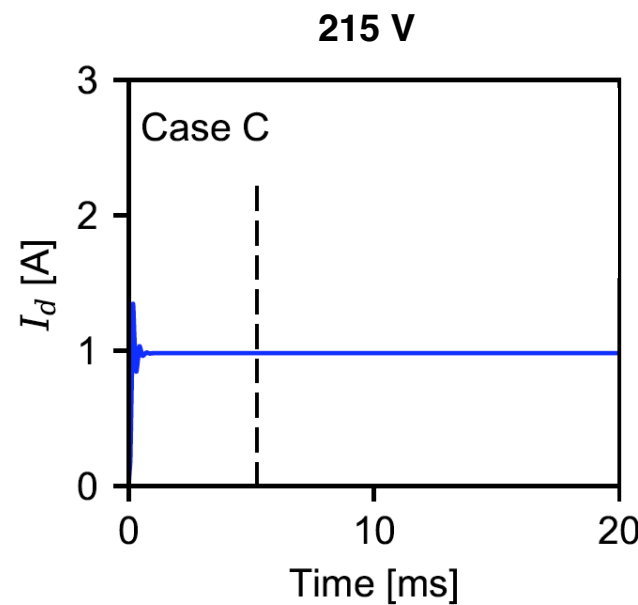
Breathing mode trigger (case B)

- **Case B:** v_i profile fixed in time
- Breathing mode again reforms after the circuit is turned off for higher voltages



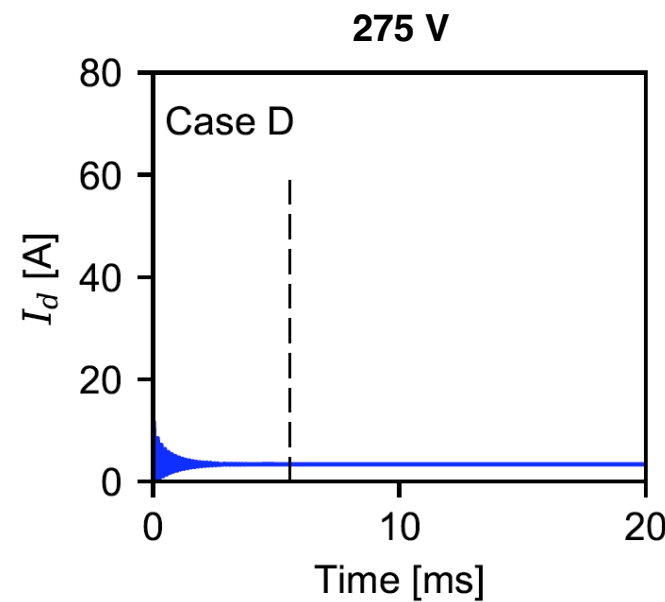
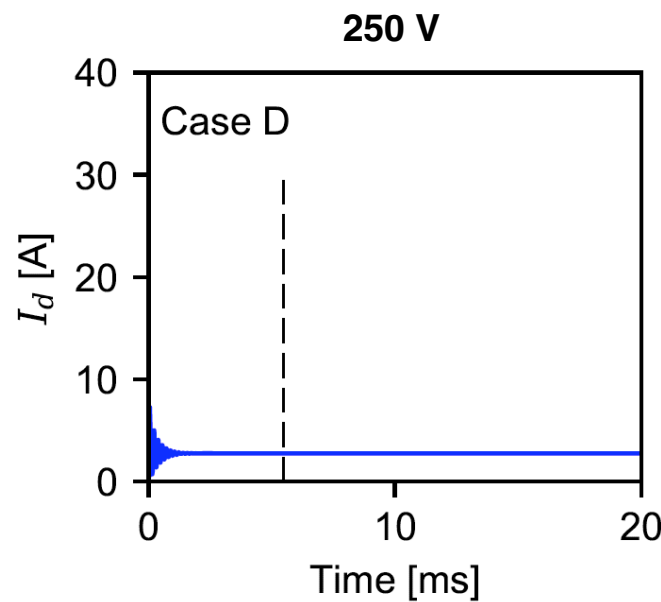
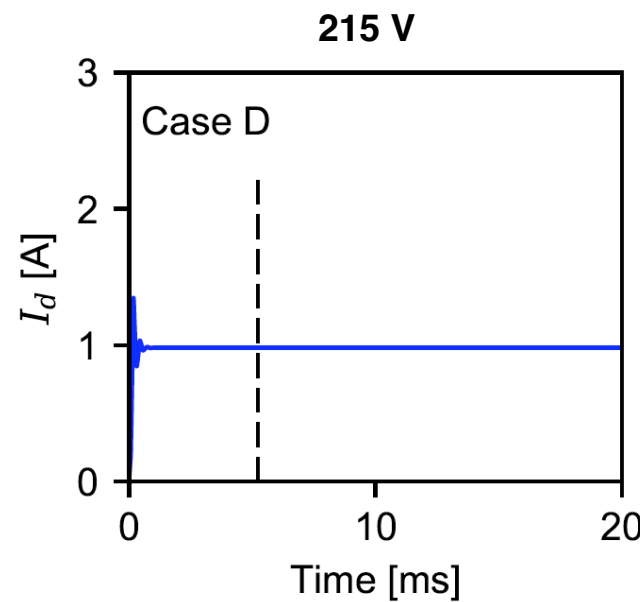
Breathing mode trigger (case C)

- **Case C:** v_i and T_e profiles fixed in time
- Breathing mode no longer reforms and system remains stable



Breathing mode trigger (case D)

- **Case D:** p_{abs} profile fixed in time
- Breathing mode again no longer reforms and system remains stable



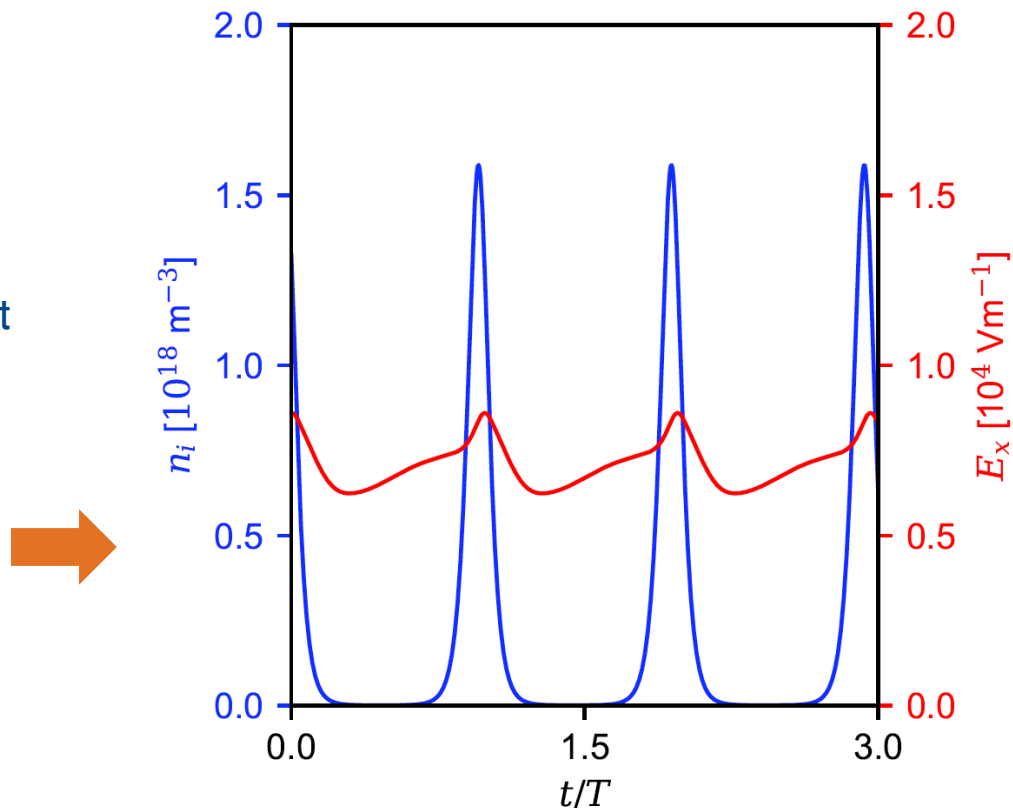
The electron energy equation, and particularly the power absorption term, is key to the formation of the breathing mode

Nonlinearity in the electron power absorption

- The electric field is given by

$$E \approx \frac{\phi_d + \int_0^L dx \frac{v_i}{\mu}}{n_i \mu \int_0^L dx \frac{1}{n_i \mu}} - \frac{v_i}{\mu}$$

- In 0D:** The electric field is effectively constant and independent of the plasma density
- In 1D:** The electric field increases in some regions when the plasma density increase
- If the electric field increases, the power absorption increases nonlinearly

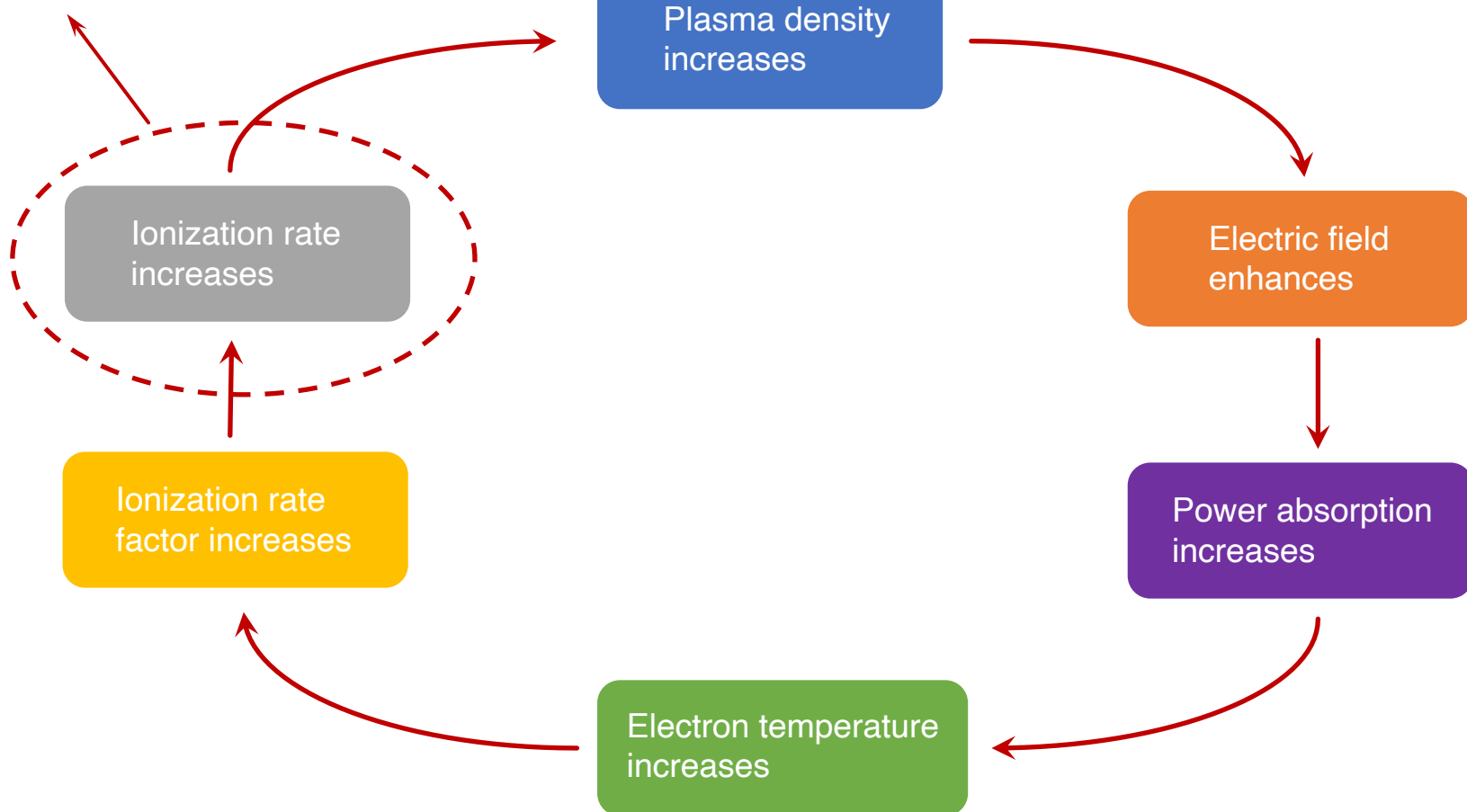


$$p_{abs} = -n_e v_e E \approx n_e \mu E^2$$

Positive feedback loop

10/11

Neutral depletion
eventually limits growth
and breaks the cycle



- The breathing mode is an ionization instability associated with nonlinearity in the electron power absorption
- A positive feedback mechanism exists where the electric field is enhanced as the plasma density increases
- Significant neutral depletion is needed before plasma growth can be halted
- By appropriately varying the discharge voltage, the breathing mode can be stabilized

$$E \approx \frac{\phi_d + \int_0^L dx \frac{v_i}{\mu}}{n_i \mu \int_0^L dx \frac{1}{n_i \mu}} - \frac{v_i}{\mu}$$

Practical need for modeling breathing mode

Benjamin Jorns



**ExB Plasmas
Workshop
2022**

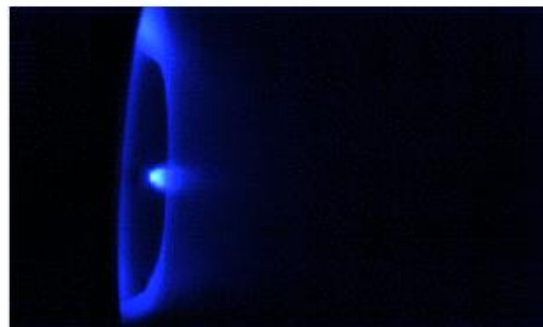
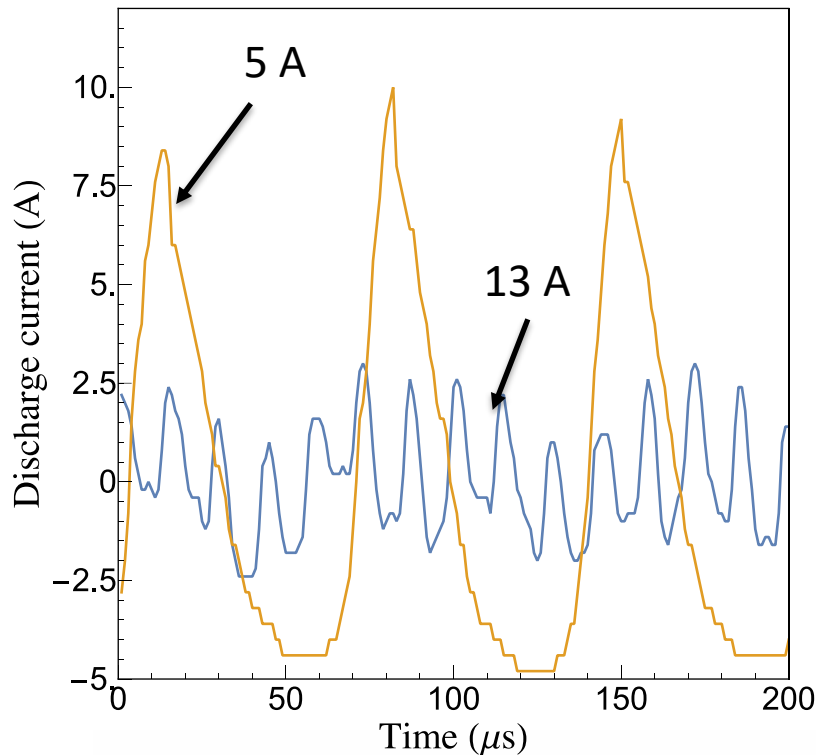
Madrid, online event



Practical need for modeling breathing mode

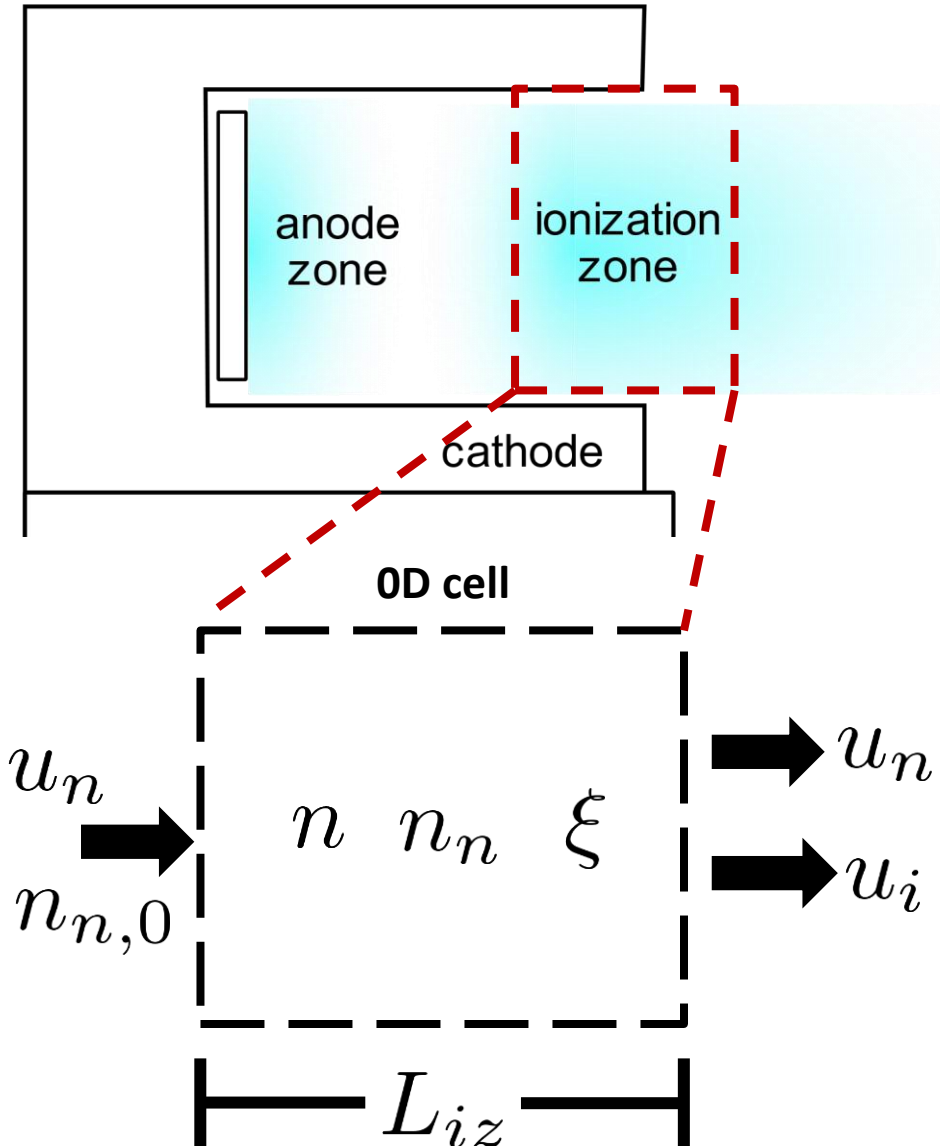
- **Breathing mode is not inherently bad:** all Hall thrusters including flight qualified devices exhibit breathing mode. In some cases, discharge oscillations exceed 100% of DC, and this is still considered acceptable.
- **Mode transitions in breathing mode can be a problem if oscillations becomes “too” unstable**
 - Lifetime limitation due to net average shift of acceleration zone downstream
 - Problem for power electronics if oscillations become too large
- **Undesirable mode transitions can occur when extending technology to new operational regime:** e.g. high specific impulse at low power or when transitioning from ground to flight
- **Modeling/understanding necessary to predict and mitigate transition in these problematic cases**

Example of mode transition for 600 V thruster





Reduced fidelity modeling of breathing mode



- Common approach historically has been based on 0D model of discharge chamber*
- Continuity equations for spatially-averaged neutral and ion population sufficient to show oscillations commensurate with breathing mode frequency

Ion continuity

$$\frac{dn}{dt} = \xi_{iz} n n_n - n \frac{u_i}{L}$$

Neutral continuity

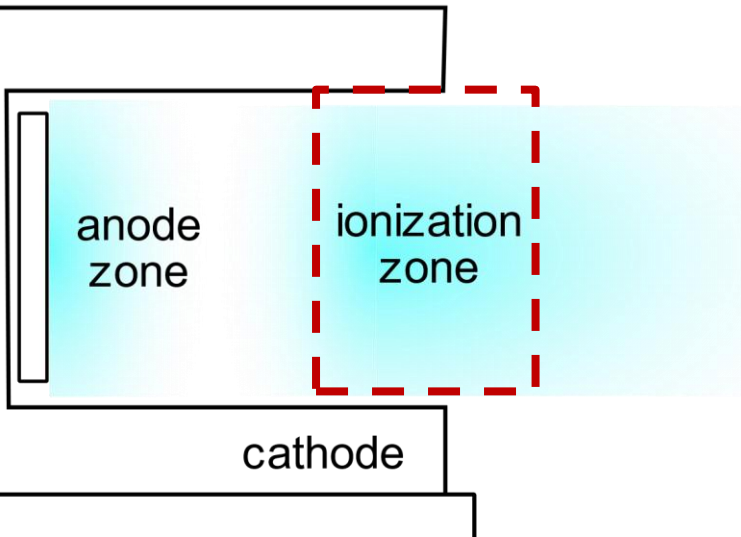
$$\frac{dn_n}{dt} = -\xi_{iz} n n_n + (n_{n,0} - n_n) \frac{u_n}{L}$$

Frequency scaling

$$\omega = \frac{\sqrt{u_i u_n}}{L_{iz}}$$

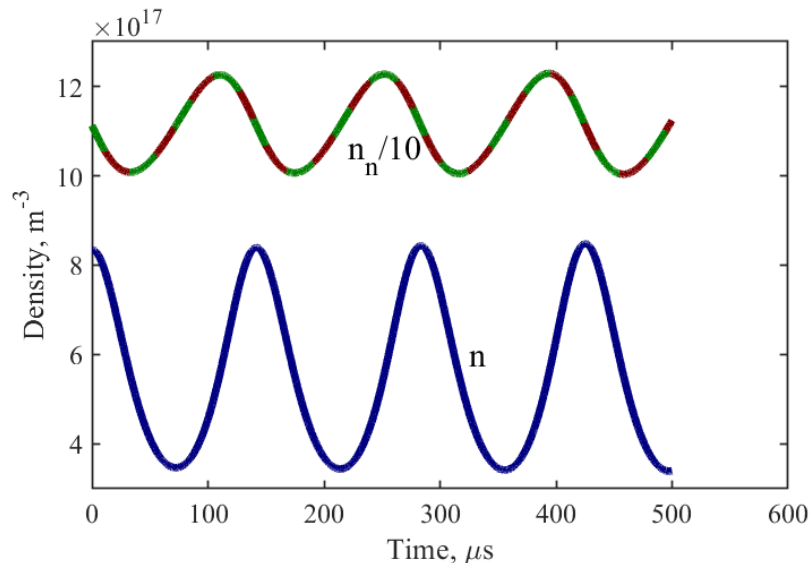


Reduced fidelity modeling of breathing mode

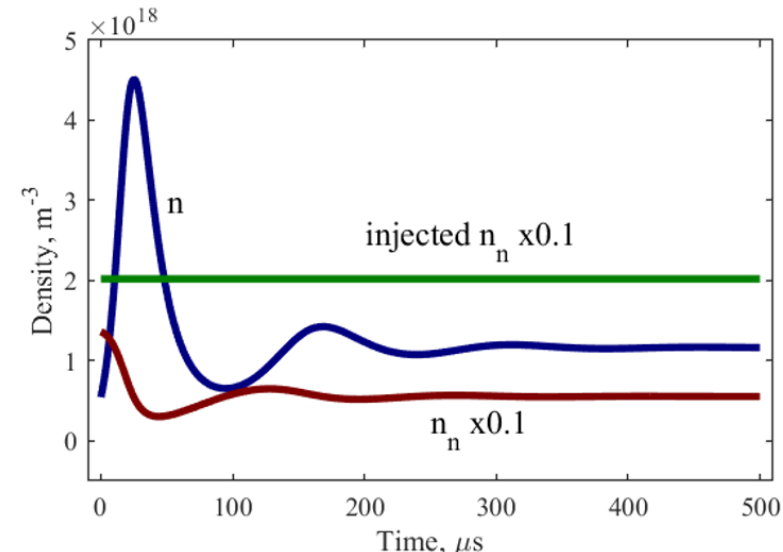


- Assuming two equation, 0D model, can show that breathing mode is a natural resonance of the thruster
- Self-consistent solution shows that predicted breathing mode from this model solution is **universally damped**
- Need to identify a model for the energy source for driving the mode unstable. Otherwise, models cannot predict onset or mode transitions**

Example of numerical solution w/o neutral injection



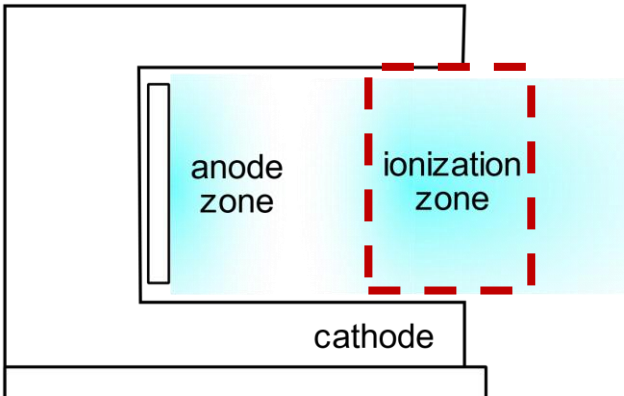
Example of numerical solution w/ neutral injection





Reduced fidelity modeling of breathing mode

In attempt to predict onset criterion analytically, additional fidelity added to represent possible energy sources. Examples include

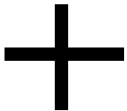


Ion continuity

$$\frac{dn}{dt} = \xi_{iz} n n_n - n \frac{u_i}{L}$$

Neutral continuity

$$\frac{dn_n}{dt} = -\xi_{iz} n n_n + (n_{n,0} - n_n) \frac{u_n}{L}$$



Adding additional 0D governing equations for momentum and energy

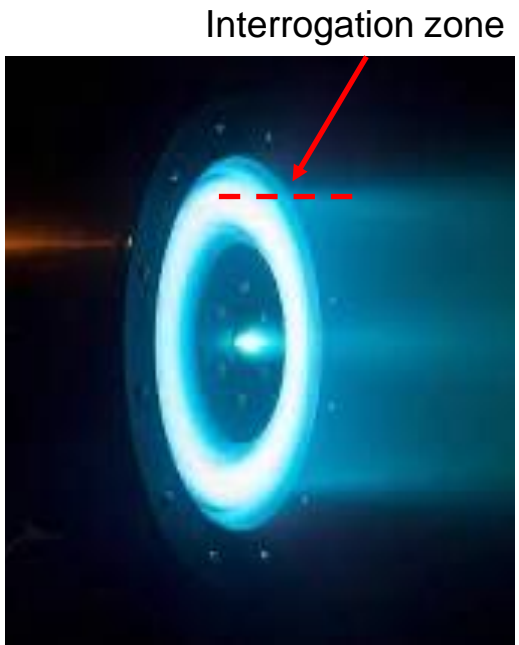
*K. Hara, M. Sekerak, I. Boyd, and A. Gallimore, PoP Vol. 21, No. 12, 2014
 *E. Dale and B. Jorns, IEPC-2017-265

Introducing non-local 0D models that add additional “dimensions,” e.g. “two-zone” approach

S. Barral and E. Ahedo. Phys Rev. E, Vol. 79, No. 4, April 2009.
 S. Barral and Z. Peradzynski, Physics of Plasmas, Vol. 17, No. 1, Jan. 2010.
 E. Dale and B. Jorns, IEPC-2019-354

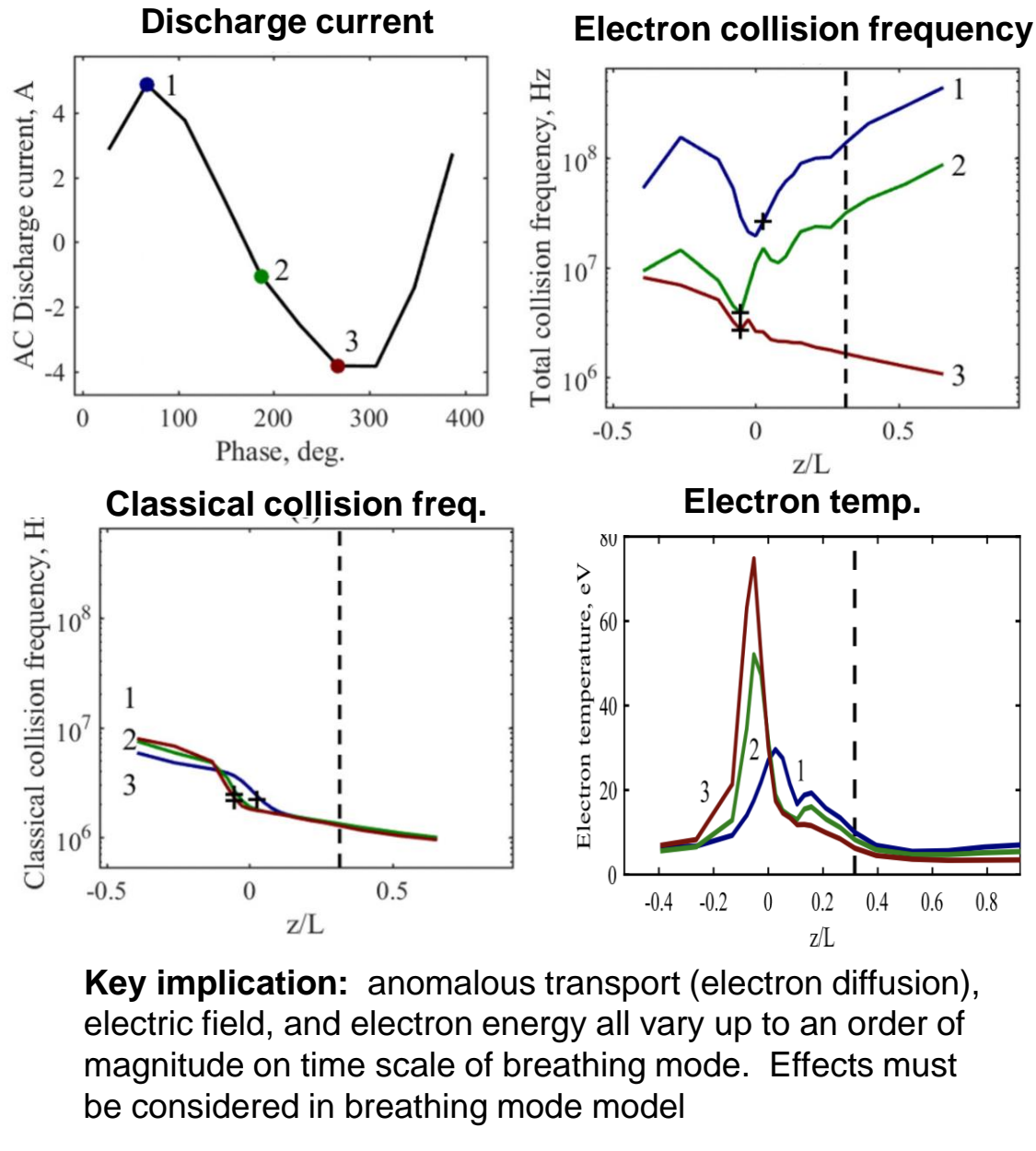
- Key question: which physics should be added to predict the transition?
- Role of experiments is to show “ground truth” for what additional fidelity or physics is needed

Experimental characterization of plasma properties on time scale of breathing mode in acceleration zone



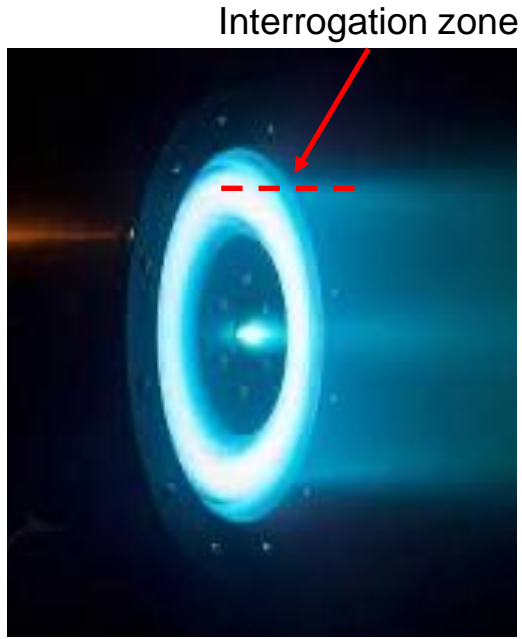
Method: time resolved laser induced fluorescence for ions combined with ion momentum equation and Ohm's law for electrons to experimentally infer plasma properties along channel centerline

Test article: H9 Magnetically shielded Hall thruster at 300 V and 2.5 kW operating on xenon



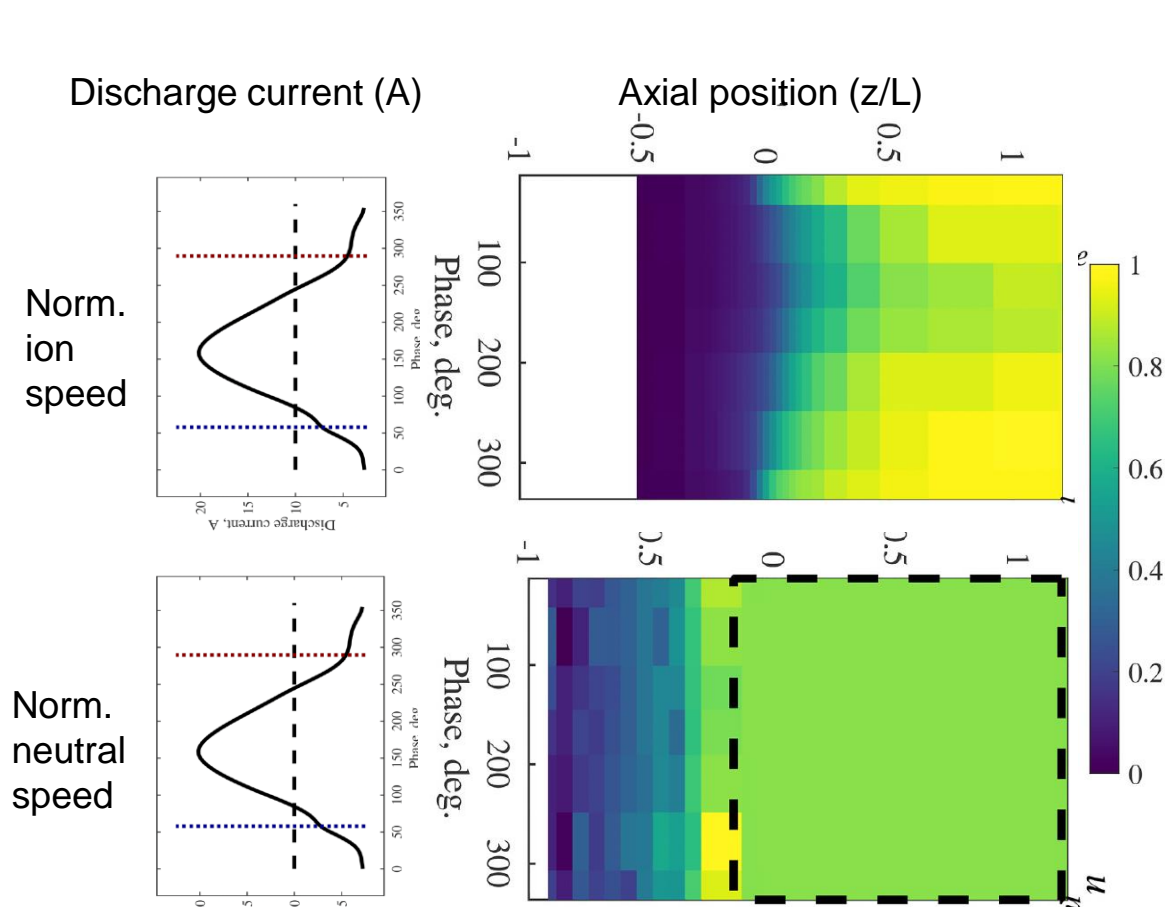
Key implication: anomalous transport (electron diffusion), electric field, and electron energy all vary up to an order of magnitude on time scale of breathing mode. Effects must be considered in breathing mode model

Experimental characterization of plasma properties on time scale of breathing mode in acceleration zone



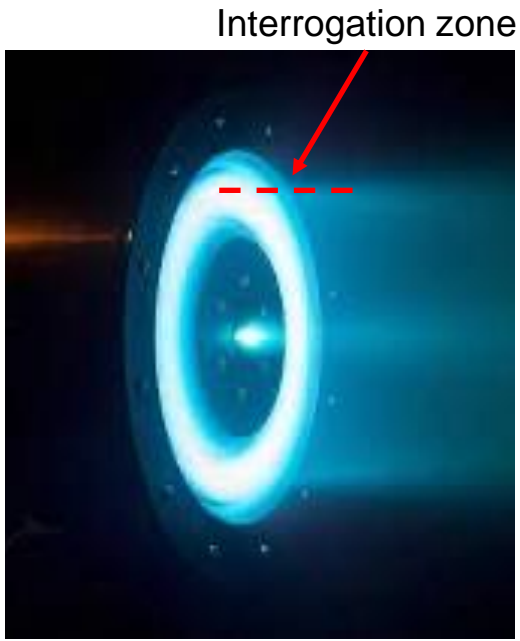
Method: time resolved laser induced fluorescence for ions and neutrals combined with ion momentum equation and Ohm's law for electrons to experimentally infer plasma properties along channel centerline

Test article: H9 Magnetically shielded Hall thruster at 300 V and 2.5 kW operating on xenon



Key implication: speeds of heavier particles perturbed but do not vary as much on time scale of oscillation compared to other quantities. May be OK to assume constant in analysis

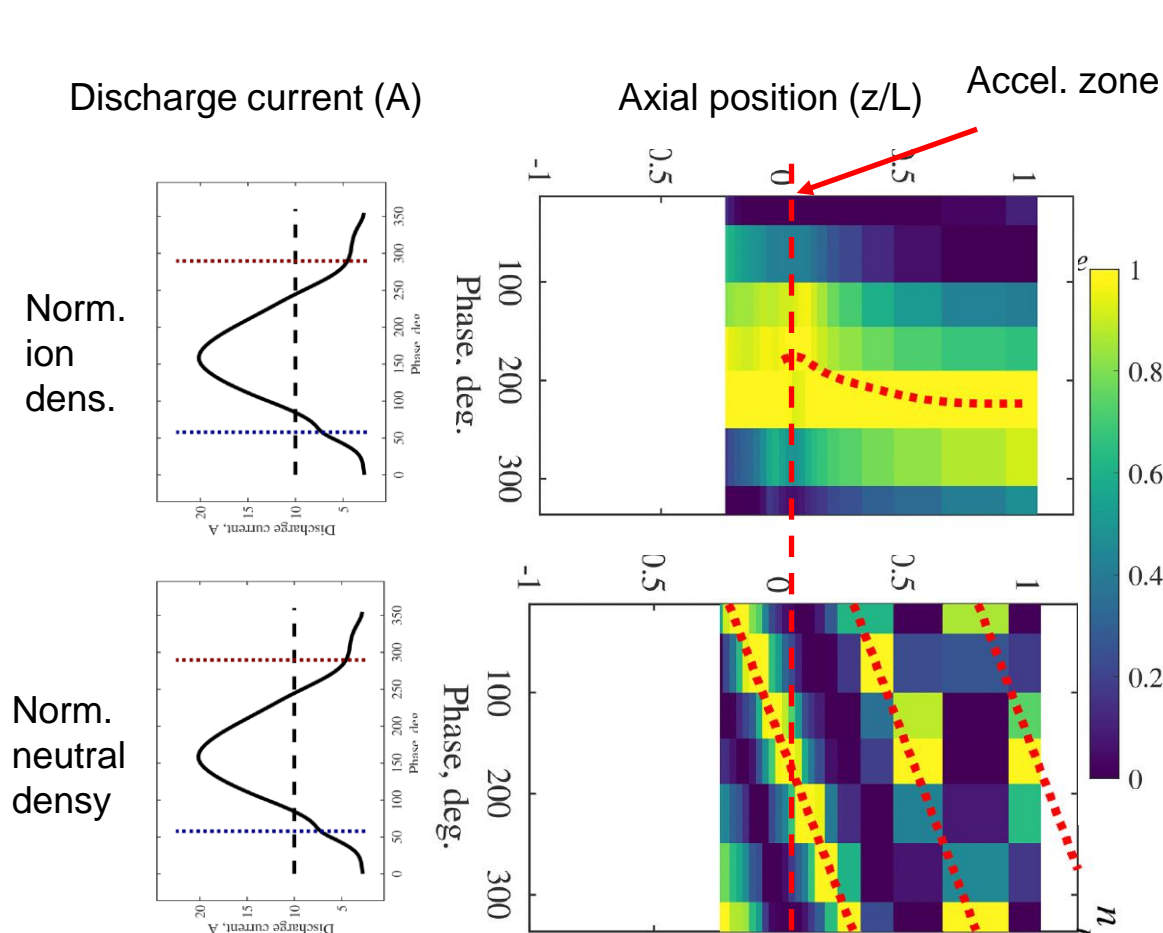
M Experimental characterization of plasma properties on time scale of breathing mode in acceleration zone



Method: time resolved laser induced fluorescence for ions and neutrals combined with ion momentum equation and Ohm's law for electrons to experimentally infer plasma properties along channel centerline

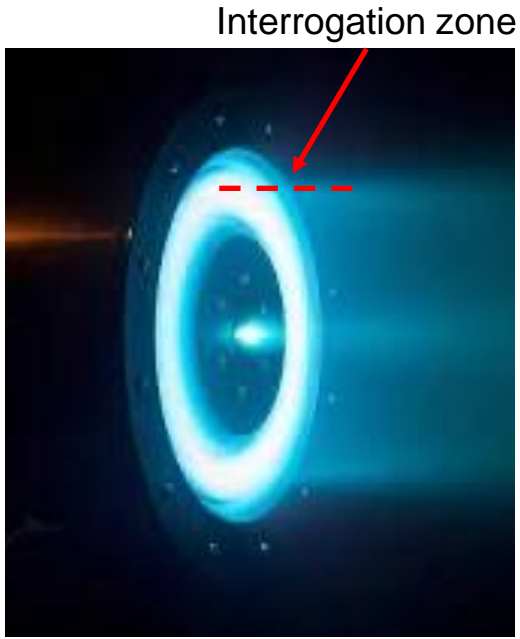
Test article: H9 Magnetically shielded Hall thruster at 300 V and 2.5 kW operating on xenon

*E. Dale and B. Jorns, JAP **130** 133302 (2021)



Key implication: Experimental evidence that the neutral and ion oscillations associated with breathing mode are convecting waves that move at drift speeds of each species. Oscillations appear to be causally linked to perturbations upstream of accel. zone

Experimental characterization of plasma properties on time scale of breathing mode in acceleration zone

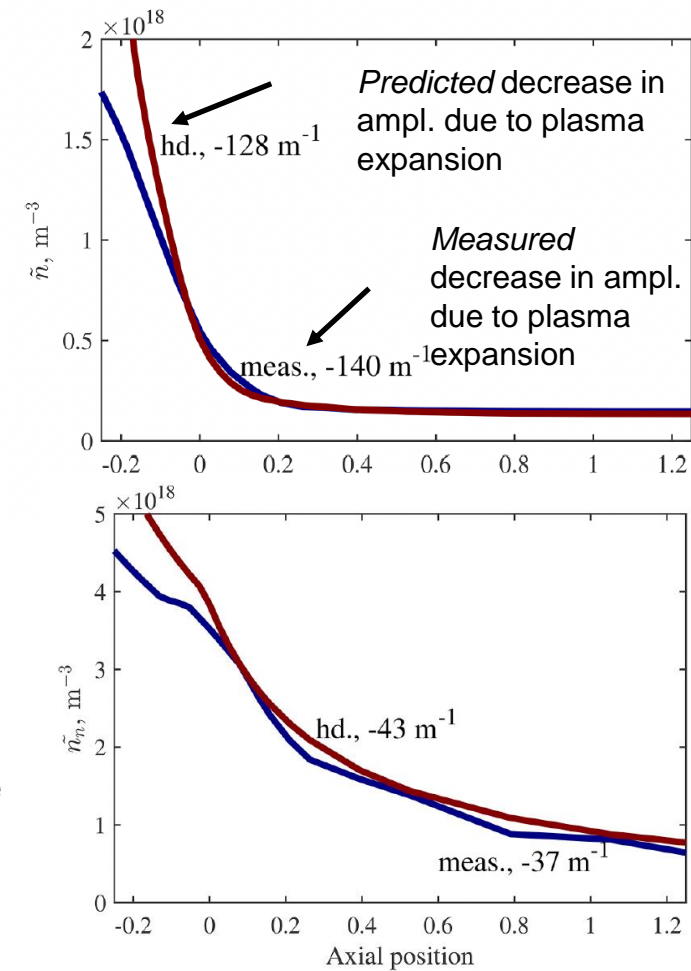


Method: time resolved laser induced fluorescence for ions and neutrals combined with ion momentum equation and Ohm's law for electrons to experimentally infer plasma properties along channel centerline

Test article: H9 Magnetically shielded Hall thruster at 300 V and 2.5 kW operating on xenon

*E. Dale and B. Jorns, JAP **130** 133302 (2021)

Amplitude of ion density fluctuations correlated with breathing mode

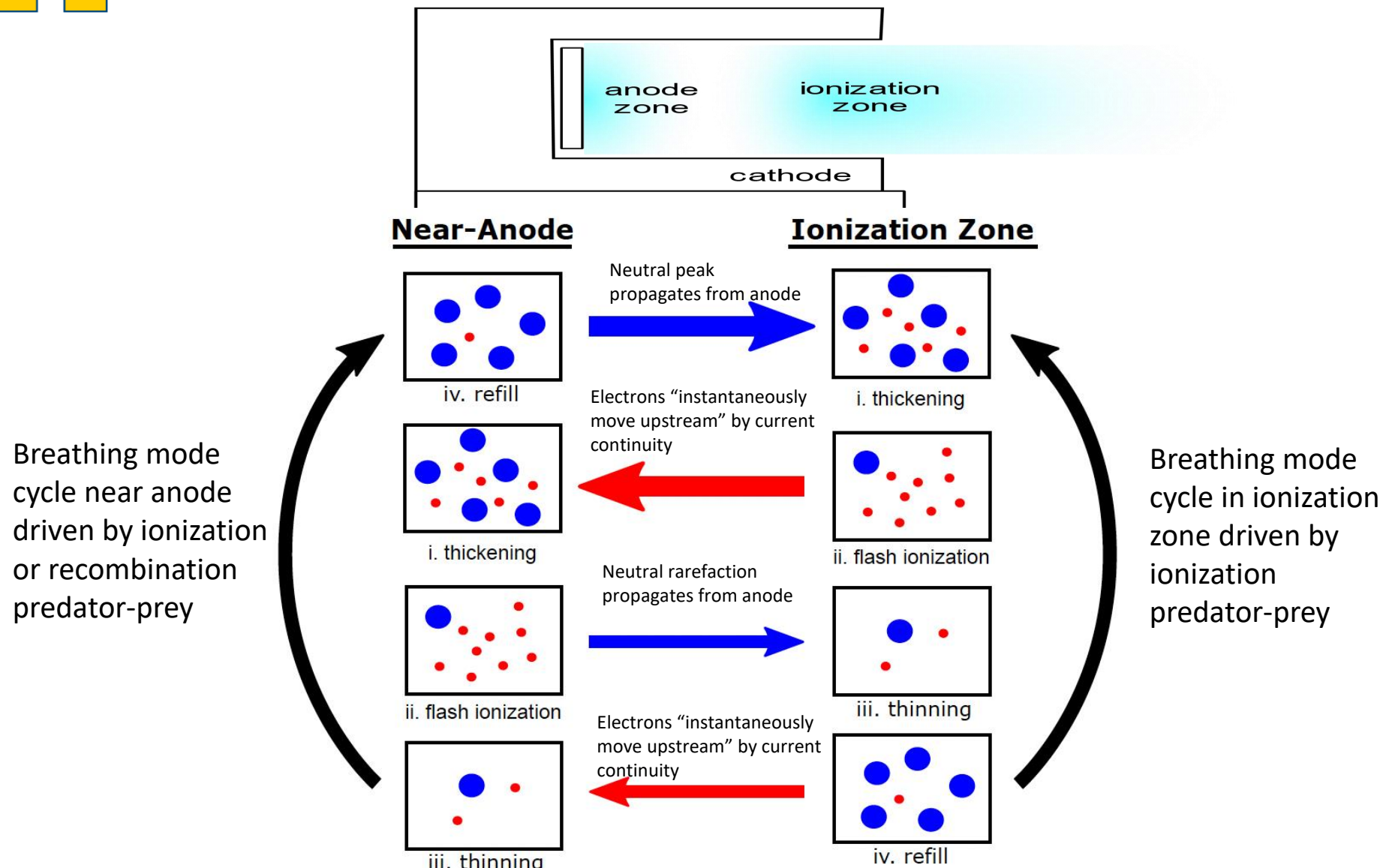


Amplitude of neutral density fluctuations correlated with breathing mode

Key implication: The amplitude of waves correlated with breathing mode decay at a rate downstream of accel zone that can be explained just by the waves propagating into a less sparse plasma ("hydrodynamic damping"). Also suggests oscillations may form upstream of accel zone.



Two zone theory inspired by experimental observation



Source of instability could be the phase delay between the two predator-prey zones that is facilitated by disparity between neutral and electron transit times. Might lead to positive feedback on both cycles



Summary of experimental findings

- Electron properties (diffusion, energy, electric field) all vary by order of magnitude on time-scale of breathing mode. Probably should be considered in formulating stability criteria.
- Propagating ion and neutral drift waves correlated with formation of breathing mode. Waves appear to convect from a region upstream of the acceleration zone
- Damping rates of perturbations also suggest that their formation may occur upstream of acceleration zone
- Experimental results suggest that both spatial effects and more plasma properties should be considered to correctly capture stability criteria for breathing mode. Two zone model is one approach to an analytical solution to capture these effects.

Numerical and Experimental Investigation of Longitudinal Oscillations in Hall Thrusters

Vittorio Giannetti, Luca Leporini, Manuel M. Saravia, Simone Camarri,
Tommaso Andreussi



**ExB Plasmas
Workshop
2022**

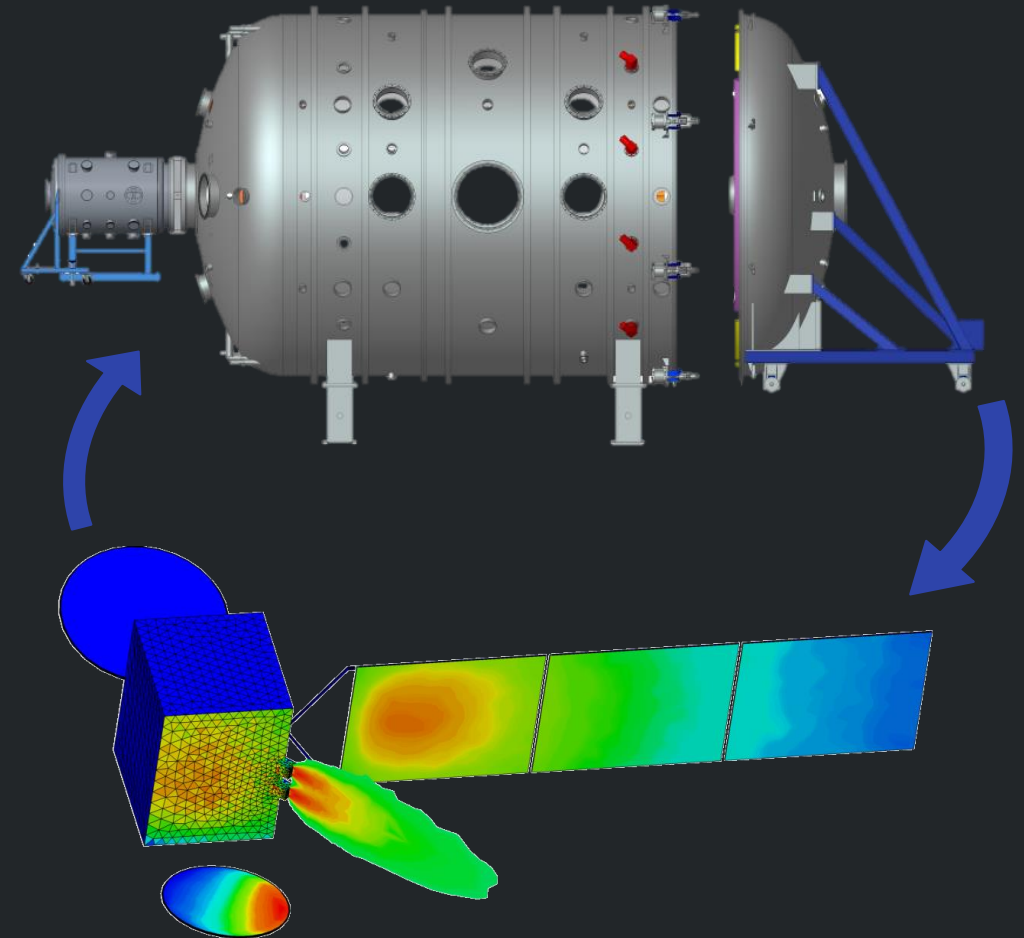
Madrid, online event

Investigation on Breathing Mode

- Introduction
- Experimental campaign
- Time-dependent fluid model
- Model calibration and simulation results
- Breathing mode onset
 - Base state
 - Linear stability analysis
 - Numerical tests

Experiments and models

- On-ground testing is fundamental for EP development but full of challenges
 - Large facilities, high pumping capability
 - Ad-hoc diagnostics
 - Long times
- Modelling and simulations are needed to
 - Support the design
 - Design experiments and verify requirements
 - Interpret the results
- At the same time, specific tests and diagnostics can validate models and numerical codes



Plasma thruster development

- Thruster development
 - Identify scaling laws
 - Performance optimization
 - Extend lifetime
 - Alternative propellants
 - ...
- Environment representativeness
 - Background pressure
 - Electrical interactions
 - Air-breathing
 - ...
- Performance evolution
 - Erosion
 - Variable operating parameters
- Fault detection and health monitoring
 - Test procedures
 - ...



Technology assessment and maturation

Qualification risks, long duration, high costs

LOW

TRL

HIGH



Plasma thruster development

- Thruster development
 - Identify scaling laws
 - Performance optimization
 - Extend lifetime
 - Alternative propellants
 - ...
- Environment representativeness
 - Background pressure
 - Electrical interactions
 - Air-breathing
 - ...
- Performance evolution
 - Erosion
 - Variable operating parameters
- Fault detection and health monitoring
 - Test procedures
 - ...



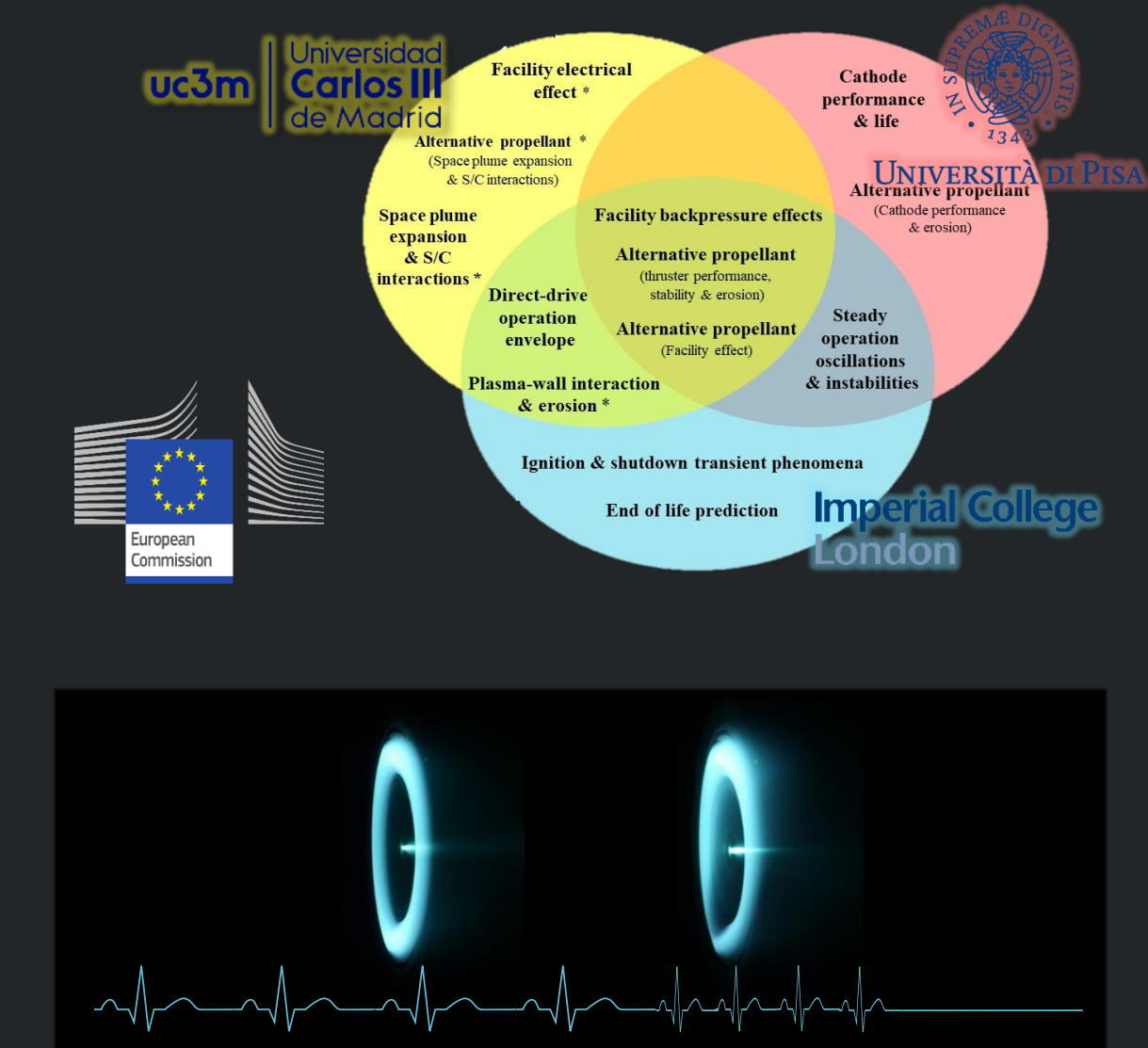
Technology assessment and maturation

Qualification risks, long duration, high costs

LOW
TRL
HIGH

Alternative strategy

- Analysis and simulations tools to predict the system behavior and drive the qualification strategy (e.g., EU H2020 ASPIRE project for the development of SITAEL's 20 kW Hall propulsion system)



- Many things can go wrong during experiments, and they will (Murphy's law)
- With Hall thrusters, looking at the **current** is a way to see if something is going wrong

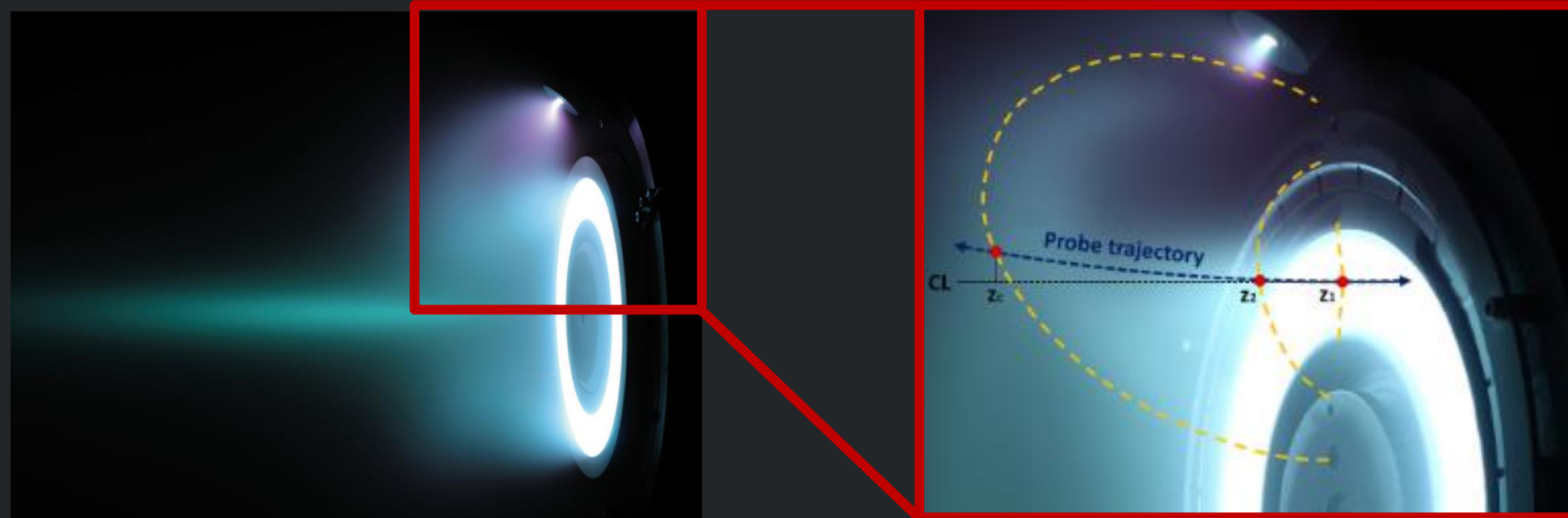
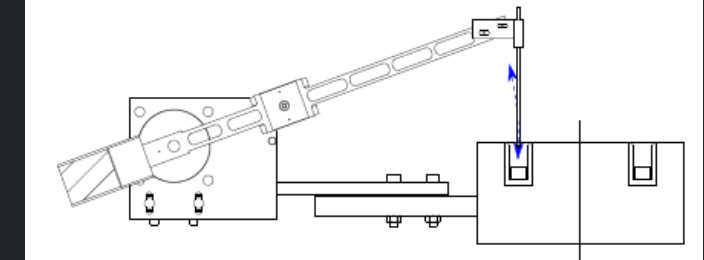
Experimental campaign

SITAEL's HT5k DM2 thruster, unshielded magnetic configuration, 2.5 kW/300 V

- **Triple Langmuir probe**
- **High speed robotic arm**
- **200 ms injection (100 ms one-way)**
- **Data sampled at 5 MHz**
- **Filtered at 120 kHz through DAQ**

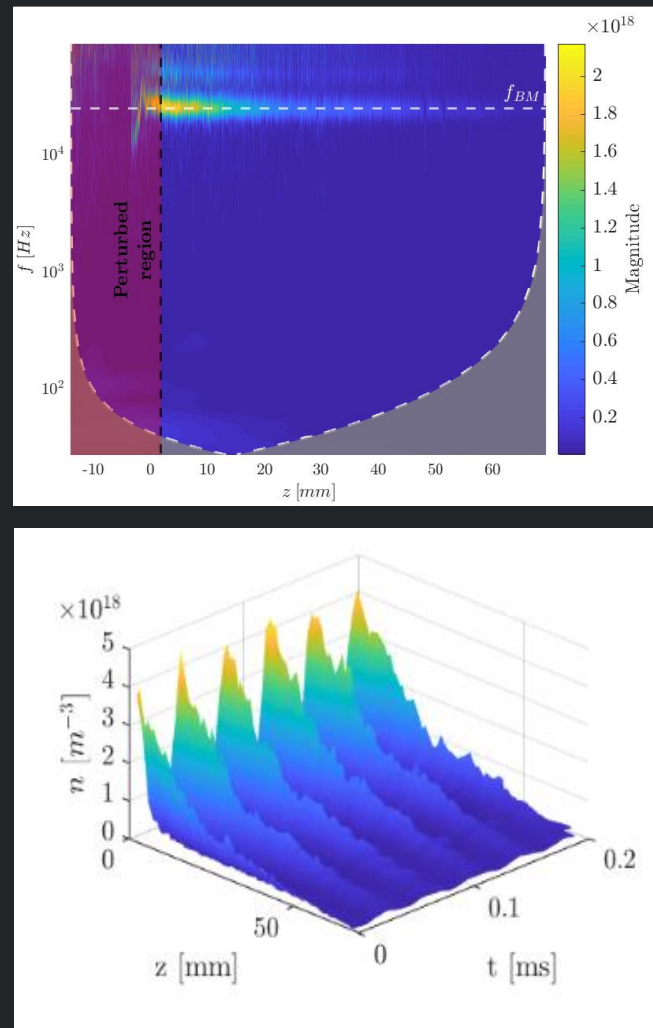
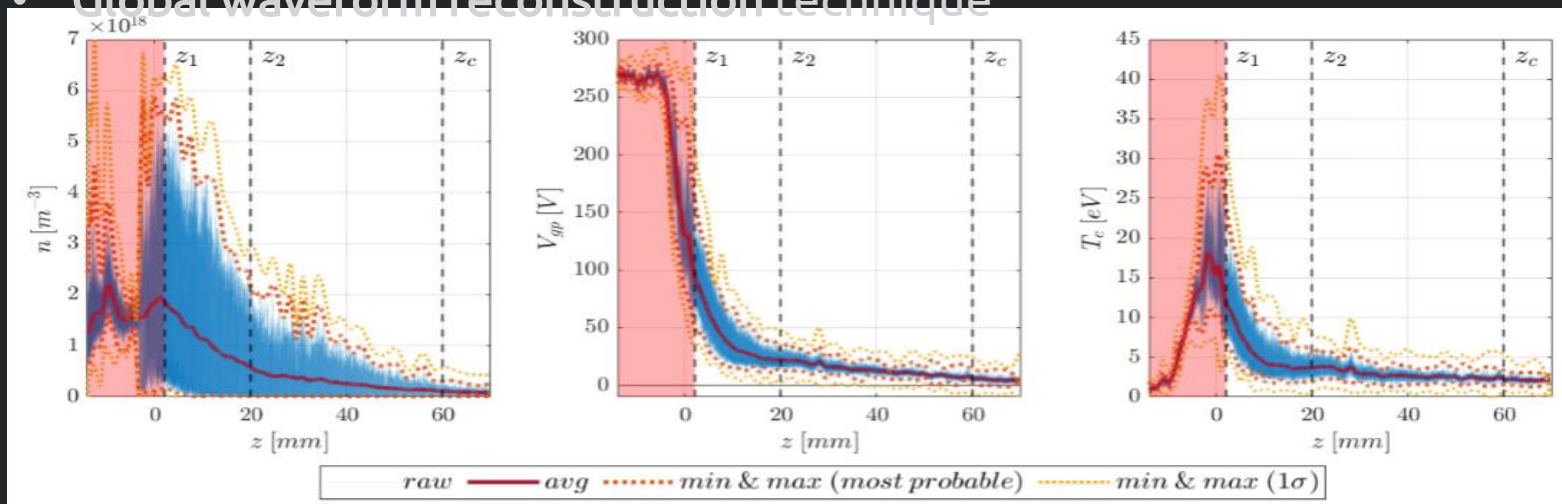
AMFR ^a [mg/s]	Voltage [V]	Current [A]	Power [W]
8	300	8.65 ^b	2595 ^b

^a Anode Mass Flow Rate
^b Time-averaged value



Experimental results

- Instantaneous measurement of plasma properties during probe insertion
- Perturbed region excluded
- Bayesian analysis of the data to extract statistically significant values of plasma properties and their local oscillations as a function of axial position.
- Time-frequency wavelet analysis → non-dispersive wave
- Global waveform reconstruction technique



Giannetti, V., Saravia, M. M., & Andreussi, T. (2020). "Measurement of the breathing mode oscillations in Hall thruster plasmas with a fast-diving triple Langmuir probe". Physics of Plasmas, 27(12), 123502.

1D time-dependent fluid model

- 3-species Fully fluid simulations.
- cold ions, hot electrons
- Anode sheath, plasma-wall interaction with SEE, Ion backflow, sonic transition, heat conduction included.

$$\frac{\partial n_n}{\partial t} + \frac{\partial}{\partial z} (u_n n_n) = -n_e n_n k_I + \dot{n}_w, \quad (1)$$

$$\frac{\partial n_i}{\partial t} + \frac{\partial}{\partial z} (u_i n_i) = n_e n_n k_I - \dot{n}_w \quad (2)$$

$$\frac{\partial}{\partial t} (n_i u_i) + \frac{\partial}{\partial z} \left(n_i u_i^2 + \frac{p_i}{m_i} \right) = -\frac{e}{m_i} n_i \frac{\partial \Phi}{\partial z} - u_i \dot{n}_w, \quad (3)$$

$$\frac{\partial n_e}{\partial t} + \frac{\partial}{\partial z} (u_e n_e) = n_e n_n k_I - \dot{n}_w, \quad (4)$$

$$n_e u_e = -\mu n_e \left(\frac{1}{e n_e} \frac{\partial n_e k_B T_e}{\partial z} - \frac{\partial \Phi}{\partial z} \right) \quad (5)$$

$$\begin{aligned} \frac{\partial}{\partial t} \left(\frac{3}{2} n_e k_B T_e \right) + \frac{\partial}{\partial z} \left(\frac{5}{2} n_e k_B T_e u_e \right) = \\ = \frac{\partial}{\partial z} \left(\frac{5 \mu}{2 e} n_e k_B^2 T_e \frac{\partial T_e}{\partial z} \right) + u_e \frac{\partial p_e}{\partial z} + n_e u_e^2 \frac{e}{\mu} - n_n n_e K - n_e W \end{aligned} \quad (6)$$

$$J = \frac{\Delta V + \int_0^{z_f} \left(\frac{u_i}{\mu} + \frac{1}{en} \frac{\partial p_e}{\partial z} \right) dz}{\int_0^{z_f} \frac{1}{en\mu} dz} \quad (7)$$

$$u_e = u_i - \frac{J}{en}. \quad (8)$$

Neutrals continuity (constant velocity)

Euler system for ions
(continuity + momentum pressure coupled)

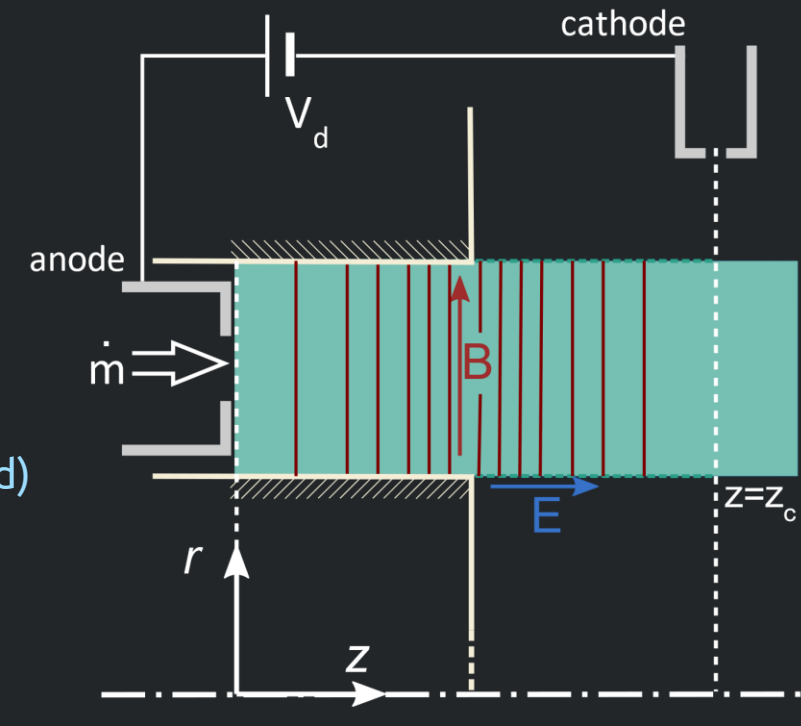
Electron continuity

Electron momentum

Electrons Internal energy

Integral equation for current

Current continuity



Three free parameters:

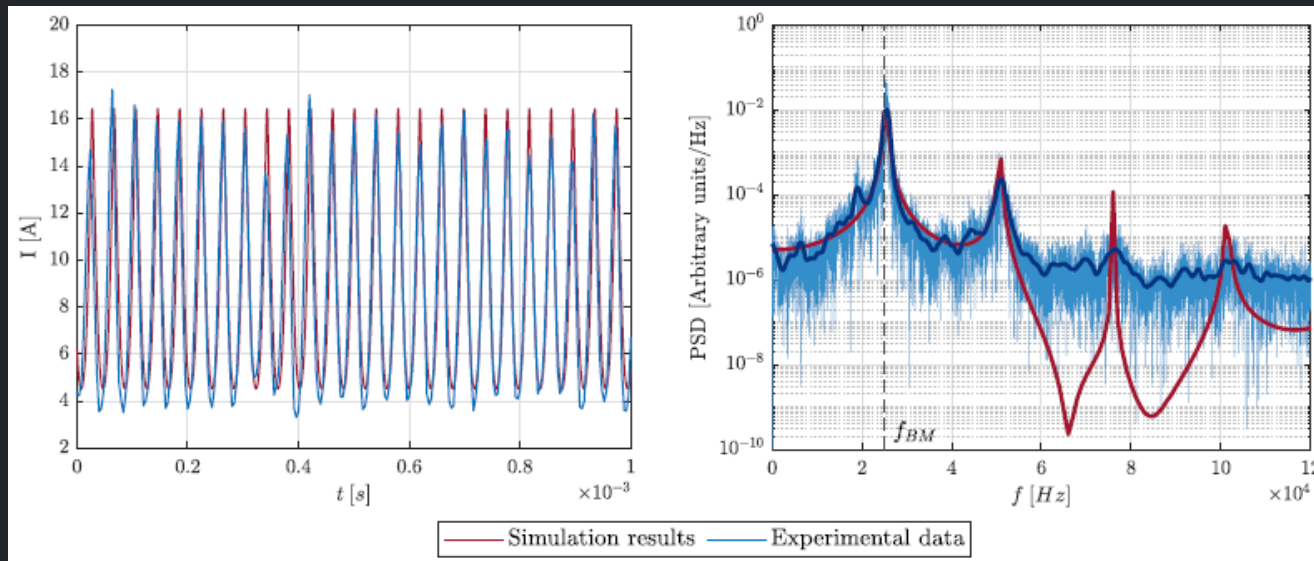
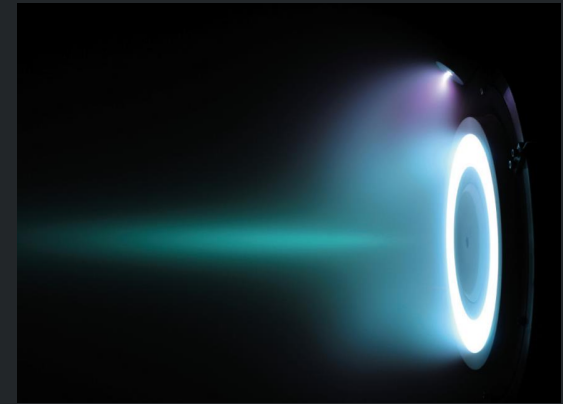
1. Neutral velocity;
2. Anomalous collisionality;
3. Wall interaction coefficient.

Numerical infrastructure validated on LANDMARK benchmark

HT5k simulations

Calibration on discharge current measurement of HT5k-DM2, M1

1. Neutral velocity: 395 m/s
2. Anomalous diffusion coefficient: 0.075 and 7.5 in the channel and near plume
3. Wall interaction coefficient: 0.115

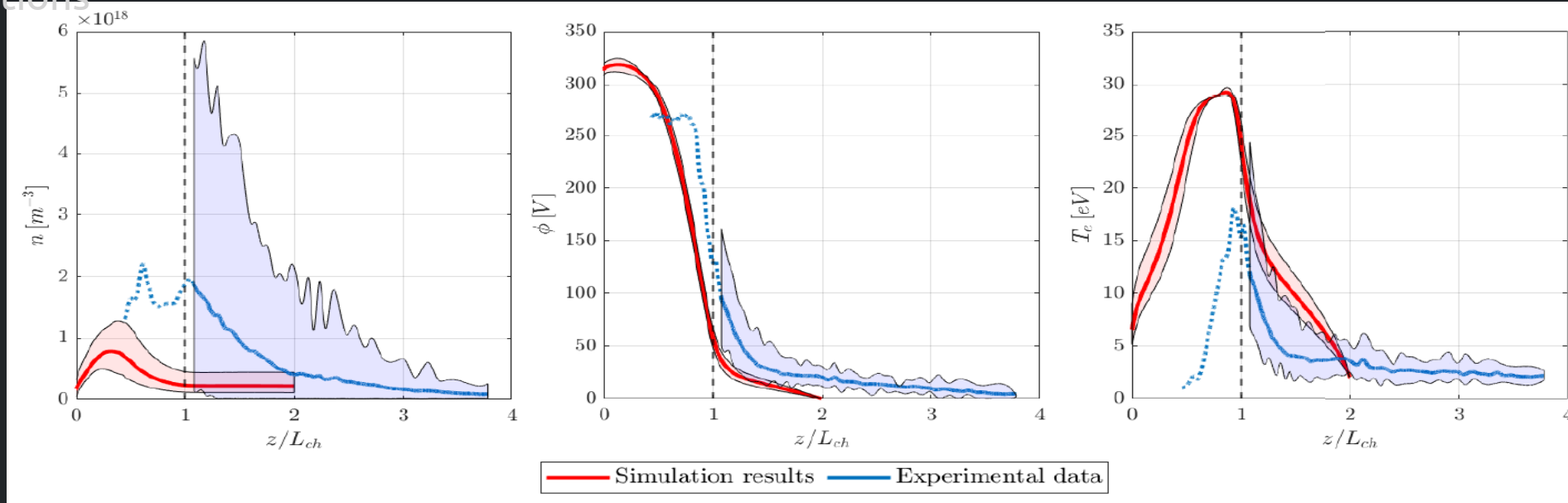


Simulated current matches remarkably well measured signal (time and frequency domain)

Parameter	Units	Measurement	Simulation
I_{avg}	[A]	8.65	8.67
I_{max}	[A]	13.9 – 17.3	16.4
I_{min}	[A]	3.3 – 5	4.5
I_{rms}	[A]	4.1	3.9
f_{BM}	[kHz]	25.4	25.3

Comparison with probe data

Following calibration on the sole discharge current signal the code can extrapolate intensive properties distributions



- **Correct order of magnitude** recovered for all plasma properties.
- **Experimental trends reconstructed**, with maximum oscillations near the channel exit section.
- **Acceleration region oscillation** is present in simulations (even if lower amplitude).
- **Plasma density value and oscillations underestimated** by simulations.
- **Simulation's acceleration region further upstream** compared with experiments.

Breathing Mode Onset

1. Base state

- Obtained using **Selective Frequency Damping (SFD)**

$$\frac{\partial n_n}{\partial t} + \frac{\partial}{\partial z} (u_n n_n) = -n_e n_n k_I + \dot{n}_w [-\chi(n_n - \bar{n}_n)]$$
$$\dot{n}_n = \frac{(n_n - \bar{n}_n)}{\Delta}$$

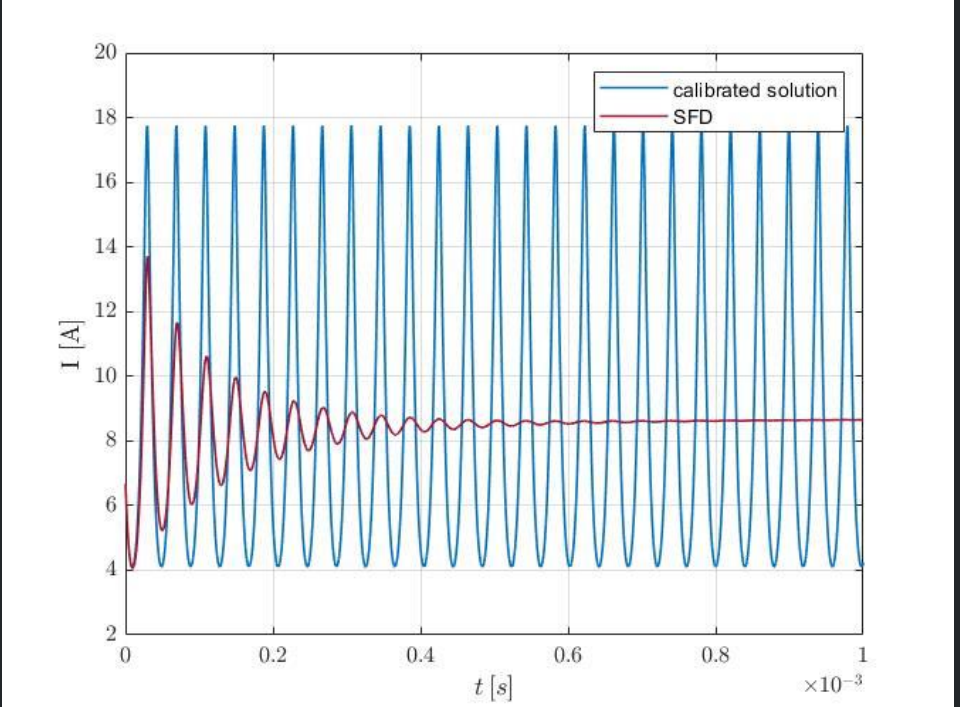
- Starting point for the stability analysis

2. Linear stability analysis

- Numerical linearization around the base state
- Linearized code is used as a time-stepper and coupled with a Krylov-based eigenvalue solver

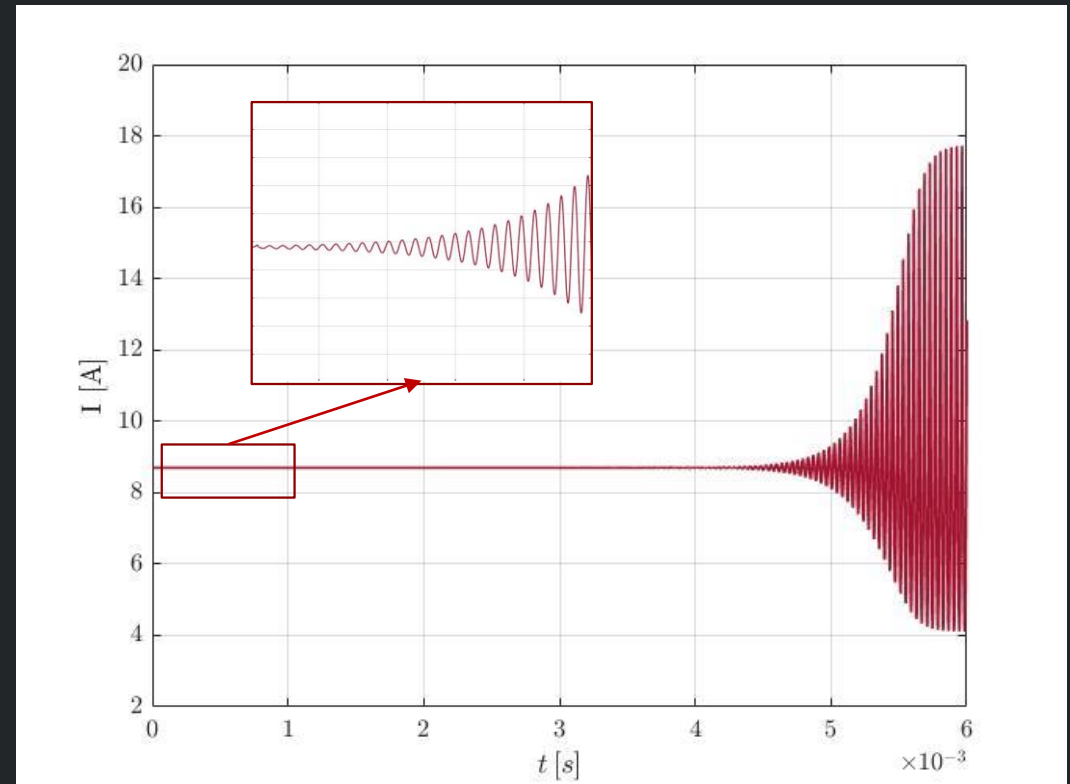
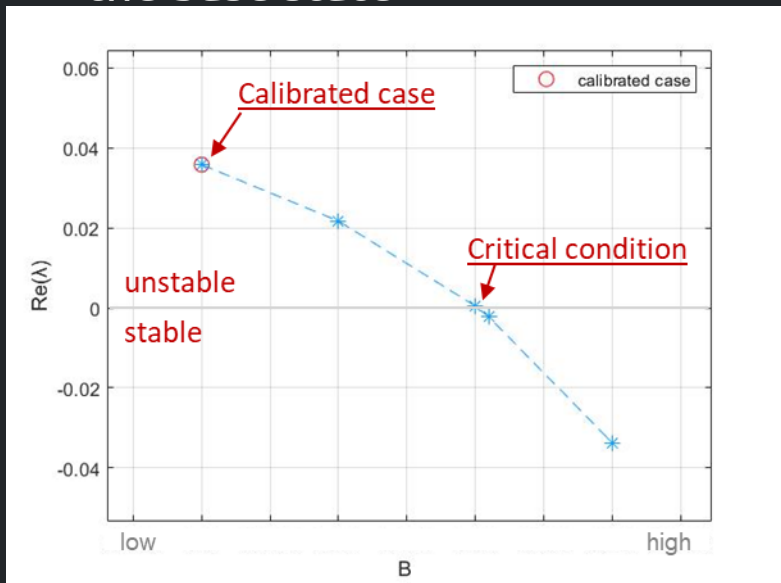
3. Numerical tests

- Analysis of the system response to a perturbation of the base state



Breathing Mode Onset

- Instability spontaneously arises starting from the base configuration
- What is the role of the various parameters in the onset of breathing mode?
- Taking B_r as control parameter, breathing mode seems to arise as a super-critical Hopf bifurcation of the base state

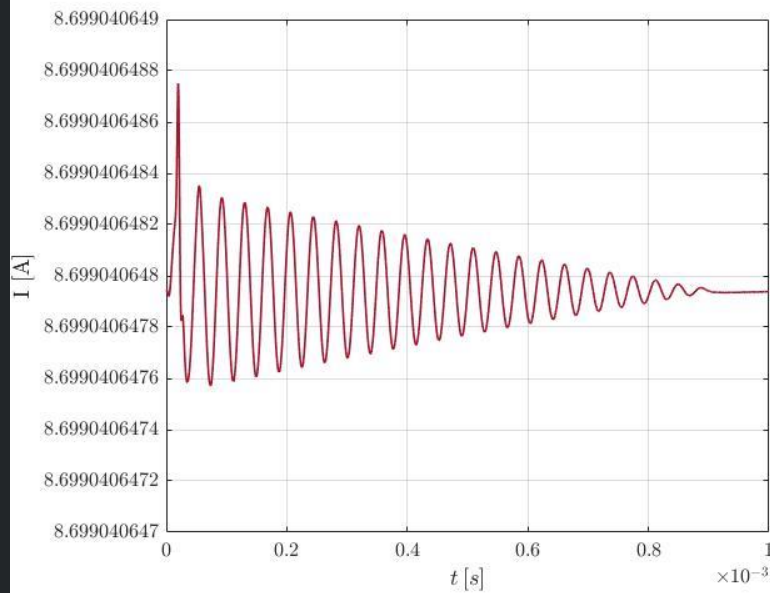


Idea: focus on the role played by electron mobility
$$\mu = \mu(n_n, T_e, B_r)$$

Breathing Mode Onset

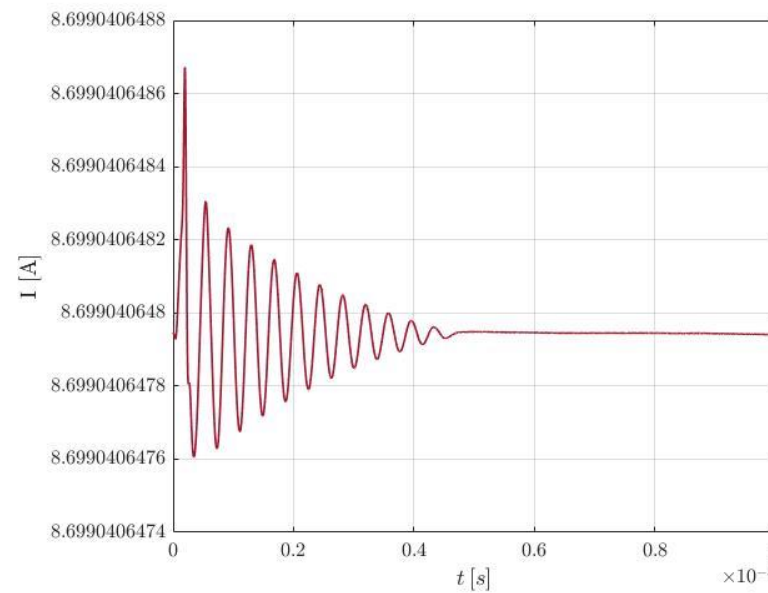
TEST 1

$$\mu = \mu_{bc} = \mu(n_{n,bc}, T_{e,bc})$$



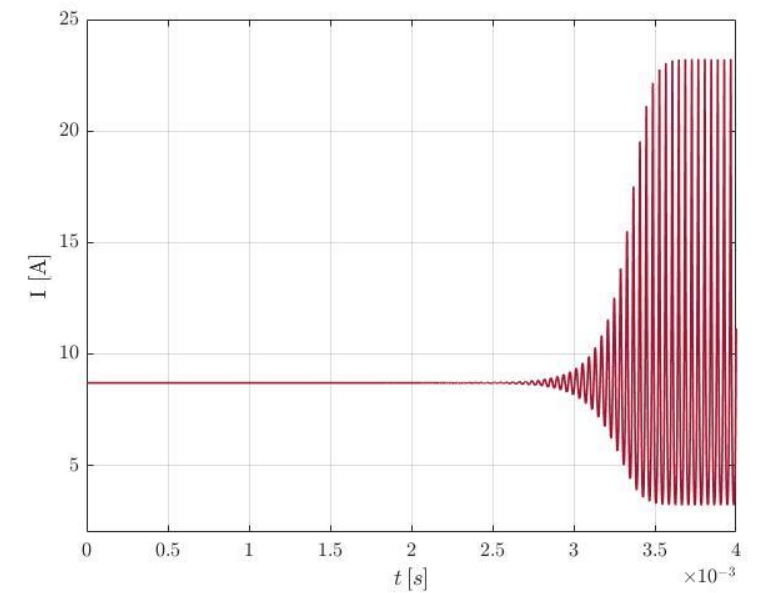
TEST 2

$$\mu = \mu(n_{n,bc}, T_e)$$



TEST 3

$$\mu = \mu(n_n, T_{e,bc})$$



Oscillations of electron mobility due to variations of neutral density are fundamentals for the onset of BM

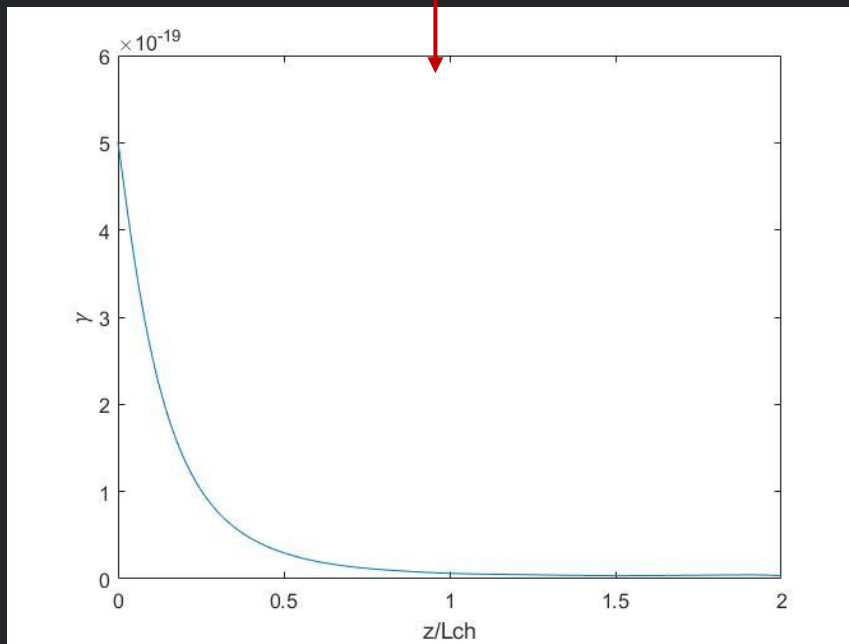
Breathing Mode Onset

- Linearization of $\mu = \mu(n_n, T_{e,bc})$ w.r.t. n_n : γ seems to act as a rigidity controlling the growth rate

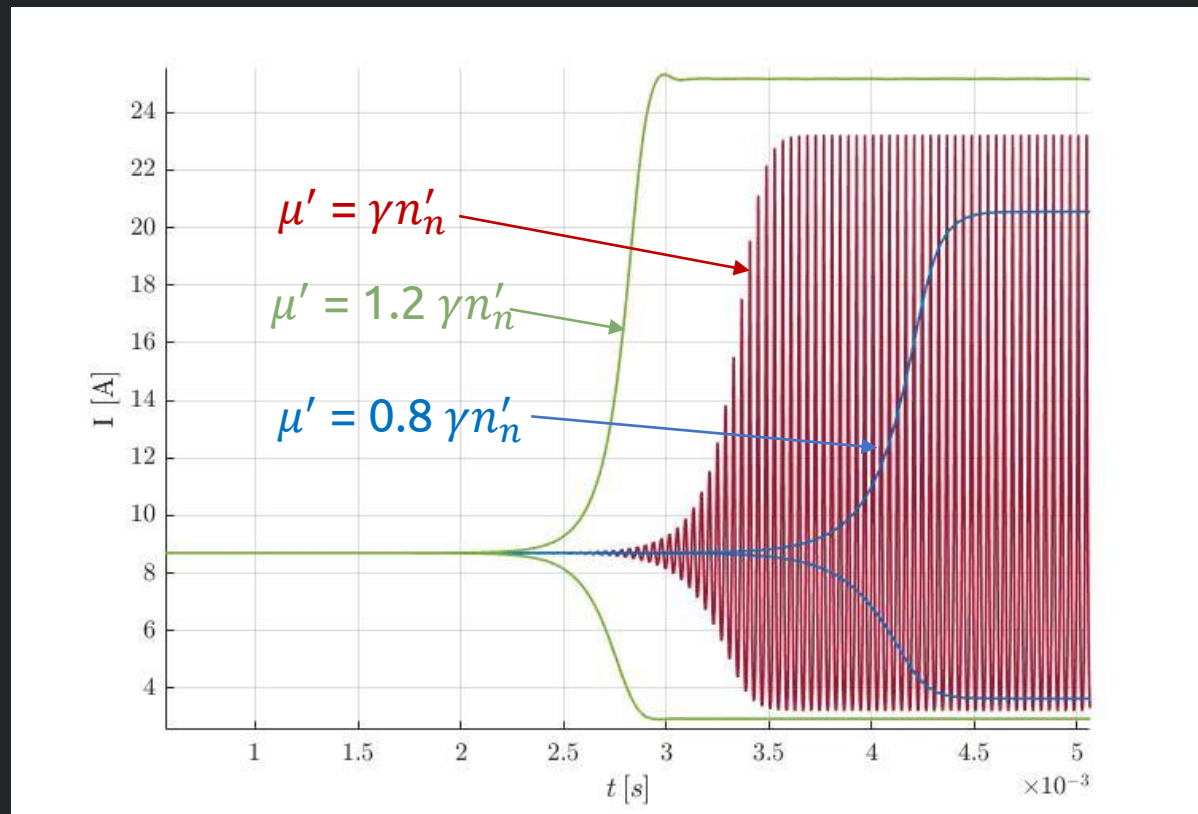
$$\mu = \mu_{bc} + \mu'$$

$$\mu' = \frac{e}{m_e(v_{bc}^2 + \omega_e^2)} \left[1 - \frac{2v_{bc}^2}{(v_{bc}^2 + \omega_e^2)} \right] k_m n'_n$$

γ



TEST 4



Conclusions

- Breathing mode oscillations are a way to understand the thruster behavior
- Fast diving of triple Langmuir probes can be used to reconstruct local plasma oscillations
- Reduced order models, calibrated on the discharge current signal, can be used to extrapolate the plasma properties
- The role of the magnetic field and, consequently, of electron mobility is crucial for the onset of the breathing mode
- The influence of neutral density on the mobility is sufficient, in the analyzed case, to sustain breathing mode oscillations

Session 4. Discussion

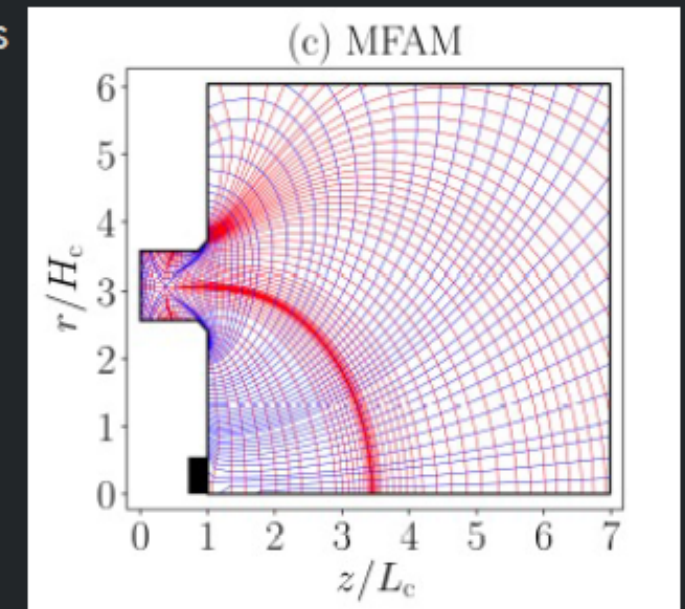


**ExB Plasmas
Workshop
2022**

Madrid, online event

Conclusions

- A physical macroscopic model of turbulent transport continues to be the most serious limitation for e-fluid models of HET and EPTs
- Other uncertainties are on: the heat flux closure and boundary conditions(BCs)
- Finally, azimuthal inertia and pressure tensor effects are not to be ignored.
- Beyond physics there are important numerical challenges with 2D e- fluid models
- The large anisotropy of $\bar{\sigma}_e$ and \bar{K}_e
 - Spurious numerical diffusion can ruin solutions in regular Cartesian meshes
 - Hall2De and HYPHEN opted for using a MFAM (magnetic field aligned mesh) [10]
 - MFAM avoids numerical diff. but involves complex numerical algorithms [11,12]
 - Is it worth working on very irregular MFAM or should we develop diffusion-free algorithms on regular meshes? [13]
- Addressing the infinite plume expansion with a finite domain
 - Issue arises because of nonlocal kinetic effects
 - Downstream BCs on finite plume are not obvious
 - Simulated thruster performances affected by plume size [14]



	F [mN]	η_F	η_{ene}	η_{div}	η_{disp}
Nominal case	7.64	0.097	0.178	0.74	0.74
Double plume	8.69	0.126	0.178	0.85	0.83

[10] Perez et al., Appl. Sci. 6, 354 (2016)

[11] Zhou et al. PSST 28, 115004 (2019)

[12] Perales et al. JAP (accepted)

[13] Modesti et al. ongoing work

[14] Zhou et al. ,PSST (submitted)

Session 4 – discussion

Axial-azimuthal PIC benchmark:

- Characteristics of instabilities in the plume
- Quasi-linear theoretical model approximates very well the instability-enhanced force
 - Validity in the context of electron drift instabilities in HETs still requires further investigation
 - The EDF is in general strongly non-Maxwellian and diverse in shape throughout the discharge: Challenge in modeling anomalous electron transport for fluid simulations

Radial-azimuthal PIC benchmark:

- How does SEE impact the conditions of appearance of the MTSI, influence on the ECDI/MTSI coupling?

Session 4 – discussion on BM

- What criteria do we have for the breathing mode (BM) excitation?
- What are the current capabilities/tools to control breathing mode in the experiment? ...
- Role of the external circuit in experiment and modelling? ...How successful are engineering efforts to stabilize BM by the external circuit?
- Do we have any working 0D model for BM? Two-zone 0D? ...
- How do we handle sensitivity to anomalous mobility and energy losses in 1D models? ...
- Calibration of BM models on BM characteristics and thruster performance: Do they agree?....
- Time dependent mobility and coupling to azimuthal modes? What are any 2D models for BM? How good are they? ...
- Where the (reduced) modeling of breathing mode should be going (excluding dreams about full 3D PIC models)?...
- Dreams about full device modeling should be pursued too!
-